Medium-chain fatty acid metabolism in hepatocytes and adipocytes

Dissertation

zur

Erlangung des Doktorgrades (Dr. rer. nat.)

der

Mathematisch-Naturwissenschaftlichen Fakultät

der

Rheinischen Friedrich-Wilhelms-Universität Bonn

vorgelegt von

Kristina Klizaite

aus

Vilnius (Litauen)

Bonn, 2016

Angefertigt mit Genehmigung der Mathematisch-Naturwissenschaftlichen Fakultät der
Rheinischen Friedrich-Wilhelms-Universität Bonn

1. **Gutachter:**
   Herr Prof. Dr. Christoph Thiele
2. **Gutachter:**
   Herr Prof. Dr. Klaus Willecke

Tag der Promotion: 21.3.2017
Erscheinungsjahr: 2017

Declaration of authorship

Hereby I declare that I am the sole author of this dissertation and that all sources I used to support my thesis are clearly indicated. The work presented in it has been generated by me as the result of my own original research. It is clearly stated, where the work is based on research done jointly with others.

Bonn ,

_____ Signature

Table of contents

Summary

Fatty acids (FAs), in free form or incorporated into complex lipids, constitute an inseparable part of the daily human diet. Different carbon atom chain length and saturation rate leads to a huge variety of FAs of which long-chain fatty acids (LCFAs) being the dominant type. The main focus of this work is medium-chain FAs (MCFAs), a group of saturated FAs, mainly found in coconut oil, palm kernel oil and milk. MCFAs have shorter carbon atom chain lengths and therefore different properties compared to longer FAs. The cellular metabolism of MCFAs is still insufficiently investigated particularly when compared to LCFAs.

This thesis analyzes the metabolism of MCFAs with aim to better comprehend their effect on the human body, to examine their unique properties, and to contribute to the general understanding of MCFAs.

The metabolism of MCFAs was investigated in different cell lines, in mouse organs, in differentiating 3T3-L1 cells, and in dedifferentiating hepatocytes. Alkyne-FAs and click labeling technique were used to analyze the metabolism of MCFAs. The triacylglycerol (TAG) synthesis from MCFAs was the main object of research. It was shown that different cell lines routinely used in cell culture experiments could not synthesize TAGs from MCFAs, however, primary hepatocytes, 3T3-L1 adipocytes and organ slices from liver and gut could. It was also found that differentiating 3T3-L1 cells gain the function of TAG synthesis from MCFAs, whereas primary hepatocytes lose this function after longer cultivation in 2D cell culture. mRNA sequencing data obtained for differentiating 3T3-L1 cells and dedifferentiating hepatocytes showed changes in various genes related to lipid metabolism.

MCFA uptake into cells was also investigated. Cells that could not synthesize MCT (medium chain triacylglycerols) could still uptake MCFAs. Moreover, a very interesting effect of CPT1 inhibitor etomoxir on the MCFA metabolism was observed. Etomoxir reduced TAG synthesis from MCFAs and enhanced the formation of unknown substances secreted into the medium by C11 MCFA fed hepatocytes.

Further, different enzymatic activities in the glycerol phosphate pathway were analyzed in Huh7 cells, primary hepatocytes and 3T3-L1 cells. It was shown that although Huh7 cells and dedifferentiated hepatocytes cannot synthesize TAGs from MCFAs, but their lysates possess different enzymatic activities for this synthesis.

This thesis is concluded by introducing hypothetical models for MCFA metabolism in hepatocytes and 3T3-L1 cells, which suggest the involvement of mitochondria in MCFA-TAG synthesis.

List of abbreviations

ACAD	acyl-CoA dehydrogenase
ACSVL	very-long-chain acyl-CoA synthetase
ADP	adenosine diphosphate
AGPAT	sn-1-acyl-glycerol-3-phosphate acyltransferase
AMP	adenosine monophosphate
ATGL	adipose triacylglycerol lipase
ATP	adenosine triphosphate
BG	background
BSA	bovine serum albumin
C10	decanoate, C10:0
C11	C11 alkyne fatty acid
C13	C13 alkyne fatty acid
C17	C17 alkyne fatty acid
C18	oleate C18:1
C19	C19 alkyne fatty acid
C9	C9 alkyne fatty acid
CACT	carnitine-acylcarnitine translocase
CD36	fatty acid translocase
CE	cholesterol ester
CL	cardiolipin
CoA	coenzyme A
CPT1	Carnitine palmitoyltransferase I
CPT2	carnitine palmitoyltransferase II
DAG	diacylglycerol
DCI	dodecenyl-CoA delta isomerase
DEXA	Dexamethasone
DGAT	diacylglycerol acyltransferase
DL-BSA	delipidated BSA
DMEM	Dulbecco's Modified Eagle Medium
ER	endoplasmic reticulum

FA	fatty acid
FABP	fatty acid binding protein
$FADH_2$	flavin adenine dinucleotide
FATP	fatty acid transport protein
FBS	Fetal Bovine Serum
G3P	glycerol-3-phosphate
GFP	green fluorescent protein
GPAT	glycerol-3-phosphate acyltransferase
HA	human influenza hemagglutinin
HSL	hormone sensitive lipase
HSLi	hormone sensitive lipase inhibitor
IBMX	3-Isobutyl-1-methylxanthine
IBMX	3-isobutyl-1-methylxanthine
LCAD	long-chain acyl-CoA dehydrogenase
LCFA	long-chain fatty acid
LCT	long-chain triacylglycerol
LD	lipid droplet
LPA	lysophosphatidic acid
LPAAT	lysophosphatidic acid acyltransferase
LPC	lysophosphatidylcholine
LPCAT	lysophosphatidylcholine acyltransferase
LPEAT	lysophosphatidylethanolamine Acyltransferase
LPI	lysophosphatidylinositol
LPS	lysophosphatidylserine
M/SCHAD	medium and short chain hydroxyacyl-CoA dehydrogenase
MAG	monoacylglycerol
MCAD	medium-chain acyl-CoA dehydrogenase
MCFA	medium-chain fatty acid
MCKAT	medium-chain 3-ketoacyl-CoA thiolase
MCT	medium-chain triacylglycerol; TAG having at least one MCFA
MGAT	monoacylglycerol acyltransferase
MGL	monoacylglycerol lipase
MTP	mitochondrial trifunctional protein

NADH	nicotinamide adenine dinucleotide
NEAAs	Non-Essential Amino Acids Solution
ON	overnight
PA	phosphatidic acid
PBS	phosphate-buffered saline
PC	phosphatidylcholine
PE	phosphatidylethanolamine
PG	phosphatidylglycerol
PI	phosphatidylinositol
PL	phospholipid
PS	phosphatidylserine
RT	room temperature
SCAD	short-chain acyl-CoA dehydrogenase
SD	standard deviation
TAG	triacylglycerol
TLC	thin layer chromatography
VLDL	very low-density lipoprotein

List of figures

List of tables

1. Introduction

Fatty acids (FAs) are important biomolecules made of a hydrocarbon chain and a terminal carboxyl group. They are building blocks for a wide variety of lipids and serve as an energy source in catabolic processes. Depending on fatty acid carbon chain length they are classified as short (>8 carbon atoms), medium (8-12 carbon atoms), long (12< carbon atoms) and very long-chain (22< carbon atoms) fatty acids. Based on the degree of saturation fatty acids can be saturated (no double bonds), monounsaturated (one double bond) or polyunsaturated (more than one double bond). The length and the degree of saturation determinate specific properties of different FAs, such as solubility in aqueous solutions, lipophilicity, melting point and susceptibility to oxidation.

The most widely investigated FAs are long-chain fatty acids (LCFAs) such as oleic acid (C18:1) and palmitic acid (C16:0), which is reasonable as they both are the most abundant FAs in human and other organisms.

In the organism FAs are stored in the form of triacylglycerols (TAGs) also known as fats or oils. In the western world fats traditionally used for cooking, such as sunflower oil, rapeseed oil, olive oil, lard and butter, are basically composed of saturated and unsaturated LCFAs.

In recent years many people have changed eating habits and are searching for alternative healthy fats. Therefore, more and more people start using coconut oil for their daily food preparation. Coconut oil is mainly made of medium-chain fatty acids (MCFAs). There is much less research data on the metabolism of these FAs compared to LCFAs. In this thesis, the metabolism MCFAs was analyzed in more detail.

1.1. Medium-chain fatty acids and medium-chain triacylglycerols

MCFAs are saturated FAs containing 8 - 12 carbon atoms (Papamandjaris et al., 1998). Octanoic acid (8:0, caprylic acid), decanoic acid (C10:0, capric acid) and dodecanoic acid (C12:0, lauric acid) belong to traditional MCFAs (Marten et al., 2006). Main natural sources of these FAs are coconut oil, palm kernel oil (which is not the same as palm oil) and mammalian milk (Marten et al., 2006), see Table 1.

Table 1. Main natural sources of MCFAs.
Numbers represent % of all FAs.

Fatty acid	Coconut oil	Palm kernel oil	Bovine milk	Human milk
Octanoic acid	6-10 % *	2-5 % *	1-3 % #	0,2-1 % §
Decanoic acid	5-10 % *	3-5 % *	2-4 % #	1,5-4 % §
Dodecanoic acid	39-54 % *	44-51 % *	2-5 % #	4-14 % §

* marks reference (Lemarié et al., 2016)

\# marks reference (Jensen, 2002)

§ marks references (Bahrami and Rahimi, 2005; Yuhas et al., 2006)

As MCFAs are saturated FAs, some people associate them with bad unhealthy fats. However, because of the smaller size MCFAs have different physicochemical properties and presumably a different metabolism as saturated LCFAs. Differences start with the hydrolysis of dietary medium-chain triacylglycerols (MCTs; natural or synthetically generated TAGs composed of MCFAs; in this thesis MCT refers to TAG having at least one MCFA).

The digestion of dietary fats starts in the stomach. Here TAGs are firstly partially hydrolyzed by gastric and lingual lipases. Then hydrolysis is completed by a pancreatic lipase in the small intestine. The hydrolysis process of MCTs in the gut facilitated by the pancreatic lipase is faster and more efficient than the hydrolysis of long-chain triacylglycerols (LCTs) (Bach and Babayan, 1982). Furthermore, MCFAs generated by hydrolysis are more effectively absorbed by intestinal cells than LCFAs (Bach and Babayan, 1982). After absorption most of the MCFAs are directly transferred to the portal vein for the transport to the liver (Nancy You et al., 2008). On the other hand, LCFAs are usually re-esterified into TAGs and then incorporated into chylomicrons (particles for lipid transport in organisms), which then enter the lymphatic system and finally reach the systemic circulation and liver (Bach and Babayan, 1982), see Figure 1.

MCTs are used in diets of patients that have specific lipid-metabolism related disorders. In cases of pancreatic insufficiency, where digestion and absorption of LCTs are impaired, MCTs could be well utilized (1994). In general, MCTs have been used in adults and children with disorders of lipid digestion, lipid absorption and lipid transport as well as in the deficiency of chylomicron synthesis.

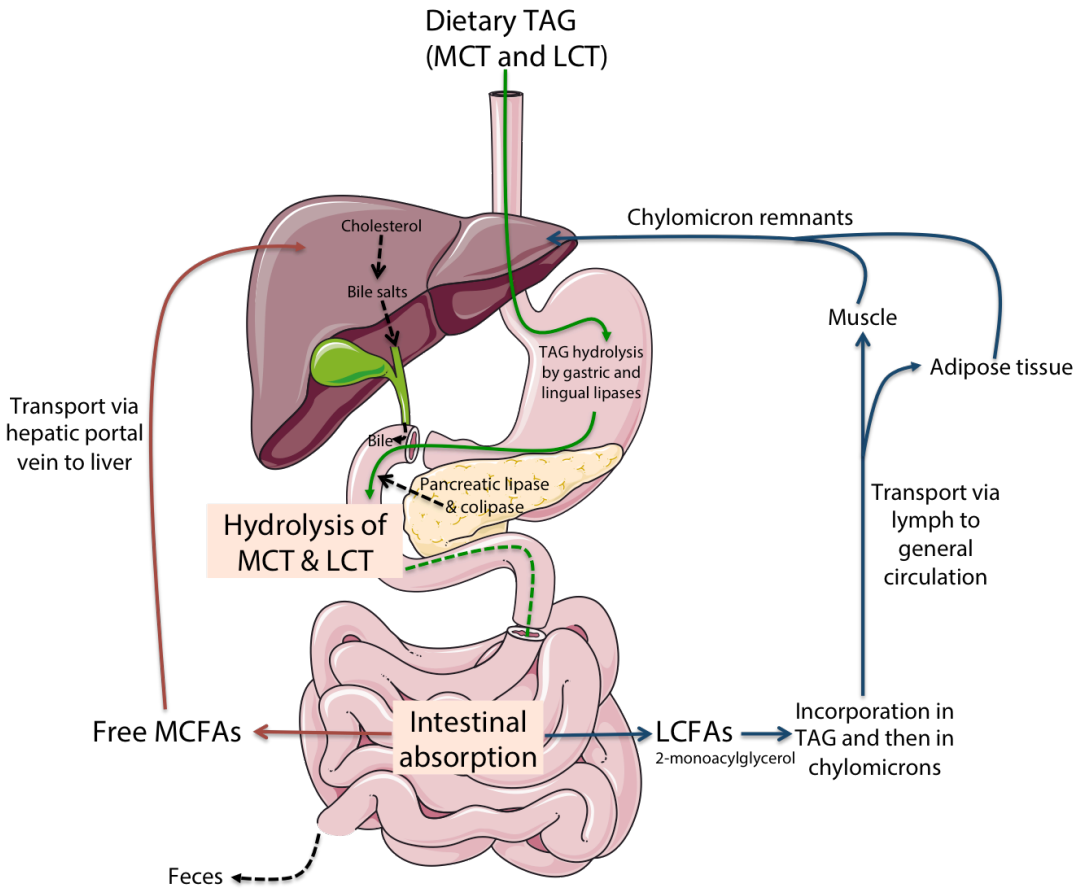

Figure 1. Digestion and absorption mechanism of dietary MCTs and LCTs.
Digestion of MCTs starts in the upper gastrointestinal tract and is mediated by gastric and lingual lipases. Both LCTs and MCTs are then finally digested in the small intestine by the action of the pancreatic lipase, which generates 2-monoacylglycerol and free fatty acids. Next intestinal absorption of FAs follows. A huge part of MCFAs is directly transferred to the liver via the portal vein in an albumin-bound form. LCFAs are re-esterified with 2-monoacylglycerol into TAGs, which are then incorporated into chylomicrons and are transferred via the lymph to the general circulation from where they reach muscle and adipose tissue. Here TAG is hydrolyzed and chylomicron remnants are formed, which are then finally taken up by the liver. Images are taken from http://www.servier.com/Powerpoint-image-bank and modified using the diagram from (Lemarié et al., 2016).

1.2. Functions of triacylglycerols

TAG consists of a glycerol backbone and three FAs attached by ester bonds (Yen et al., 2008). This neutral lipid is a highly reduced molecule and stores energy in the form of carbon-hydrogen bonds. TAG is known as the most effective molecule for energy storage in human organism (Yen et al., 2015).

The primary place for TAG synthesis and storage is the adipose tissue. TAG is also synthesized in the liver for the production and assembly of very low-density lipoproteins (VLDL) to transport neutral lipids to other tissues as well as in the

mammary gland for the production of milk fat globules (Yen et al., 2015). In the intestine TAG synthesis is related to absorption and re-esterification of digested dietary fats.

The main well-known TAG function is the storage of FAs later used for energy utilization and synthesis of membrane lipids (Yen et al., 2008). TAG is also important for the formation of the moisture barrier of the skin (Yen et al., 2008). It acts as a mechanical cushion around internal organs and within joints and has a great role in insulation (Coleman and Mashek, 2011). The TAG synthesis in cells may protect them from potentially toxic membrane-damaging effects of excess FAs and acyl-CoAs (Coleman, 2004; Yen et al., 2008).

However, there are also some negative aspects related to TAG overload in organisms. Excessive accumulation of TAG in human adipose tissue leads to obesity and is related to organ dysfunction in non-adipose tissues (Yen et al., 2008). An overload of TAG in insulin-sensitive organs other than adipose tissue, such as liver and skeletal muscle, results in an inhibition of insulin action (insulin resistance) (Friedman, 2002). The accumulation of TAG in the liver causes the non-alcoholic fatty liver disease (NAFLD) (Cohen et al., 2011; Fabbrini et al., 2010) in the heart it leads to cardiomyopathy (Pulinilkunnil et al., 2014; Sharma et al., 2004).

The main focus of the current work is the TAG synthesis from MCFAs and the catabolism of these FAs. For this reason, different steps in TAG synthesis and FA breakdown via the β-oxidation will be discussed in the upcoming chapters. But before being able to participate in any cellular lipid metabolism, FAs need to get inside the cell, and therefore FA transport will be initially discussed.

1.3. Fatty acid transport

Experiments have shown that FAs can cross the plasma membrane both by passive diffusion and by protein-mediated transport. Scientists still debate, which way of FA transport is the dominant one (Hamilton et al., 2001, 2002; Kamp et al., 2003; Schwenk et al., 2010). However, it is now believed that protein-mediated transport is the major way for cellular FA uptake especially in tissues with elevated FA metabolism, such as the heart, skeletal muscle (Wu et al., 2006), liver (Doege et al., 2006) and adipose tissue (Schaffer and Lodish, 1994). Several candidate proteins are thought to be involved in FA transport across the plasma membrane, including fatty acid translocase (FAT/CD36),

plasma membrane-associated fatty acid binding protein (FABPpm) and fatty acid transport proteins (FATPs). There are six known FATPs that belong to a class of solute carrier family 27 (SLC27). FATPs also function as very long-chain acyl-CoA synthetases (ACSVLs), see chapter 1.4.1.

Once transported inside the cells, FAs are bound to cytosolic fatty acid binding proteins (FABPs). They are thought to facilitate LCFA movement inside the cell and to protect cell membranes from a detergent-like action of FAs (Grevengoed et al., 2014). In cells such as hepatocytes, adipocytes and cardiomyocytes, where FA metabolism is very intensive, FABPs comprise 1-5% of total cytosolic proteins (Haunerland and Spener, 2004). The FABP family consists of at least nine protein-coding genes (Smathers and Petersen, 2011).

1.4. TAG synthesis

In eukaryotes TAG is synthesized by two major pathways, the glycerol phosphate and the monoacylglycerol (MAG) pathway (Takeuchi and Reue, 2009), see Figure 2. The glycerol phosphate pathway is present in most cells. In contrast, the MAG pathway is only found in enterocytes, hepatocytes and adipocytes (Yen et al., 2008). These pathways use glycerol-3-phosphate (G3P) and MAG respectively as initial acyl acceptors (Yen et al., 2015). Both pathways use fatty acyl-CoA thioesters as donors of acyl groups (Grevengoed et al., 2014). In the glycerol phosphate pathway, G3P is stepwise acylated with two acyl-CoA molecules to form lysophosphatidic acid (LPA) and subsequently phosphatidic acid (PA). PA is then dephosphorylated to generate diacylglycerol (DAG). In the final step, DAG is converted to TAG by the action of diacylglycerol acyltransferases (DGATs). In the MAG pathway, DAG is directly synthesized from MAG by acylation and is then converted to TAG. This pathway for the TAG synthesis is most prominent in the small intestine, where TAG is mainly synthesized from components of hydrolyzed dietary fats (Mansbach and Gorelick, 2007).

Separate steps in the TAG synthesis pathway will be discussed in more detail in upcoming chapters starting with acyl-CoA synthesis.

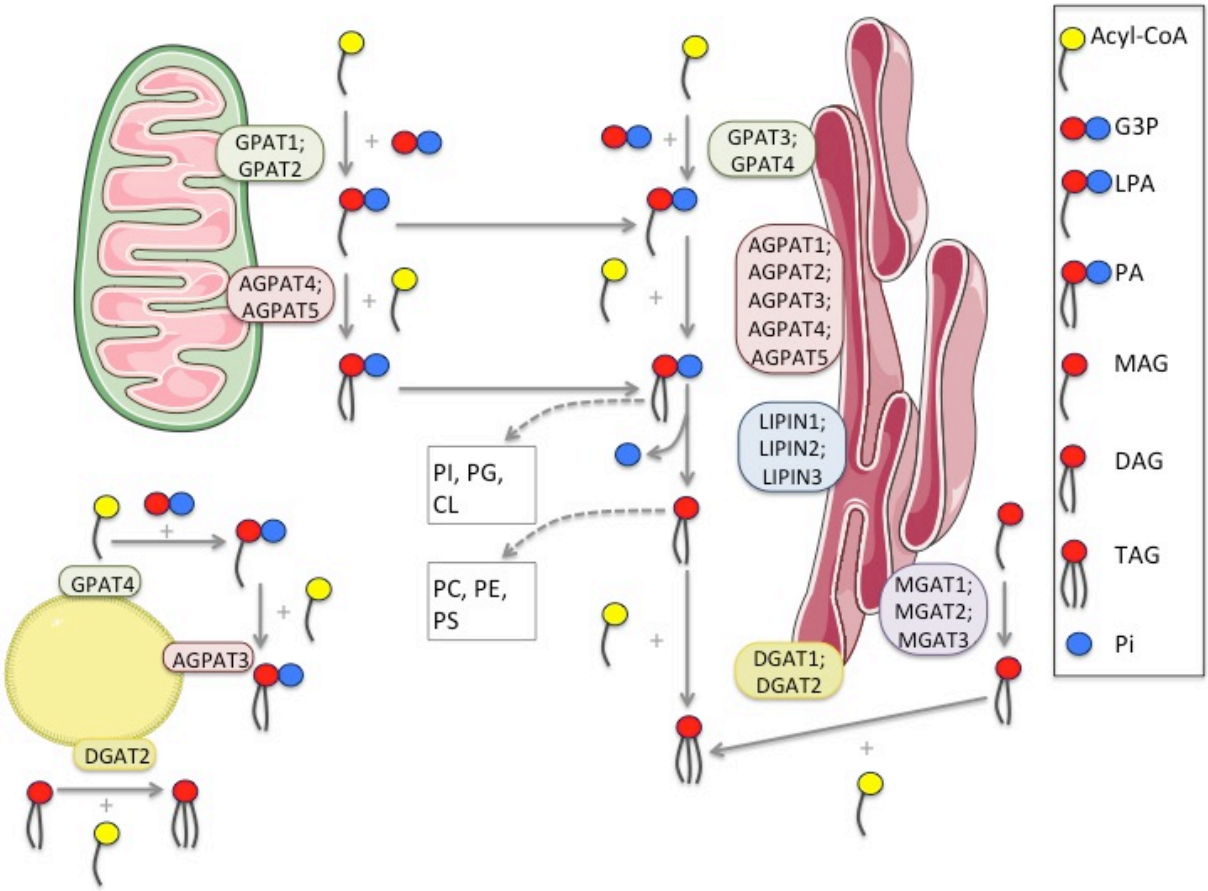

Figure 2. Pathways of TAG synthesis.
Proteins participating in *de novo* TAG synthesis can be found on mitochondria, endoplasmic reticulum (ER) and lipid droplets (LDs). The first step in TAG synthesis is the generation of LPA from acyl-CoA and G3P and is catalyzed by GPAT enzymes. The next step is the formation of PA facilitated by AGPAT (LPAAT) activity. PA is dephosphorylated by the action of lipins to form DAG. The final step in the pathway is the acylation of DAG into TAG. PA is a precursor lipid which can be used for the synthesis of other lipids such as PI, PS, PG or CL. Similarly, phospholipids such as PC and PE can be synthesized from DAG via Kennedy pathway. In liver, intestine and adipose tissue, TAG can be synthesized from MAG by the action of MGAT followed by DGAT. (PA, phosphatidic acid; DAG, diacylglycerol; TAG, triacylglycerol; MAG, monoacylglycerol; P, phosphate; LPA, lysophosphatidic acid; G3P, glycerol-3-phosphate; PI, phosphatidylinositol; PG, phosphatidylglycerol; CL, cardiolipin; PC, phosphatidylcholine; PE, phosphatidylethanolamine; PS, phosphatidylserine.) Images of mitochondria, endoplasmic reticulum and lipid droplet are from http://www.servier.com/Powerpoint-image-bank.

1.4.1. Acyl-CoA synthesis

The initial substrates for TAG synthesis are G3P and acyl-CoAs. G3P can be synthesized from the glycolysis intermediate dihydroxyacetone phosphate (DHAP), as well as from glycerol by the action of the glycerol kinase or from pyruvate via glyceroneogenesis (Kalhan et al., 2001). Acyl-CoA is synthesized from coenzyme A (CoA) and FA by proteins called acyl-CoA synthetases. In the human genome 26 acyl-CoA synthetase genes were identified (Watkins et al., 2007). Depending on the FA length of the

preferred substrate, acyl-CoA synthetases are categorized into short-chain, medium-chain, long-chain and very-long-chain acyl-CoA synthetases (Grevengoed et al., 2014). However, the FA acid chain length specificity of these enzymes is not strict and their substrate preference overlap (Watkins et al., 2007). Multiple isoforms of acyl-CoA synthetases are expressed in different cell types and are located in the membranes of different organelles and some even on the plasma membrane (Grevengoed et al., 2014). Medium-chain acyl-CoA synthetases (ACSMs) are localized in the mitochondria.

1.4.2. LPA synthesis

In the glycerol phosphate pathway, the first committed step is the acylation of *sn*-glycerol-3-phosphate at *sn1* position with acyl-CoA to form 1-acyl-*sn*-glycerol-3-phosphate, also known as lysophosphatidic acid (LPA) (Grevengoed et al., 2014). This step is catalyzed by glycerol-3-phosphate acyltransferases (GPATs). GPAT enzymes are considered to be rate limiting in the TAG synthesis (Wendel et al., 2009). Two isoforms of GPAT (GPAT1 and GPAT2) are present in the outer mitochondrial membrane, whereas other two isoforms (GPAT3 and GPAT4) reside in the endoplasmic reticulum (ER), see Figure 2 (Wendel et al., 2009). It was shown that GPAT4 is also localized to lipid droplets (LDs) (Wilfling et al., 2013).

1.4.3. PA synthesis

The second step in the glycerol phosphate pathway is the acylation of LPA at the *sn*2 position of the glycerol backbone to form PA (Yamashita et al., 2014). This reaction is catalyzed by lysophosphatidic acid acyltransferases (LPAATs). The nomenclature of these proteins is rather confusing. Originally LPAATs 1-5 were assigned to sn-1-acyl-glycerol-3-phosphate acyltransferase (AGPAT) family and were known as AGPATs 1-5. Other members of AGPAT family (AGPAT 6-11) have activities like GPAT, lysophosphatidylcholine acyltransferase (LPCAT) or lysophosphatidylethanolamine acyltransferase (LPEAT). There was a proposal to rename AGPAT enzymes based on their substrate specificities and by the order in which their cloning was reported (Shindou et al., 2009). However, this proposal did not fully take the effect and the AGPAT name rather then LPAAT still dominates in the literature.

LPAAT 1 and 2 (AGPAT 1 and 2) are the best-characterized LPAATs having a broad tissue distribution and acyl-CoA preference (Yamashita et al., 2014). They are both localized to the ER (Eberhardt et al., 1999). LPAAT 3 and 5 show relatively low enzymatic LPAAT activity compared to LPAAT2 and their role in TAG synthesis may be minimal at best (Prasad et al., 2011). It was shown that overexpressed LPAAT5 is localized to the mitochondria (Prasad et al., 2011). LPAAT4 has a relatively high expression in the brain and possesses LPAAT activity with a preference for docosahexaenoyl-CoA (DHA-CoA) (Eto et al., 2014). It was shown that LPAAT3 is localized to LDs (Wilfling et al., 2013).

PA is an important branch point in TAG synthesis as it is a precursor of CDP-diacylglycerol, which in turn is a precursor of phosphatidylglycerol (PG), phosphatidylinositol (PI), phosphatidylserine (PS) and cardiolipin (CL).

1.4.4. DAG synthesis

The third step in the glycerol phosphate pathway is the dephosphorylation of PA, which is performed by phosphatidic acid phosphatases (PAPs), also known as lipins. Three existing mammalian lipin isoforms (lipin1-3) are localized in the cytosol and translocate to the ER to hydrolyze PA in the presence of FAs or acyl-CoAs (Gomez-Muñoz et al., 1992; Takeuchi and Reue, 2009). Lipin1 was identified first and was shown to be prominently expressed in the mouse adipose tissue, skeletal muscle and testis (Péterfy et al., 2001). Lipin2 is mainly expressed in the mouse liver and brain, while lipin3 is mostly found in the gastrointestinal tract (Donkor et al., 2007).

DAG, which is synthesized in this step of glycerol phosphate pathway, is a precursor for phosphatidylcholine (PC) and phosphatidylethanolamine (PE).

1.4.5. DGAT activity - the final step in TAG synthesis

The acylation of DAG at the *sn3* position with acyl-CoA is the final step in the glycerol phosphate pathway and is catalyzed by the DGAT enzymes DGAT1 and DGAT2. Although they catalyze the same reaction, these enzymes belong to different protein families and do not share significant sequence homology (Yen et al., 2015). DGAT1 belongs to a membrane bound O-acyl transferase (MBOAT) family together with Acyl-CoA

cholesterol acyltransferases (ACATs), whereas DGAT2 belongs to a diacylglycerol acyltransferase family together with monoacylglycerol acyltransferases (MGATs) and some wax synthases (Yen et al., 2008). In humans DGAT1 is highly expressed in the small intestine, testis, adipose tissues, mammary glands, thymus, skeletal muscle, spleen, heart and skin; in mice – in the small intestine, testis, adipose tissues, mammary gland and skin (Yen et al., 2008). The highest expression of human DGAT2 is in the liver, adipose tissue, mammary gland, testis, peripheral leukocytes and heart. In the mouse DGAT2 has highest expression in the liver, testis, heart, kidney, stomach, small intestine, skeletal muscle, skin and uterus (Yen et al., 2008). The functional importance of both enzymes was shown by DGAT1 and DGAT2 knockout mouse models. DGAT2 seems to be the dominant DGAT protein as the DGAT2 knockout mice died a few hours after birth and their carcass TAG content was reduced by 90% compared to wild-type animals. Furthermore, their permeability barrier function in the skin was impaired (Stone et al., 2004). DGAT2 is localized to ER and LDs (Cao et al., 2007; Kuerschner et al., 2008; Stone et al., 2009). DGAT1 knockout mice were viable, had reduced adiposity and were resistant to diet-induced obesity (Smith et al., 2000).

An alternative, acyl-CoA independent way for TAG synthesis has been identified in the rat intestine (Lehner and Kuksis, 1993). An enzyme having transacylase activity could convert two DAG molecules into TAG and MAG, however, the gene coding for a protein with such activity has not been identified (Lehner and Kuksis, 1993; Yen et al., 2015).

1.4.6. Monoacylglycerol pathway

As mentioned before in chapter 1.4, TAG can be synthesized via the MAG pathway. The main players here are MGATs. They perform the initial step of this pathway, which is the acylation of MAG. MAG comes mainly from TAG hydrolysis. Three MGATs (MGAT1-3) were identified in humans. MGAT3 is only found in humans and higher mammals, but not in mice and other rodents (Shi and Cheng, 2009). MGATs together with DGAT2 belong to the same protein family. *In vitro* MGAT3 possesses both MGAT and DGAT activities (Brandt et al., 2016). Being on the same line DGAT1 possesses MGAT activity in a cell-free assay (Yen et al., 2005). All three MGAT proteins are localized to the ER (Cao et al., 2007; Yen and Farese, 2003; Yen et al., 2002, 2015).

The second step in the MAG pathway is the same as in the last step of the glycerol phosphate pathway, namely the acylation of DAG via DGAT enzymes, see Figure 2.

1.5. TAG mobilization

When energy demand in the organism increases, TAG is broken down in adipose tissue and generated free FAs are delivered within the bloodstream to peripheral tissues for β-oxidation and ATP production (Lass et al., 2011). The complete TAG hydrolysis is enabled by three lipases: the adipose TAG lipase (ATGL), the hormone sensitive lipase (HSL) and the monoacylglycerol lipase (MGL). These proteins sequentially hydrolyze TAG to generate glycerol and FAs.

ATGL is the major TAG hydrolase in adipose tissue. It catalyzes the initial rate-limiting step of TAG breakdown (Zimmermann et al., 2004). ATGL predominantly generates *sn*-1,3 and *sn*-2,3 DAG (Eichmann et al., 2012). This DAG is then hydrolyzed by HSL to produce MAG, which in the final step is hydrolyzed by MGL.

In mice ATGL is highly expressed in white and brown adipose tissue and to a lesser extent in the testis, heart, skeletal muscle and other tissues (Zimmermann et al., 2004). ATGL knockout mice have increased body fat mass and neutral lipids accumulate in most tissues (Haemmerle et al., 2006).

In vitro, HSL can hydrolyze various substrates such as TAG, DAG, MAG, cholesterol ester (CE), however, the highest relative activity is towards DAG (Fredrikson et al., 1981). As the name implies, HSL is regulated by hormones such as catecholamine, adrenocorticotropic hormones and glucagon that stimulate the activity of this lipase (Kraemer and Shen, 2002). The hormonal activation of HSL occurs via phosphorylation by cyclic AMP-dependent protein kinase (PKA) (Kraemer and Shen, 2002).

Under energy demand TAG hydrolysis takes place in the adipose tissue. Free FAs are released from adipocytes into the blood, bound to albumin and delivered to other tissues. FAs can also be delivered to ectopic tissues in form of TAG. Such TAGs are packed into chylomicrons in enterocytes or into VLDLs in the liver. These lipoproteins are then released into the blood stream and TAGs are hydrolyzed by endothelium-bound lipoprotein lipase (Goldberg, 1996). By hydrolysis released FAs or whole VLDLs are taken up by the cells (Goldberg, 1996; Pillutla et al., 2005). Once inside the cell, FAs are activated by forming thioesters with CoA (Aon et al., 2014), see chapter 1.4.1. Activated FAs can then be utilized for β-oxidation.

1.6. Mitochondrial β-oxidation

FAs generated by TAG hydrolysis can be used for energy production via β-oxidation. This is a process for subsequent FA degradation into acetyl-CoA molecules. Although the β-oxidation can also take place in peroxisomes, the mitochondrion is the major organelle for this type of fatty acid oxidation (Aon et al., 2014).

LCFAs activated to long-chain acyl-CoAs cannot directly enter the mitochondria as the mitochondrial membrane is impermeable for them (Houten and Wanders, 2010). This problem is solved by the carnitine shuttle. Carnitine palmitoyltransferase I (CPT1) initiates the transport by converting an acyl-CoA into the acylcarnitine (Houten and Wanders, 2010), see Figure 3. Acylcarnitine gets into mitochondrial intermembrane space and from here it is translocated across the inner mitochondrial membrane by the enzyme called carnitine-acylcarnitine translocase (CACT), which exchanges carnitines from the matrix for acylcarnitines from the intermembrane space. Once translocated, acylcarnitines are converted back to acyl-CoAs by the action of carnitine palmitoyltransferase II (CPT2), which is located on the internal face of the inner mitochondrial membrane. Generated acyl-CoA can then enter β-oxidation cycle, which consists of four reactions. After one full cycle, acyl-CoA is shortened by two carbon atoms and these two carboxy-terminal carbon atoms are released as acetyl-CoA (Houten and Wanders, 2010).

Figure 4 shows four reactions of the mitochondrial β-oxidation cycle. In the first reaction, acyl-CoA is dehydrogenated to form *trans*-2-enoyl-CoA, which has a *trans*-double bond between C2 and C3 carbon atoms, see Figure 4, (Thorpe and Kim, 1995). This step is performed by acyl-CoA dehydrogenases (ACADs). ACADs are classified into very long-chain acyl-CoA dehydrogenases (VLCADs), long-chain acyl-CoA dehydrogenases (LCADs), medium-chain acyl-CoA dehydrogenases (MCADs) and short-chain acyl-CoA dehydrogenases (SCADs) (Houten and Wanders, 2010) depending on the acyl-CoA chain length, see Figure 3.

In the second step of mitochondrial β-oxidation, the double bond of trans-2-enoyl-CoA is hydrated by the enoyl-CoA hydratase to yield L-3-hydroxy-acyl-CoA, which is subsequently dehydrogenated to 3-keto-acyl-CoA in the third step by the action of hydroxyacyl-CoA dehydrogenase (Houten and Wanders, 2010). In the final step, 3-keto-acyl-CoA is cleaved by 3-keto-acyl-thiolase to generate acetyl-CoA and acyl-CoA,

shortened by two carbon atoms, see Figure 4. Acetyl-CoA can then be used for the citric acid cycle and acyl-CoA can then enter another cycle of β-oxidation. Each β-oxidation cycle yields one flavin adenine dinucleotide ($FADH_2$) and one nicotinamide adenine dinucleotide (NADH) (Houten and Wanders, 2010). These both electron carriers can be used in electron transport chain for ATP production via the oxidative phosphorylation.

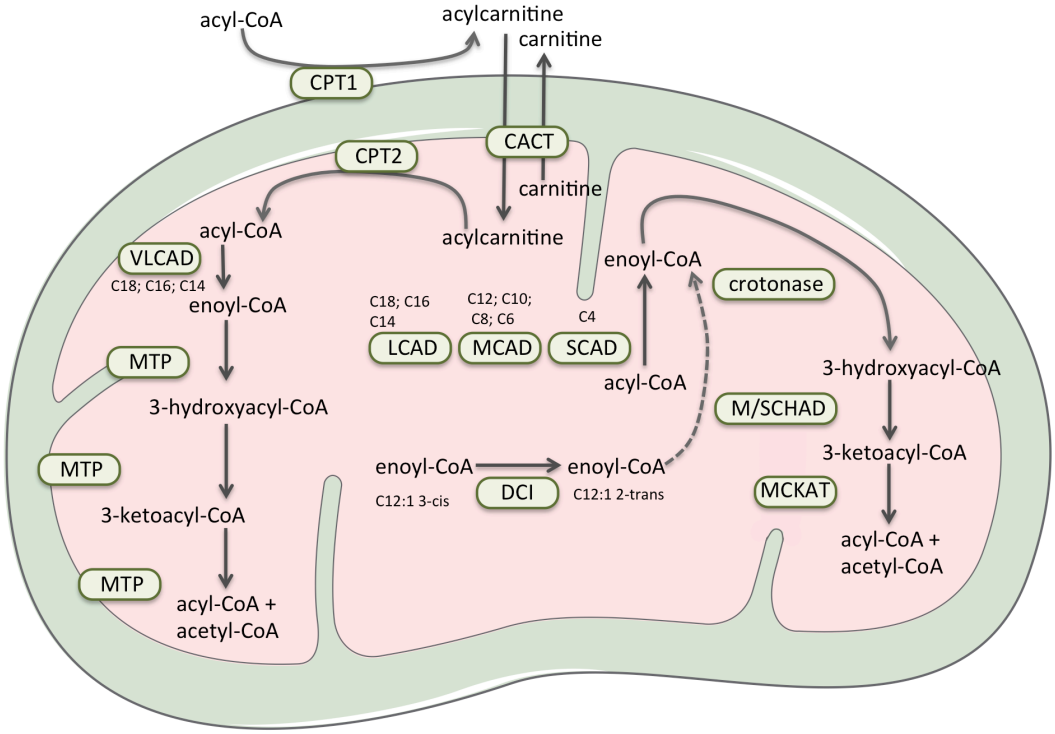

Figure 3. Mitochondrial β-oxidation.
Acyl-CoA is converted to acylcarnitine by CPT1. Afterward, acylcarnitine is transported into the mitochondria. This process is facilitated by CACT. Once inside the mitochondria acylcarnitine is converted back to acyl-CoA by CPT2. VLCAD, LCAD, MCAD, SCAD (according to acyl-CoA chain length) convert acyl-CoA to enoyl-CoA. Enoyl-CoA is hydrated to 3-hydroxyacyl-CoA by the hydratase subunit of the MTP protein (for long-chain acyl-CoAs) or by the crotonase (for medium/short-chain acyl-CoAs). MTP is a mitochondrial trifunctional protein that has hydratase, LCHAD and thiolase activities. LCHAD and M/SCHAD transform 3-hydroxyacyl-CoA to 3-ketoacyl-CoA, which is subsequently converted to acyl-CoA and acetyl-CoA by MCKAT for medium and short-chain 3-ketoacyl-CoAs and MPT thiolase subunit for long-chain 3-ketoacyl-CoAs. Acyl-CoA can then enter the second cycle of β-oxidation. The oxidation of unsaturated FAs requires the action of DCI. C4 to C18 represent the length of acyl-CoAs. (CPT1, carnitine palmitoyltransferase I; CACT, carnitine-acylcarnitine translocase; CPT2, carnitine palmitoyltransferase II; VLCAD, LCAD, MCAD, SCAD - very long, long, medium, short-chain acyl-CoA dehydrogenases; LCHAD, long-chain hydroxyacyl-CoA dehydrogenase; M/SCHAD, medium and short chain hydroxyacyl-CoA dehydrogenase, MCKAT, medium-chain 3-ketoacyl-CoA thiolase; DCI, dodecenoyl-CoA delta isomerase) Modified from (Houten and Wanders, 2010). Image of mitochondria is taken from http://www.servier.com/Powerpoint-image-bank.

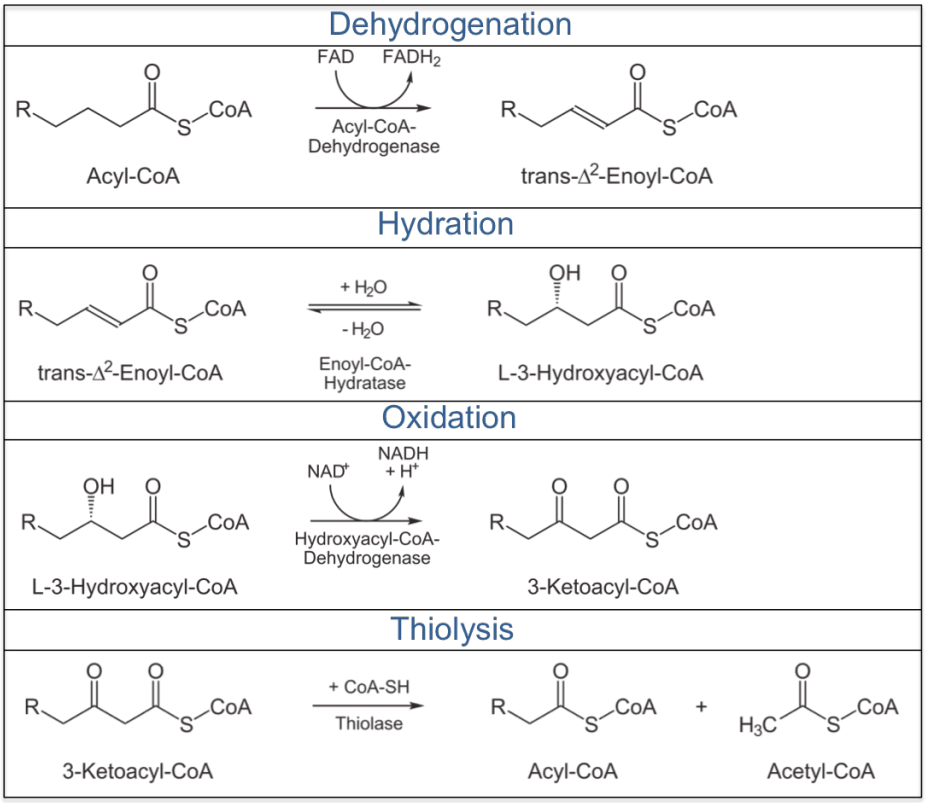

Figure 4. Reactions of β-oxidation showing substrates, products, enzymes and cofactors. Reaction schemes were taken from https://en.wikipedia.org/wiki/Beta_oxidation.

1.7. Click labeling in lipid research

In order to follow the metabolism or the cellular localization of the lipid of interest, it needs to be labeled. It is relatively easy to label proteins using different tags together with molecular cloning approach. Lipids, however, cannot be labeled genetically. Moreover, they are relatively small molecules that need small labels. For decades scientists have been using radioactive labeling with ^{14}C or ^{3}H for lipid research. Such labeling does not interfere with the structure of a lipid and is sensitive. However, work with radioactive materials is an expensive, tedious and relatively dangerous tool, which requires specific laboratories and regulations. Recently, a new method for labeling of lipids based on click chemistry/click reaction was established (Gaebler et al., 2013; Thiele et al., 2012). The click reaction is based on a [3+2] cycloaddition of terminal alkynes with azides described by Huisgen (Huisgen, 1963). Originally this reaction takes place at high temperature and pressure conditions and is not suitable for biological systems or routine laboratory work. In 2002 two independent groups found that upon

addition of Cu(I) catalyst the same reaction could take place at room temperature and mild conditions (Rostovtsev et al., 2002; Tornøe et al., 2002). Since then click reaction found the way in biological applications. In this work lipids that are labeled with terminal alkynes were used. The terminal alkyne group is very small and can be incorporated into FAs without much disturbing the structure of the hydrocarbon chain (Thiele et al., 2012). When fed with such labeled FAs, cells incorporate them in different cellular lipids. After lipid extraction, the click reaction is performed with azide coupled coumarin, which is used as the reporter dye, see Figure 5. Lipids can then be separated using thin layer chromatography (TLC) and the fluorescence of coumarin can be detected with a camera.

The click method could also be used for the labeling of proteins (Dieterich et al., 2006), carbohydrates (Hsu et al., 2007) and DNA (Salic and Mitchison, 2008); nevertheless, it has an especially high potential in lipid research.

In this thesis the click labeling method was used to investigate the metabolism of MCFAs.

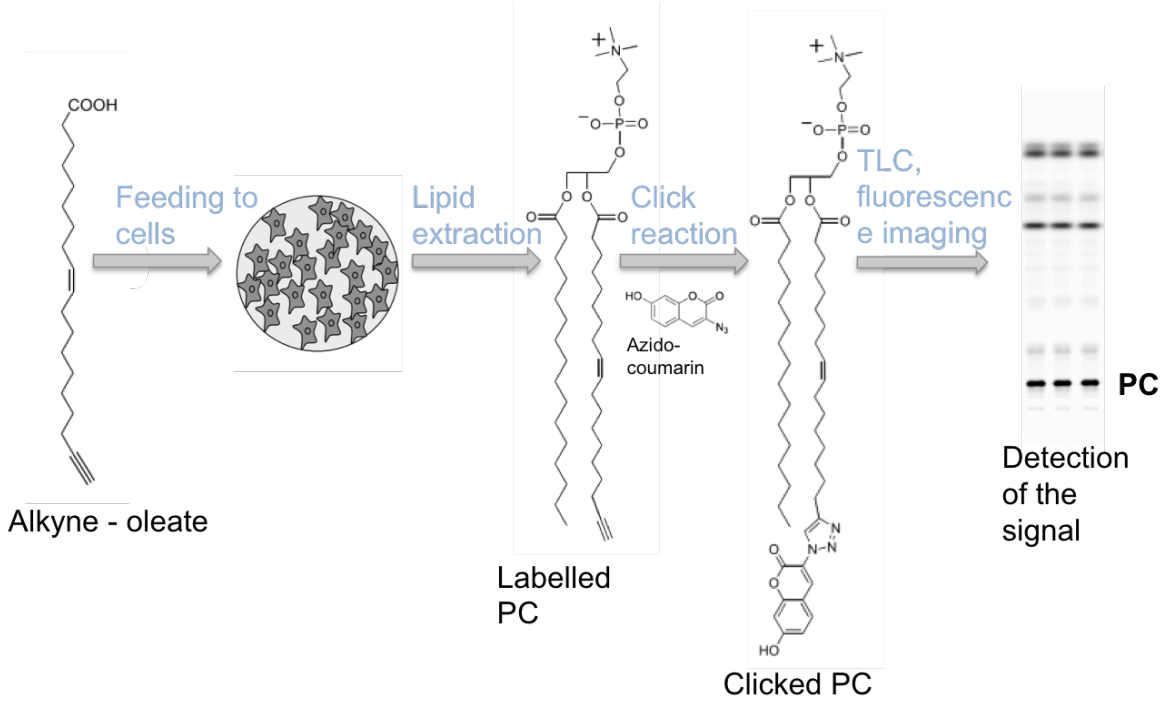

Figure 5. Schematic representation of the experiment, where lipids with terminal alkyne tags are used.

In this particular case, FA alkyne-oleate is fed to cells for a specific time period. Cells take up FAs and incorporate them in different cellular lipids, one of which is PC. After lipid extraction click reaction with azido-coumarin follows and coumarin labeled fluorescent lipids are formed. Lipids are separated using TLC. After excitation fluorescence signal is detected, which can then be quantified. Modified from (Thiele et al., 2012).

2. Aim of this study

MCFAs, which are a particular type of FAs, do contribute to the modern human diet. We ingest MCFAs with our nutrition, especially with coconut oil or milk. With the increasing occurrence of these FAs both in home made and in industrially processed food, there is a need to better understand their metabolism. The scientific literature on MCFA metabolism is relatively sparse and contradictive, nevertheless showing different trends compared to LCFA metabolism. The aim of this thesis is to contribute to a better understanding of MCFA metabolism in two cell types important for lipid metabolism, namely adipocytes and hepatocytes. To do this several key questions will be addressed:

- Which cells and organs can synthesize TAG from MCFAs?
- Do cells that are unable to synthesize MCTs can uptake MCFAs?
- What is the rate of MCFA uptake compared to LCFAs?
- Which enzymatic activities in glycerol phosphate pathway contribute to MCT synthesis?
- What are the possible mechanisms that enable MCT synthesis in differentiated 3T3-L1 cells and primary hepatocytes?

3. Materials and Methods

3.1. Materials

3.1.1. Cell lines, cell culture media and supplements

Table 2. Cell medium and supplements.

Product	Company and catalog number
DEXA (Dexamethasone)	Sigma-Aldrich Chemie GmbH; Munich, Germany, D4902
DMEM (Dulbecco's Modified Eagle Medium)	Life Technologies GmbH; Darmstadt, Germany, 31966047
DMSO (dimethyl sulfoxide)	Sigma-Aldrich Chemie GmbH; Munich, Germany, 276855
FBS (Fetal Bovine Serum)	Life Technologies GmbH; Darmstadt, Germany, 10270106
Gln (L-Glutamine (200 mM))	Life Technologies GmbH; Darmstadt, Germany, 25030123
IBMX (3-Isobutyl-1-methylxanthine)	Sigma-Aldrich Chemie GmbH; Munich, Germany, I5879
Insulin solution, human	Sigma-Aldrich Chemie GmbH; Munich, Germany, I9278
NEAA (MEM Non-Essential Amino Acids Solution (100X)	Life Technologies GmbH; Darmstadt, Germany, 11140068
Opti-MEM	Life Technologies GmbH; Darmstadt, Germany, 31985047
P/S (Penicillin-Streptomycin Solution)	Life Technologies GmbH; Darmstadt, Germany, 15140130
Rosi (Rosiglitazone)	Sigma-Aldrich Chemie GmbH; Munich, Germany, R2408
RPMI 1640	PAN Biotech GmbH; Aidenbach, Germany, P04-17500
Trypsin-EDTA (0.05%)	Life Technologies GmbH; Darmstadt, Germany, 25300062
William's E Medium	PAN Biotech GmbH; Aidenbach, Germany, P04-29510

Table 3. Cell lines and cell line specific medium conditions.

Name	Description	Medium	Medium supplements
3T3-L1	Fibroblast-like mouse embryonic cell line	DMEM	20% FBS; for differentiation additionally: • 5 µg/ml insulin, • 10 µM dexamethasone, • 0.5 mM IBMX • 5.6 µM rosiglitazone
A431	Human epidermoid carcinoma cell line	DMEM	10% FBS
Cos7	Fibroblast-like monkey kidney cell line	DMEM	10% FBS
HCT	Human colorectal carcinoma cell line	DMEM	10% FBS
Hek293	Human embryonic kidney cell line	DMEM	10% FBS
HepG2	Human liver carcinoma cell line	DMEM	10% FBS
Huh7	Human liver carcinoma cell line	RPMI	10% FBS, 10 mM HEPES, 0.1 mM NEAAs, 2 mM Gln
Primary mouse hepatocytes	Isolated from mouse liver	William's E Medium	10% FBS, 2 mM Gln, 100 U/ml Penicillin, 100 µg/ml Streptomycin

3.1.2. Chemicals, reagents and lipids

Table 4. Chemicals, reagents and lipids.

Product	Company
10:0 DAG (1,2-didecanoyl-*sn*-glycerol)	Avanti Polar Lipids Inc.; Alabaster, USA
12:0 DAG (1,2-didodecanoyl-*sn*-glycerol)	Avanti Polar Lipids Inc.; Alabaster, USA
18:0 DAG (1-2-dioleoyl-*sn*-glycerol)	Avanti Polar Lipids Inc.; Alabaster, USA
3-Azido-7-Hydroxy-Coumarin	Thiele et al., 2012
8:0 DAG (1,2-dioctanoyl-*sn*-glycerol)	Avanti Polar Lipids Inc.; Alabaster, USA
Acetic acid	VWR International GmbH; Langenfeld, Germany
Acetonitrile	VWR International GmbH; Langenfeld, Germany
Acrylamide (30% solution)	Applichem GmbH; Darmstadt, Germany
Agarose, UltraPure	Life Technologies GmbH; Darmstadt, Germany

Ammonium persulfate	Sigma-Aldrich Chemie GmbH; Munich, Germany
ATP	Applichem GmbH; Darmstadt, Germany
Bromophenol Blue	Sigma-Aldrich Chemie GmbH; Munich, Germany
BSA (Bovine serum albumin fraction V)	Applichem GmbH; Darmstadt, Germany
Chloroform ($CHCl_3$), stabilized with EtOH	VWR International GmbH; Langenfeld, Germany
CoA (Coenzyme A trilithium salt)	Sigma-Aldrich Chemie GmbH; Munich, Germany
Collagen (type I) from rat tail	Sigma-Aldrich Chemie GmbH; Munich, Germany
Collagenase NB G4 from Clostridium histolyticum	Serva GmbH; Duisburg, Germany
Cu(I)TFB (Tetrakis(acetonitrile)copper(I) tetrafluoroborate)	Sigma-Aldrich Chemie GmbH; Munich, Germany
Decanoyl coenzyme A monohydrate	Sigma-Aldrich Chemie GmbH; Munich, Germany
Decanoic acid (C10:0)	Sigma-Aldrich Chemie GmbH; Munich, Germany
Deoxycholate	Sigma-Aldrich Chemie GmbH; Munich, Germany
DL-BSA (Bovine serum albumin H2, delipidated)	Applichem GmbH; Darmstadt, Germany
EDTA	Applichem GmbH; Darmstadt, Germany
EGTA	Carl Roth GmbH; Karlsruhe, Germany
Ethanol (EtOH)	VWR International GmbH; Langenfeld, Germany
Ethyl acetate	Julius Hoesch GmbH; Düren, Germany
G3P (L-α-Glycerol phosphate bis(cyclohexylammonium) salt)	Sigma-Aldrich Chemie GmbH; Munich, Germany, G7886
Glycerol	Grüssing GmbH; Filsum, Germany
Glycine	Applichem GmbH; Darmstadt, Germany
HBSS (Hanks' Balanced Salt Solution)	Sigma-Aldrich Chemie GmbH; Munich, Germany, H1387
HCl (Hydrochloric Acid, 12M, 37%)	VWR International GmbH; Langenfeld, Germany
Heparin-Natrium-25000-ratiopharm®	Ratiopharm GmbH; Ulm, Germany
HEPES	Applichem GmbH; Darmstadt, Germany
Hexan	Sigma-Aldrich Chemie GmbH; Munich, Germany
HSLi (Hormone-sensitive lipase inhibitor)	Cayman Chemical Company; Ann Arbor, USA, CAY10499

Hünig's base (*N*,*N*-Diisopropylethylamine)	TCI Deutschland GmbH; Eschborn, Germany
Isopropanol	VWR International GmbH; Langenfeld, Germany
Ketamine	Pfizer Inc.; New York, USA
KH_2PO_4	Sigma-Aldrich Chemie GmbH; Munich, Germany
KOH (Potassium hydroxide pellets)	Merck Chemicals GmbH; Darmstadt, Germany
Lipase from porcine pancreas (from Lipase Basic Kit)	Sigma-Aldrich Chemie GmbH; Munich, Germany
Lipofectamine 2000	Life Technologies GmbH; Darmstadt, Germany
LPA (1- oleoyl -2-hydroxy-*sn*-glycero-3-phosphate)	Avanti Polar Lipids Inc.; Alabaster, USA
LPC (1-Oleoyl-sn-glycero-3-phosphocholine)	Sigma-Aldrich Chemie GmbH; Munich, Germany
MeOH (methanol)	Sigma-Aldrich Chemie GmbH; Munich, Germany
$MgCl_2$	Applichem GmbH; Darmstadt, Germany
Milk powder	Heirler-Cenovis GmbH; Radolfzell, Germany
Na_2HPO_4	Sigma-Aldrich Chemie GmbH; Munich, Germany
NaCl	Th. Geyer GmbH & Co. KG; Lohmar, Germany
NaOH (Sodium hydroxide, 1M)	Sigma-Aldrich Chemie GmbH; Munich, Germany
Oleic acid (C18:1)	Sigma-Aldrich Chemie GmbH; Munich, Germany
Oleoyl coenzyme A lithium salt	Sigma-Aldrich Chemie GmbH; Munich, Germany
PC (lecithin from soybean)	Applichem GmbH; Darmstadt, Germany
Protease Inhibitor Cocktail, cOmplete™, EDTA-free	Roche Diagnostics Deutschland GmbH; Mannheim, Germany
Rompun	Bayer AG; Leverkusen, Germany
SDS	Applichem GmbH; Darmstadt, Germany
Silica gel 60 (0.063-0.200 mm)	Merck Chemicals GmbH; Darmstadt, Germany
Sucrose (D-Sucrose)	Carl Roth GmbH; Karlsruhe, Germany
TEMED	Sigma-Aldrich Chemie GmbH; Munich, Germany
Tris	Applichem GmbH; Darmstadt, Germany
Trypan blue	Sigma-Aldrich Chemie GmbH; Munich, Germany
Tween-20	Applichem GmbH; Darmstadt, Germany
β-Mercaptoethanol	Applichem GmbH; Darmstadt, Germany

3.1.3. Buffers, solutions and kits

Table 5. Buffers, solutions and kits.

Buffer	Composition
10x PBS	27 mM KCl
	17.6 mM KH_2PO_4
	1.38 M NaCl
	101 mM Na_2HPO_4
1x Running buffer	25 mM Tris
	192 mM glycine
	0.1% (w/v) SDS
4x Separating gel buffer	1.5 M Tris-HCl pH 8.8
	0.4% (w/v) SDS
4x Stacking gel buffer	0.5 M Tris-HCl pH 6.8
	0.4% (w/v) SDS
5x Laemmli buffer	250 mM Tris-HCl pH 6.8
	40% Glycerol
	12% (w/v) SDS
	5% β-mercaptoethanol
	0.01% bromophenol blue
Blocking buffer	PBST
	5% milk
Blotting buffer	40% 1x Running buffer
	40% water
	20% methanol
BSA solution	50 mg/ml in 75 mM Tris-HCl, pH 7.4
Coupled assay buffer	75 mM Tris-HCl, pH 7.4
	10 mM $MgCl_2$
DGAT assay buffer	100 mM Tris-HCl, pH 7.4
	2 mM $MgCl_2$
	200 mM sucrose
	1 mg/ml DL-BSA
EDTA	0.5 M, pH 7.4
EGTA	100 mM, pH 7.4

GPAT assay buffer	75 mM Tris-HCl, pH 7.4 2 mM $MgCl_2$ 1 mg/ml DL-BSA
HBSS buffer **pH 7.4**	1 package of HBSS powder for 1L of buffer 0.35 g/L $NaHCO_3$
LPAAT assay buffer	60 mM Tris-HCl, pH 7.4 3 mM $MgCl_2$ 1 mg/ml DL-BSA
Lysis buffer	10 mM Tris-HCl, pH 7.4 250 mM sucrose 1x protease inhibitor
MACS buffer	50 ml HBSS buffer 2 mM EDTA 0.005 g/ml BSA
PBST	1x PBS 0.1% Tween-20
Perfusion buffer	50 ml William's E medium 0.5 mg/ml Collagenase
Pre-perfusion buffer	50 ml HBSS buffer 500 µM EGTA 50 µl Heparin (250 international units)
Wash buffer	1x PBS 2% DL-BSA

3.1.4. Nomenclature of alkyne lipids used or mentioned in this work

In this work FAs having alkyne group at the end of carbon atom chain were used. Figure 6 (chapter 4.1.1) illustrates the structure of two FAs most relevant to this work, namely C11-alkyne-FA and C19-alkyne-FA. Alkyne lipids used in this thesis are listed in Table 6. C11-alkyne-FA belongs to MCFAs and represents C10:0 FA; C19 alkyne-FA represents C18:1 FA. For simplicity C11-alkyne-FA will be called C11-FA. TAG, PC, acyl-CoA and other lipids that have C11-FA incorporated in their structure will be called C11-TAG, C11-PC, C11-CoA respectively. The same naming scheme is used for C19 and other alkyne-FAs.

Table 6. Alkyne lipids.

Lipid name in the thesis	Source
C9-alkyne-FA (C9-FA)	Synthesized in AG Thiele
C11-alkyne-FA (C11-FA)	TCI Deutschland GmbH; Eschborn, Germany
C13-alkyne-FA (C13-FA)	Synthesized in AG Thiele
C17-alkyne-FA (C17-FA)	Synthesized in AG Thiele
C19-alkyne-FA (C19-FA)	Synthesized in AG Thiele
C11-alkyne-CoA	Synthesized in AG Thiele
C19-alkyne-CoA	Synthesized in AG Thiele
sn2-C11-FA-TAG; *sn3*-C11-FA-TAG	Synthesized in AG Thiele
sn1-C19-FA-2-hydroxy-*sn*-glycero-3-phosphate (C19-LPA)	Synthesized in AG Thiele

3.1.5. Reagent systems and kits

Table 7. Reagent systems and kits.

Product	Company
BCA reagent (Pierce™ BCA Protein Assay Kit)	Thermo Fisher Scientific GmbH; Dreieich, Germany
CD11 MicroBeads, human and mouse	Miltenyi Biotec GmbH; Bergisch Gladbach, Germany
ECL reagent	Produced in AG Thiele

3.1.6. Consumables

Table 8. Consumables.

Product	Company
1.5 ml, 2 ml, 1.5 ml micro tubes	Sarstedt AG & Co; Nümbrecht, Germany
24-well plate, 12-well plate, 6-well plate, type red	Sarstedt AG & Co; Nümbrecht, Germany
Biosphere® Fil. Tip 10 µl, 200 µl, 1000 µl	Sarstedt AG & Co; Nümbrecht, Germany
Cannula BD Neoflon™ 26 GA 0.6 x 19 mm 13 ml/min	BD GmbH; Kerpen, Germany
Capillaries, glass open end	Hilgenberg GmbH; Malsfeld, Germany, 1413017
Cell culture dish ∅10 cm	Sarstedt AG & Co; Nümbrecht, Germany

Cell culture dish with gripping ring ∅ 6 cm	VWR International GmbH; Langenfeld, Germany
Cell strainer 40 µm, EASYstrainer™	Greiner Bio-One GmbH; Frickenhausen Germany
Cell strainer 70 µm, 100 µm	Corning Inc.; NY, USA
CryoPure Tube 2.0 ml	Sarstedt AG & Co; Nümbrecht, Germany
Disposable scalpels, Cutfix®	VWR International GmbH; Langenfeld, Germany
Falcon centrifuge tubes 15 ml, 50 ml	Corning Inc.; NY, USA
Fast-Read 102 disposable counting chambers	BioSigma S.r.l.; Venice, Italy
Filtropur V50 500ml 0.2 µm	Sarstedt AG & Co; Nümbrecht, Germany
Glass Beads ∅ 0.25-0.5 mm	Carl Roth GmbH; Karlsruhe, Germany
LS Columns	Miltenyi Biotec GmbH; Bergisch Gladbach, Germany
Needles 21 G, 0.8 x 120 mm	Braun Melsungen AG; Melsungen, Germany
Needles BD Microlance™ 3, 30 G 1/2", 0.3 x 13 mm	BD GmbH; Kerpen, Germany
Nitrocellulose membrane Protran BA85	GE Healthcare; Chicago, USA
PARAFILM® M	Sigma-Aldrich Chemie GmbH; Munich, Germany
Pasteur Pipets, glass, long tip	VWR International GmbH; Langenfeld, Germany
Pipette tips 10 µl, 200 µl, 1000 µl	Sarstedt AG & Co; Nümbrecht, Germany
Safe-Lock tubes 1.5 ml, 2 ml	Eppendorf Vertrieb Deutschland GmbH; Wesseling, Germany
Screw cap micro tubes, 1.5 ml	Sarstedt AG & Co; Nümbrecht, Germany
Serological pipettes 5 ml, 10 ml, 25 ml	Sarstedt AG & Co; Nümbrecht, Germany
Silica gel 60 (0.063-0.200 mm)	Merck Chemicals GmbH; Darmstadt, Germany
Syringe 1 ml, 3ml Luer-Lok™	BD GmbH; Kerpen, Germany
Syringe 1ml Sub-Q, 0.45 mm (26G) x 12.7mm	BD GmbH; Kerpen, Germany
Syringe filter, pore size 0.2 µm	GE Healthcare; Chicago, USA
T-75 flask, type red	Sarstedt AG & Co; Nümbrecht, Germany
Whatman paper (VWR®Grade 703 Blotting Paper)	VWR International GmbH; Langenfeld, Germany

3.1.7. Plasmids and antibodies

Table 9. Plasmids.

Plasmid name	Resistance	Tag	Gene	Source
Flag-hAGPAT9	Kanamycin	Myc-DDK	Human AGPAT9	Origene technologies Inc.; Rockville, USA
Flag-hDGAT2	Ampicillin	Flag	Human DGAT2	Scot Stone
pEGFP-C1	Kanamycin	EGFP	-	Monika Suchanek
plk91/pMoHA_hDGAT2wt	Ampicillin	-	Human DGAT2	Lars Kuerschner
pMoHA_ACSL1	Ampicillin	3HA	Human ACSL1	Christine Moessinger
plk24/pMoHA-hDGAT2	Ampicillin	3HA	Human DGAT2	Lars Kuerschner

Table 10. Antibodies.

Antibody	Host, Clonality	Dilution in WB	Source
Anti-ACSL1	Rabbit, polyclonal	1:500	Sigma-Aldrich*
Anti-Agpat9	Rabbit, polyclonal	1:500	Sigma-Aldrich*
Anti-Flag	Rabbit, polyclonal	1:1000	Sigma-Aldrich*
Anti-GAPDH	Mouse, monoclonal	1:3000	Novus Biologicals$
Anti-HA	Mouse, monoclonal	1:1000	Santa Cruz#
Anti-mouse	Goat, polyclonal	1:2500	Jackson &
Anti-rabbit	Goat, polyclonal	1:2500	Jackson &

* Sigma-Aldrich Chemie GmbH; Munich, Germany

$ Novus Biologicals LLC; Littleton, USA

Santa Cruz Biotechnology Inc.; Santa Cruz, USA

& Jackson ImmunoResearch Laboratories Inc.; Baltimore Pike, USA

3.1.8. Equipment

Table 11. Equipment used for experimental work.

Device	Company
Bio-Rad Mini protean	Bio-Rad Laboratories Inc.; Hercules, USA
Cell cracker	EMBL workshop; Heidelberg, Germany
Centrifuges 5417R; 5424; 5430R; 5810	Eppendorf Vertrieb Deutschland GmbH; Wesseling, Germany
CO_2 incubator CB210	Binder GmbH; Tuttlingen, Germany
CO_2 incubator Midi 40	Thermo Fisher Scientific GmbH; Dreieich, Germany
Concentrator plus	Eppendorf Vertrieb Deutschland GmbH; Wesseling, Germany
Eppendorf Research plus pipettes	Eppendorf Vertrieb Deutschland GmbH; Wesseling, Germany

LEDs, 10 x 1 W420 nm	Roithner Lasertechnik; Viena, Austria
Mini-Beadbeater-8	BioSpec Products Inc.; Bartlesville, USA
Mouse dissection instruments	Fine Science Tools GmbH; Heidelberg, Germany
NanoDrop 2000	Thermo Fisher Scientific GmbH; Dreieich, Germany
Nikon eclipse TS100 inverted microscope	Nikon GmbH; Düsseldorf, Germany
Peristaltic Pump Drive PD 5001	Heidolph Instruments GmbH & Co. KG, Schwabach, Germany
QuadroMACS separator	Miltenyi Biotec GmbH; Bergisch Gladbach, Germany
Rolera MGI plus EMCCD camera	Decon Science Tec GmbH; Hohengandern, Germany
Rotary evaporator	Heidolph Instruments GmbH & Co. KG; Schwabach, Germany
Sterile bench	Weiss Pharmatechnik GmbH; Sonnenbühl-Genkingen, Germany
Thermomixer comfort	Eppendorf Vertrieb Deutschland GmbH; Wesseling, Germany
TLC developing chamber for 20 x 20 cm plate	VWR International GmbH; Langenfeld, Germany
Vacuum controller CVC 3000	Vacuubrand GmbH & Co. KG; Wertheim, Germany
Vacuum pump, Vacusafe comfort	INTEGRA Biosciences AG; Fernwald, Germany
Vibratom VT 1200	Leica Camera AG; Wetzlar, Germany
Vortex Genie 2	Scientific Industries Inc.; Bohemia, USA
Water bath	Memmert GmbH & Co. KG; Schwabach, Germany

3.1.9. Computer programs

Table 12. Computer programs and their usage.

Program	Company/Developer	Usage
Fiji (ImageJ 2.0.0-rc-48)	Johannes Schindelin, Albert Cardona	Image processing
Microsoft Office 2011	Microsoft Corporation; Washington, USA	Text, image processing, calculations
Adobe Illustrator CS5	Adobe Systems Inc.; California, USA	Image processing
Gel-Pro Analyzer 6.0	Media Cybernetics; Washington, USA	Analysis of TLC plates, WBs
GraphPad Prism 6	GraphPad Software Inc.; La Jolla; USA	Statistics, data processing

3.2. Methods

3.2.1. Methods of cell biology

3.2.1.1. Cell culture

Cell lines used for experiments were maintained in specific medium indicated in Table 3, in a humidified incubator at 37° C and 5 % CO_2. To avoid overgrowth, dividing cells were passaged on regular basis using trypsin-EDTA.

3.2.1.2. Cell freezing and thawing

One confluent T-75 flask of cells was used to prepare 5 cryo tubes (note: 30% confluent flasks were used when freezing undifferentiated 3T3-L1 cells). Cells were trypsinized, pelleted at 500 g for 5 min and mixed with the freezing medium, containing cell type specific medium (see Table 3), 20% FBS and 10% DMSO. Then the cells were transferred to cryo tubes. The tubes were placed into a freezing container filled with isopropanol and stored at -80° C overnight. The following day the tubes were transferred into a liquid nitrogen container.
Vials containing frozen cells were thawed at room temperature (RT). The thawed cells were transferred to T-75 flasks and fresh medium was added.

3.2.1.3. Differentiation of 3T3-L1 cells

3T3-L1 cells were grown to 100% confluence. Two days later differentiation induction medium consisting of DMEM medium, 20% FBS, 5 µg/ml insulin, 10 µM DEXA, 0.5 mM IBMX and 5.6 µM rosiglitazone was added. When differentiation induction medium was introduced the so-called day 0 of differentiation was started. On day 3 of differentiation, induction medium was changed to insulin medium (DMEM medium containing 20% FBS and 5 µg/ml insulin). On day 5 insulin medium was exchanged (i.e., fresh insulin medium was added). On day 7 a normal growth medium with 20% FBS was added to the cells. Cells differentiated for 4-11 days were used for experiments.

3.2.1.4. DNA transfection with Lipofectamine 2000

Normally cells were transfected in 24-well plate format. Transfections in other plate/dish types were adjusted to this format. The day before transfection 80.000–100.000 of cells were seeded into each well of a 24-well plate. On the day of transfection cell confluence was 60–70%. For transfection 250 ng of plasmid DNA was mixed with 12.5 µl of Opti-MEM medium. Then 0.75 µl of Lipofectamine 2000 was mixed with 12.5 µl of Opti-MEM medium. Both mixtures were incubated for 5 min at RT. Then both of them were combined and incubated for further 20 min. The final DNA:Lipofectamine 2000 ratio was 1:3. In the meantime, cells were washed once with PBS and 250 µl of Opti-MEM medium was added to each well. After incubation the DNA:Lipofectamine 2000 mixture was added to cells. 24 hours after transfection the cells were used for experiments.

3.2.1.5. Feeding cells with click lipids

Cells were usually fed with 50 µM of FAs for 1.5 hours. For pulse experiments longer or shorter feeding times were used. For pulse-chase experiments cells were first fed with 50 µM of FAs for 1 hour, when click lipids were removed and chase medium was added for in experiment indicated incubation time. In competition experiments varying concentrations of FAs were used.

3.2.2. Organ slices and primary cell culture

3.2.2.1. Preparation and culture of organ slices

A mouse was anesthetized using a mixture of Ketamine and Rompun (90 mg/kg body weight and 9.4 mg/kg body weight respectively). Organs were dissected out of the animal and transferred to cold HBSS buffer. The following organs were used: liver, kidney, brain, heart, muscle, spleen, lung, small intestine, eye, pancreas and testis. 4% agarose solution in HBSS was prepared and boiled in the microwave. Afterward, it was transferred into a 50˚C water bath and kept there for approx. 10 min until the agarose reached 50˚C temperature. A 12-well plate was placed on ice and 2/3 of one well was filled with agarose. The organ was taken out of the HBSS buffer, dried with tissue, laid

down on an agarose layer and additional agarose was added to cover the organ completely. Then the next organ was handled. Gut, pancreas and testis were left in the buffer. Organs were cut with a vibratome in either 200 µm (liver, kidney, brain, heart) or 300 µm (muscle, lung, spleen) slices. For 200 µm slices, the sectioning speed was 0.4 mm/s and for 300 µm slices – 0.7 mm/s. Gut, eye, pancreas and testis were cut with a scalpel because it was not possible to cut them with the vibratome. Organ slices were transferred to wells of a 24-well plate. 0.5 ml of DMEM medium with 10% horse serum and click fatty acids was added to each well and the plate with slices was incubated for 1.5 hours at 37°C and 5% CO_2.

3.2.2.2. Isolation of primary hepatocytes

Falcons with buffers used for hepatocyte isolation were placed in the water bath at 42˚C. A mouse was first injected with 150 µl of heparin. 10 min later a mixture of Ketamine and Rompun (90 mg/kg body weight and 9.4 mg/kg body weight respectively) was injected. The anesthetic depth of the mouse was monitored by pinching its feet with anatomic forceps. The anesthetized mouse was fixed to an operation desk. The abdomen was opened and the intestine was moved to the right to make the portal vein visible. A cannula was pricked into the portal vein, the needle was discarded and the cannula was connected to a tube of the peristaltic pump, which was already turned on and pumped the pre-perfusion buffer at 4 ml/min flow rate corresponding to 52 rpm. When the liver turned yellow, the vena cava was cut and the mouse was pre-perfused with pre-perfusion buffer for further 5 min. After that pre-perfusion buffer was changed to perfusion buffer containing collagenase. The liver was perfused with perfusion buffer for further 10 min. Then the perfused liver was carefully dissected by cutting into the diaphragm and placed into a beaker glass. 45 ml of pre-warmed primary hepatocyte medium was added and liver was shaken and rubbed against the glass. The achieved suspension of liver cells was then transferred to a 50 ml falcon and centrifuged for 2 min at 8 g. The supernatant was removed, 30 ml of fresh medium was added, cells were resuspended and passed through a 100 µm cell strainer. The living cell number was counted using cell counting chambers and trypan blue. 150.000 hepatocytes were plated in every well of a 12-well plate and 200.000 or 400.000 cells were plated in every well of

a 6-well plate or 3.5 cm dish. All plates and dishes used for hepatocyte plating were coated with collagen. For hepatocyte isolation 18-20 week old male mice were used.

3.2.2.3. Coating of dishes with collagen

The plates and dishes for the primary hepatocytes have to be coated with collagen, to ensure attachment of the cells. The coating was performed under a sterile bench. 0.26 mg/ml sterile solution of collagen was added to the plates and dishes (1 ml for one well of a 12-well plate and 2 ml for one well of a 6-well plate or 6 cm dish). After 30 min the collagen solution was withdrawn and collected. It was reused up to 5 times. Dishes were opened and left for 20 min to dry in the laminar flow hood with a UV lamp turned on. Plates can be stored up to 2 weeks at RT.

3.2.2.4. Depletion of macrophages from isolated hepatocytes using MACS

For mRNA sequencing it was important to achieve a very pure hepatocyte suspension, which would be free from macrophages. For this MACS cell separation system with CD11b MicroBeads was used. These beads consist of specific antibodies, which recognize macrophages (liver macrophages are known as Kupffer cells). These antibodies are conjugated to super paramagnetic particles. Anti-CD11b antibodies specifically bind macrophages which during separation then stay in the column where a magnetic field is applied. Other cell types are collected in the flow-through. The isolation of hepatocytes was done as in chapter 3.2.2.2. However, after removal of supernatant and addition of new medium cells were centrifuged one more time for 2 min at 8 g. The supernatant was removed and 20 ml of fresh medium was added. The cells were first passed through a 70 µm cell strainer and then through a 40 µm cell strainer. Afterward, the cells were centrifuged for 2 min at 8 g, the supernatant was removed and 20 ml of fresh medium was added. The cells were counted and centrifuged for 3 min at 15 g. The supernatant was removed completely and 90 µl of MACS buffer per 10 million of cells was added. Additionally, 10 µl of CD11b MicroBeads per 10 million of cells was added. The cell suspension was mixed well and incubated in the refrigerator (4˚C) for 12 min. After incubation the cells were washed with 1 ml of MACS buffer per 10 million of cells, centrifuged for 3 min at 400 rpm and resuspended in 500 µl of MACS buffer. While cell

incubation proceeded, an LS column was placed in the magnetic field of the QuadroMACS separator. The column was prepared for separation by rinsing it with 3 ml of MACS buffer. The resuspended cell suspension was applied onto the column. The flow-through containing unlabeled cells was collected. This flow-through is the macrophage-free cell suspension as macrophages stayed in the column, because of the magnetic label and all other cell types passed through. The column was washed 3 times with 3 ml of MACS buffer. All flow-through fractions were combined together. Cells were centrifuged for 3 min at 15, resuspended in 10 ml of medium, counted and plated on coated dishes. It is worth mentioning that 70-80% of hepatocytes still stays in the column after 3 times of washing. Further washing increases cell number only by approx. 2% per 3 ml of MACS buffer.

3.2.3. Methods of protein biochemistry

3.2.3.1. SDS-polyacrylamide gel electrophoresis (SDS-PAGE) and western blot

SDS-PAGE is a technique, which enables protein separation according to their molecular weight and is not affected by protein charge or structure. The protein samples for SDS-PAGE were prepared in either 1x or 2x Laemmli Buffer followed by heating at 95˚C for 5 min. 2x Laemmli Buffer was used for protein extraction directly from the plate, where cells were grown. The Bio-Rad Mini protean system was used to cast a discontinuous gel consisting of an upper stacking gel part and a lower separating gel part. The separating gel part was made of 4x Separating gel buffer, 10-12% acrylamide, water, ammonium persulfate (from 10% stock solution) and TEMED, see Table 13. The stacking gel was made of 4x Stacking gel buffer, acrylamide, water, ammonium persulfate (from 10% stock solution) and TEMED, see Table 13. Protein samples were loaded on the gel and separated in 1x running buffer at 40 mA for 1-1.5 hours. Next, proteins from the gel were blotted onto a nitrocellulose membrane using the Bio-Rad Mini protean system and blotting buffer at 350 mA for 1 hour. After blotting the membrane was blocked for 1h at RT in blocking buffer. Then the membrane was incubated with a primary antibody, which was diluted in blocking buffer. Dilutions of primary antibodies can be found in Table 10. Incubation lasted either 1h at RT or overnight at 4˚C. After incubation the membrane was washed with PBST buffer 3x for 5 min followed by incubation with HRP-conjugated secondary antibodies for 1 hour at RT. The secondary antibodies were

diluted 1:2500 in blocking buffer. Finally, the membrane was washed with PBST buffer 2x for 10 min followed by washing with PBS 1x for 10 min. Protein detection was performed using ECL reagents and an EMCCD camera controlled by a Gel-Pro Analyzer Software.

Table 13. Amounts of components for 10 % separating gels and stacking gels.
According to this recipe two gels can be prepared.

	Separating gel	**Stacking gel**
Buffer (separating or stacking)	2.5 ml	0.75 ml
Acrylamide	3.3 ml	0.5 ml
Water	4.2 ml	1.75 ml
Ammonium persulfate	100 µl	12.5 µl
TEMED	20 µl	5 µl

3.2.3.2. Cell lysates for enzymatic assays and western blot

Cells were homogenized using a cooled EMBL cell cracker with a cylinder diameter of 8.02 mm. For all cell types, a clearance of 12 µm (8.008 mm ball) was used. Up to two confluent 10 cm dishes of Huh7 or 3T3-L1 cells or 10-30 million of primary hepatocytes were used for homogenization. The cells were washed once with PBS and scraped in 1 ml of ice-cold lysis buffer. A long 21-gauge needle was used to suck the cell suspension into the 3 ml syringe, which was then fixed to the cell cracker. 13 syringe strokes were applied to each side of the cracker. A cell homogenate was centrifuged for 10 min at 1000 g and 4°C to pellet the nuclei. Post-nuclear supernatant was transferred to a new tube and its protein concentration was measured with a NanoDrop or/and BCA Protein Assay Kit according to the manufacturer's instructions using BSA as a standard.

3.2.4. Enzymatic assays

3.2.4.1. DGAT assay

Information concerning the amount and concentration of substrates can be found in Table 14. First, DAG dissolved in $CHCl_3$ was added to a 1.5 ml tube and $CHCl_3$ was evaporated. Then 2.4 µl of the PC solution in $CHCl_3$ was added to DAG and this mixture was vortexed for 2 min. Next, 100 µl of DGAT assay buffer containing acyl-CoA and HSLi was pipetted into the tube. Afterward, 30 µg of protein (cell lysate) was added, which before was adjusted to 50 µl by adding lysis buffer. The reaction mixture (total volume 150 µl) was first vortexed and then incubated for 30 min at 30˚C while shaking at 800 rpm. Finally, the reaction was stopped by adding 800 µl of $CHCl_3$/MeOH 1/3. After this final step lipid extraction followed, see chapter 3.2.5.1.

Table 14. Substrates for enzymatic assays.

Substrate	Concentration of stock solution in mM	Concentration in assay buffer in µM	Amount taken for the assay in µl
18:0 DAG	4	200	7.5
12:0 DAG	4.38	200	6.8
10:0 DAG	5	200	6
8:0 DAG	5.8	200	5.2
PC	13	208	2.4
C19-CoA	0.5	25	7.5
C11-CoA	0.57	25	6.6
HSLi	10	10	0.15
LPA	2	10	0.75
LPC	4	10	0.38
LPA*	2	40	3
LPC*	4	40	1.5
G3P	10	500	7.5
ATP	0.5	10	4.5
CoA	29.3	390	2
C11-FA	20	200	1.5
C10 CoA	5	25	0.75
C18 CoA	5	25	0.75
alkyne-LPA	10	10	0.15
C19-FA	20	200	1.5

* used in coupled acyl-CoA LPAAT or LPCAT assay

3.2.4.1. LPAAT and LPCAT assay

Information concerning the amount and concentration of substrates can be found in Table 14. 100 µl of LPAAT/LPCAT assay buffer containing LPA or LPC, acyl-CoA and HSLi was mixed with 30 µg of protein, which before was adjusted to 50 µl by adding lysis buffer. The reaction mixture (total volume 150 µl) was first vortexed and then incubated for 30 min at 30˚C while shaking at 800 rpm. Finally, the reaction was stopped by adding 800 µl of $CHCl_3$/MeOH 1/3. After this final step lipid extraction followed, see chapter 3.2.5.1.

3.2.4.2. GPAT assay

Information concerning the amount and concentration of substrates can be found in Table 14. First 2.4 µl of the PC solution in $CHCl_3$ was added to a 1.5 ml tube and $CHCl_3$ was evaporated. Then 100 µl of the GPAT assay buffer containing G3P, acyl-CoA and HSLi was pipetted into the tube. Next, 30 µg of protein (cell lysate) was added, which before was adjusted to 50 µl by adding lysis buffer. This mixture was first vortexed and then incubated for 30 min at 30˚C while shaking at 800 rpm. Finally, the reaction was stopped by adding 800 µl of $CHCl_3$/MeOH 1/3. After this final step lipid extraction followed, see 3.2.5.1.

3.2.4.3. Coupled acyl-CoA – LPAAT/LPCAT assay

As a direct acyl-CoA assay was not compatible with the click reaction (data not shown), acyl-CoA assay was coupled with either an LPAAT or LPCAT assay. Information concerning the amount and concentration of substrates can be found in Table 14. Firstly, FAs and LPA were mixed in a 1.5 ml reaction tube and the liquid phase was evaporated. Then 13 µl of the BSA solution was added and the tube was vortexed for 2 min. Next, 100 µl of the coupled assay buffer containing CoA and ATP was pipetted into. Afterward, 200 µg of protein (cell lysate) was added, which before was adjusted to 50 µl by adding lysis buffer. Then this mixture was first vortexed and then incubated for 30 min at 30˚C while shaking at 800 rpm. Finally, the reaction was stopped by adding 800 µl of $CHCl_3$/MeOH 1/3. After this final step lipid extraction followed, see 3.2.5.1.

3.2.5. Lipid extraction and click reaction

3.2.5.1. Lipid extraction after enzymatic assays

After stopping the enzymatic reaction with $CHCl_3$/MeOH 1/3, 400 µl of water was added. The tube was vortexed and centrifuged at 20.238 g for 30 s. The lower $CHCl_3$ phase, which contained lipids, was then transferred to a new reaction tube. Lipids from the reaction tube were extracted a second time. For this 200 µl of $CHCl_3$ was added to the reaction tube. The tube was first vortexed and then centrifuged at 20.238 g for 30 s. The lower $CHCl_3$ phase was combined with the $CHCl_3$ phase from the first extraction. Lipids were used for the click reaction.

3.2.5.2. Lipid extraction from organ slices

When the incubation time was over (see 3.2.2.1) the medium was discarded and organ slices were washed once with 2% delipidated BSA (DL-BSA) in PBS and once only with PBS. 1.5 ml screw cap micro tubes were filled with glass beads to approx. 200 µl mark and 1 ml of $CHCl_3$/MeOH 1/1 was added to each tube. Each slice was added to a prepared tube. The tubes were tightly screwed and bead-beated for 4 min at max speed. Afterward, the tubes were centrifuged at 20.238 g for 30 s. The liquid phase was transferred to a new 2 ml tube and 800 µl of water was added. Samples were vortexed and centrifuged again at 20.238 g for 30 s. The lower $CHCl_3$ phase was transferred to a new 1.5 ml tube. Then the usual click procedure followed, see chapter 3.2.5.5.

3.2.5.3. Lipid extraction from cells grown in plates

Cells were grown in 6-well, 12-well or 24-well plates and in 3.5 cm or 6 cm dishes. After feeding the cells with click lipids the medium was removed and the cells were washed once with wash buffer and once with PBS. After washing 800 µl of the MeOH/ $CHCl_3$ 3/1 mixture was added to each well of either plate type and was incubated for 1 min by swinging the plate. The mixture from each well was transferred to a separate tube. 400 µl of water and 150 µl of $CHCl_3$ were added. The tube was first vortexed and then centrifuged at 20.238 g for 30 s. The lower $CHCl_3$ phase containing lipids was transferred to the new reaction tube. Lipids were either stored or used for the click reaction, see chapter 3.2.5.5.

3.2.5.4. Lipid extraction from the medium

In FA uptake experiments a lipid extraction was performed from the medium in which cells were incubated for in experiment indicated time and with indicated amount of FAs. After incubation time was over, the medium with FAs was collected and cells were subjected to lipid extraction, see 3.2.5.3. 50 µl of this collected medium was transferred to the reaction tube used for lipid extraction. 800 µl MeOH/ $CHCl_3$ 3/1 mixture, 400 µl of 1% acetic acid and 150 µl of $CHCl_3$ were added to the medium. The tube was first vortexed and then centrifuged at 20.238 g for 30 s. The lower $CHCl_3$ phase containing lipids was transferred to a new reaction tube. Lipids were directly used for the click reaction, see 3.2.5.5.

3.2.5.5. Click reaction

The $CHCl_3$ phase, which was transferred to a new tube after lipid extraction (see 3.2.5.1 - 3.2.5.4), was first dried in a vacuum concentrator, then 7 µl of $CHCl_3$ was added and the tube was vortexed for 5 min. In the meantime, the click reaction mixture was prepared by mixing 10 µl of the 3-azido-7-hydroxycoumarin solution (2mg/ml) with 250 µl of the Cu(I)TFB solution (10 mM) in acetonitrile and 850 µl of ethanol. 30 µl of the click mixture was added to the previously prepared tube containing lipids and $CHCl_3$. The mixture was briefly vortexed, centrifuged and incubated at 43˚C for 2.5 hours or overnight. A higher concentration click reaction mixture was used while working with coupled CoA synthesis assays as the molar amount of alkyne-FAs used in these assays was very high, see chapter 3.2.4.3 and Table 14.

3.2.5.6. Lipid separation by thin layer chromatography (TLC)

After the click reaction, the tube was centrifuged to collect the liquid, which was condensed under the cap. Then the tube was vortexed for 10 min. In the meantime, the TLC plate was prepared. A line was drawn at 1.5 cm distance from the bottom of the TLC plate and spaces for lipid loading were marked. The clicked lipids were loaded on the TLC plate using glass capillaries. The plate was placed in a TLC developing chamber, which was filled with solution I (chloroform/methanol/water/acetic acid 65/25/4/1), and kept there until the front line of the solvent reached 6.5-9.5 cm height measured

from the bottom. The plate was taken out, dried and placed in the second TLC developing chamber with solution II (hexane/ethyl acetate 1/1). It was kept there until the front line reached 1 cm mark when measured from the top of the plate. Eventually, the plate was taken out, dried, soaked in 4% Hünig's base solution in hexane and dried again. After this procedure TLC plate was ready for the lipid detection.

3.2.5.7. Detection and quantification of click labeled lipids

Lipids were detected and quantified using a system described in Thiele et al., 2012. The LED light filtered through a colored glass was used for excitation of clicked lipids. Images were acquired with an EMCCD camera in two channels equipped with different filters. Filter 494/20 was used in a channel for detection of the coumarin fluorescence and filter 572/28 was used in a channel for detection of background fluorescence. Images were acquired and quantified using a Gel-Pro Analyzer software.

3.2.6. Methods of lipid biochemistry

3.2.6.1. Alkaline hydrolysis

Alkaline hydrolysis was used to break down ester bonds of lipids to identify if lipids having ester bonds were present in samples of interest. This technique was applied to unknown lipids found in the medium (4.5.2.6). After lipid extraction (3.2.5.4) The $CHCl_3$ phase was divided into two parts. One part was used for hydrolysis and the other one for control. $CHCl_3$ was evaporated from both parts. Further steps were performed only with the part used for hydrolysis. 300 µl of MeOH/EtOH 1/1 and 30 µl of 2 M KOH was added. The tube was flushed with argon, sealed with parafilm and incubated for 2 hours at 60˚C under gentle agitation. After that, solvents were evaporated and 100 µl of 1 M HCl along with 300 µl of $CHCl_3$ were added. The mixture was vortexed, centrifuged at 20.238 g for 2 min. The $CHCl_3$ phase was transferred to a new tube and $CHCl_3$ was evaporated. After this click reaction was performed with both hydrolyzed lipids and control lipids.

3.2.6.2. Separation of neutral lipids from phospholipids

Before performing TAG hydrolysis with a pancreatic lipase (see 3.2.6.3) neutral lipids were separated from other lipid classes. First, a cellular lipid extract, which was devoted for hydrolysis, was mixed with 200 µl of $CHCl_3$ in a tube. This mixture was sonicated for 5 min. Then 500 µl of hexane/ethyl acetate 5/1 was added. A small column made of a Pasteur pipette and a silica gel was washed with hexane/ethyl acetate 5/1. Cellular lipids were added to the column. The column was washed with 5 ml of hexane/ethyl acetate 5/1 and all the flow-through containing neutral lipids was collected. Polar lipids that remained in the column were washed out with 5 ml of MeOH/$CHCl_3$/H_2O 65/35/8 and then the usual lipid extraction followed. The hexane/ethyl acetate solution was evaporated from the neutral lipid fraction with a rotary evaporator. The dried neutral lipids were ready for hydrolysis with a pancreatic lipase.

3.2.6.3. TAG hydrolysis with a pancreatic lipase

For TAG hydrolysis 600 µl of 1 mM pH 8 Tris-HCl was added to the dried lipids. This mixture was sonicated for 3 min followed by the addition of 100 µl of 22 % $CaCl_3$ and 125 µl of 0.1 % deoxycholate. The tube was incubated at 40˚C for one minute. 2 mg of the pancreatic lipase dissolved in 200 µl of water was added and the reaction mixture was vortexed for 3 min. The reaction was terminated with 400 µl of 1 M acetic acid. After that 500 µl of MeOH/ $CHCl_3$ 3/1 was added and the reaction tube was vortexed and centrifuged at 20.238 g for 30 s. The $CHCl_3$ phase was transferred to a new tube. The second extraction with 200 µl $CHCl_3$ followed. Both $CHCl_3$ phases were combined and then washed with 500 µl of water. $CHCl_3$ was evaporated and the click reaction was performed.

3.2.7. Statistical analysis

The data are presented as a mean ±/+ standard deviation (SD). The statistical analysis was performed with GraphPad Prism6 program. For comparison of two groups, unpaired t-test was used. For more groups, one-way ANOVA analysis was applied. * stands for $p \leq 0.05$; ** $p \leq 0.01$; *** $p \leq 0.001$

4. Results

4.1. Metabolism of MCFAs and LCFAs in different cell lines and mouse organs

4.1.1. Metabolism of different chain length FAs in 3T3-L1 adipocytes and Huh7 cells

In Thiele et al., 2012 it was shown that two distinct cell lines metabolize FAs of different carbon chain length in a different manner. This interesting finding triggered the research described in this thesis. In experiments of this work alkyne-FAs that can be labeled with a fluorescent dye by applying click reaction (1.7) were used. The structures of two main FAs used in this thesis can be found in Figure 6. It is assumed that C9 alkyne-FA represents C8:0 natural fatty acid octanoate; C11 represents C10:0 FA decanoate (C10); C13 – C12:0 FA dodecanoate; C17 – C16:0 FA palmitate and C19 – C18:1 FA oleate (C18). The detailed comparisons between all natural and alkyne-FAs was not done but in Thiele et al., 2012 it was shown that C19-alkyne-FA in many aspects resembled oleate.

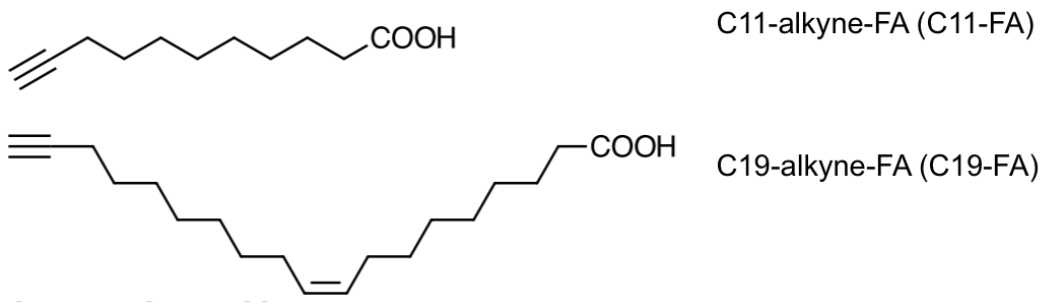

Figure 6. Structures of C11-FA and C19-FA.

As illustrated in Figure 7A, lanes 3-8, differentiated 3T3-L1 adipocytes incorporated FAs having seven or more carbon atoms into cellular lipids, while Huh7 cells, which represent a liver carcinoma cell line, only incorporated FAs having not less than 13 carbon atoms (Figure 7B, lanes 6-8). At first it was considered that this is an organ-specific behavior. For later experiments C11 MCFA was chosen, which was incorporated into cellular lipids by differentiated 3T3-L1 cells (Figure 7A, lane 5), but not by Huh7

cells (Figure 7B, lane 5). To compare C11-FA metabolism with LCFA metabolism, the C19-FA representing oleate was taken. Next step was to find out which organs can metabolize C11 and C19-FAs.

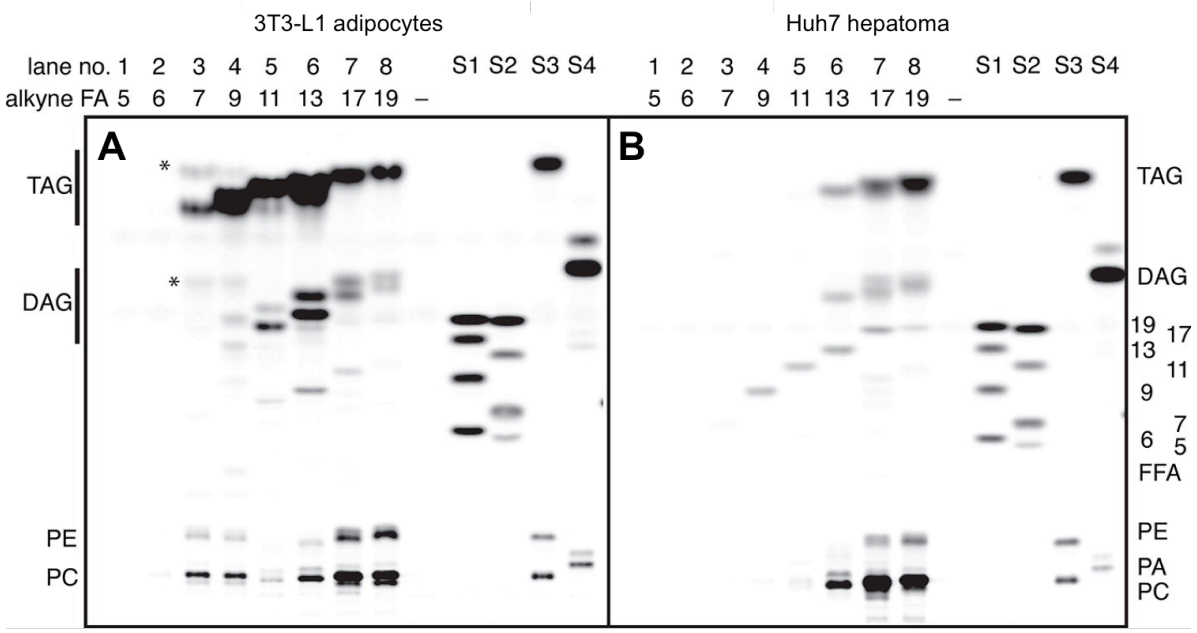

Figure 7. Metabolism of different chain length FAs in 3T3-L1 adipocytes and Huh7 hepatoma cells.
3T3-L1 cells (A) were grown in 3.5 cm dishes and Huh7 cells (B) were grown in 6 cm dishes. Both cell types were supplemented for 1 hour with 50 µM of different chain length FAs. The cells were incubated and washed. Lipids were extracted from the cells and the click reaction was performed. Finally, lipids were separated on TLC plate and fluorescence was detected by fluorescence imaging. Numbers on the top of the image at the line "alkyne FA" indicate the total carbon atom chain length of FA. 5–17 are saturated FAs (except for the ω-alkyne group), 19 is alkyne oleate. S1-S4 are synthetically synthesized standards as indicated on the right side of the image. The image was taken from Thiele et al., 2012, figure 6 panels A and B.

4.1.2. C11-FA and C19-FA metabolism in different mouse organs

Different organs were dissected from a mouse and organ slices were prepared. These slices were incubated with a mixture of C11-FA and C19-FA to compare their ability to incorporate these FAs into TAG. From Figure 8A (lane 1 and 4) it can be seen that liver and gut most effectively incorporated C11-FA in TAG. In these organs more than 50% of the detected lipid signal was assigned to C11-TAG (Figure 8B). The C11-TAG signal here was stronger than the C19-TAG signal (Figure 8A, lanes 1 and 4). A lower amount of C11-TAG was also detected in the kidney, testis and muscle (Figure 8A lanes 2, 3 and 7, B). Although the muscle, in general, had a very low signal in all lipid classes (Figure 8A, lane 7), most of it could be assigned to C11-TAG. The brain, lung, spleen and eye were most ineffective in incorporating C11-FA into TAG (under 5%, Figure 8B). The fact that liver could very efficiently synthesize C11-TAG was unexpected as previous data from Huh7 cells showed that liver cells do not incorporate C11-FA into TAG (Figure 7B). A plausible explanation would be that the hepatoma cell line lost the ability to metabolize C11-FA. It is well described in the literature that the hepatoma cell lines differ from primary cells and that they have lost some metabolic functions (Castell et al., 2006). Next, it was analyzed if other cancer and non-cancer cell lines that are often used in cell culture were able to metabolize C11-FA.

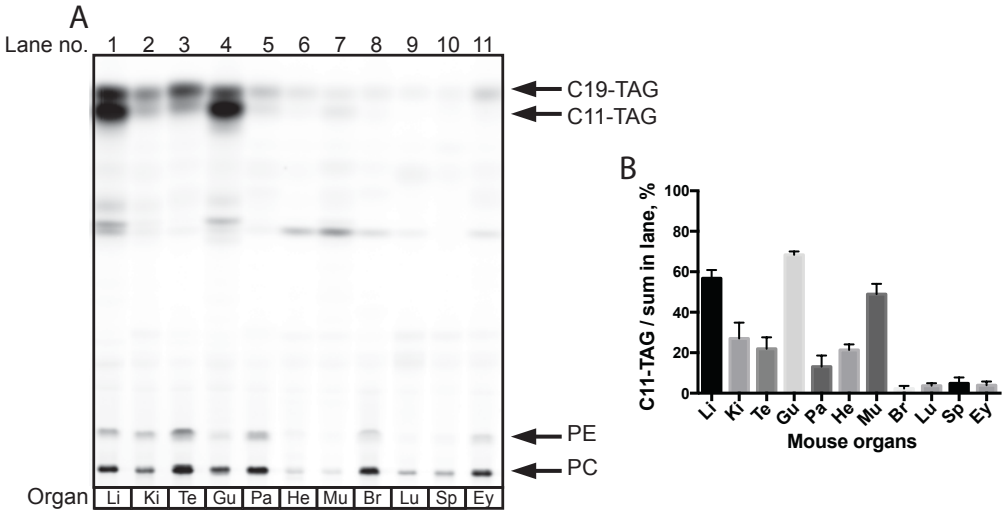

Figure 8. Metabolism of C11 and C19-FAs in slices of different mouse organs.
(A) Different organs were dissected from a mouse and organ slices were prepared. A mix of 50 µM C11 and 50 µM C19-FAs was added to the slices for 1.5 hours. The organ slices were washed and lipids were extracted from the slices. The click reaction was performed, lipids were separated on a TLC plate and fluorescence was detected by fluorescence imaging. Abbreviations: Li – liver, Ki – kidney, Te – testis, Gu – gut, Pa – pancreas, He – heart, Mu – muscle, Br – brain, Lu – lung, Sp – spleen, Ey – eye. (B) Quantification of data in panel A. Values represent the fluorescence intensity of C11-TAG divided by sum fluorescence intensity of C11-TAG, C19-TAG, PE and PC. Data represent mean +SD, n=3.

4.1.3. C11 and C19-FA metabolism in different cell lines

The ability to incorporate C11-FA into TAG was examined in several cell lines often used in cell culture as well as in primary hepatocytes. As shown in figure 9, all cell lines could incorporate C19-FA into TAG. However, only primary hepatocytes could synthesize C11-TAG (figure 9, lane 16). It should be mentioned that undifferentiated 3T3-L1 cells could not incorporate C11-FA in TAG (Figure 9, lane 10), whereas, differentiated 3T3-L1 cells could (Figure 7A). Therefore it was examined in which step of differentiation 3T3-L1 cells gained the function to synthesize C11-TAG.

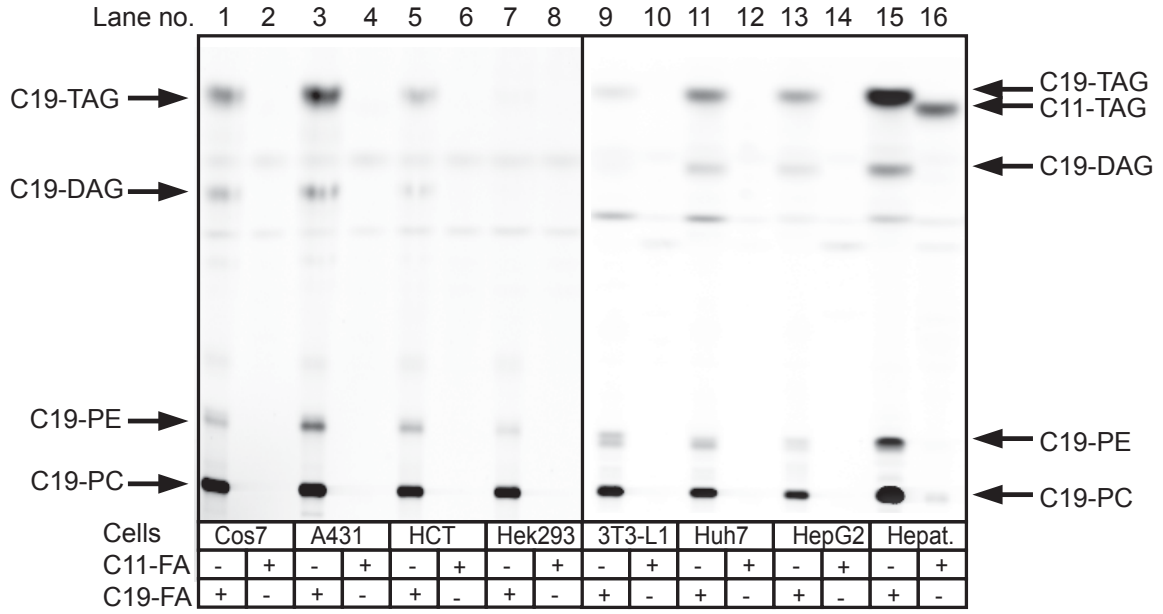

Figure 9. C11 and C19-FA metabolism in different cell lines.
Different cell lines were grown in 24-well plates until confluence. 300.000 of primary hepatocytes were plated on 6 cm dishes coated with collagen. 50 μM of either C11 or C19-FA was added to cells for 1.5 hours. The cells were washed and lipids were extracted from the cells. The click reaction was performed, lipids were separated on a TLC plate and fluorescence was detected by fluorescence imaging. The description of different cell lines can be found in Table 3. Hepat. stands for mouse primary hepatocytes. The different lipid classes in which FAs were incorporated are indicated at both sides of the image.

4.2. C11 and C19-FA metabolism in differentiating 3T3-L1 cells

On day 0 differentiation medium was added to 3T3-L1 cells. At day 1, 2, 3, 4 and 11 differentiating cells were incubated with C11 and C19-FAs. As evident from Figure 10A lane 3 and Figure 10B, cells start to incorporate C11-FA into TAG at day 2 of

differentiation. To determine this point in time more precisely, a second experiment was conducted where cells were differentiated for up to 72 hours. As indicated in Figure 10C and D, 3T3-L1 cells gain the function to metabolize C11-FA between the 36th and 42nd hour after the start of differentiation. C19-TAG was present in all conditions, where C19-FA was fed to cells (Figure 10A and C). Following the subject, the process of dedifferentiation of primary hepatocytes was later analyzed.

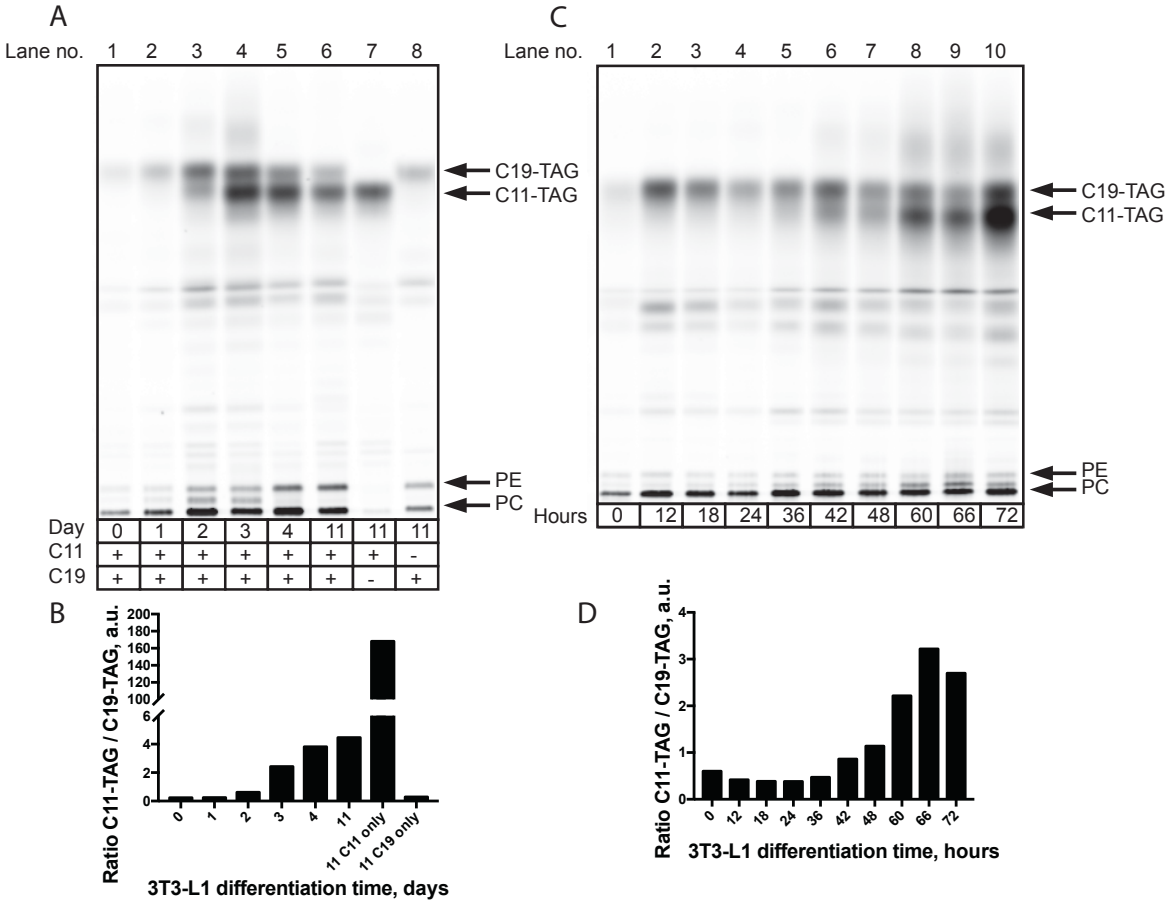

Figure 10. Differentiation of 3T3-L1 cells in days and hours.
(A, C) 3T3-L1 cells, grown on gelatin-coated 6-well plates, were differentiated for different periods of time. At indicated time point of differentiation, a mix of 50 µM of C11 and 50 µM C19-FAs was added to the cells for 1 hour. On day 11 the cells were also fed with single C11 or C19-FAs (panel A lanes 7-8). The cells were washed and lipids were extracted from the cells. The click reaction was performed, lipids were separated on a TLC plate and fluorescence was detected by a fluorescence imaging. Day 0 represents control cells without differentiation medium. The different lipid classes, in which FAs were incorporated, are indicated on the right side of the images. (B, D) Quantifications of ratio C11-TAG to C19-TAG for panels A and C correspondingly. The data are taken from laboratory rotation report of Marlene Buller, 2015.

4.3. C11 and C19-FA metabolism in dedifferentiating hepatocytes

It is well described in the literature that freshly isolated primary hepatocytes start to dedifferentiate rapidly and lose hepatocyte-specific functions when maintained in 2D cell culture (Bell et al., 2016; Elaut et al., 2006; Rowe et al., 2013). This raises the question if hepatocytes are able to metabolize C11-FA during dedifferentiation. To test this, freshly isolated hepatocytes were kept in 2D cell culture for an indicated time period. Then fresh and older cells were fed with either C11 or C19-FAs. As can be seen in Figure 11A lanes 1-5, the cells lost a great deal of their potential to synthesize C11-TAG already on day 1 after isolation (lane 2). However, C19 metabolism was nearly unchanged (Figure 11A lanes 6-10). An hourly dedifferentiation experiment was performed to determine, when dedifferentiating hepatocytes lose the potential to incorporate C11-FA into TAG. Figure 11B shows that the ability to incorporate C11-FA into TAG was greatly diminished in the time period between 8 and 18 hours, whereas the amount of C19-TAG remained relatively constant.

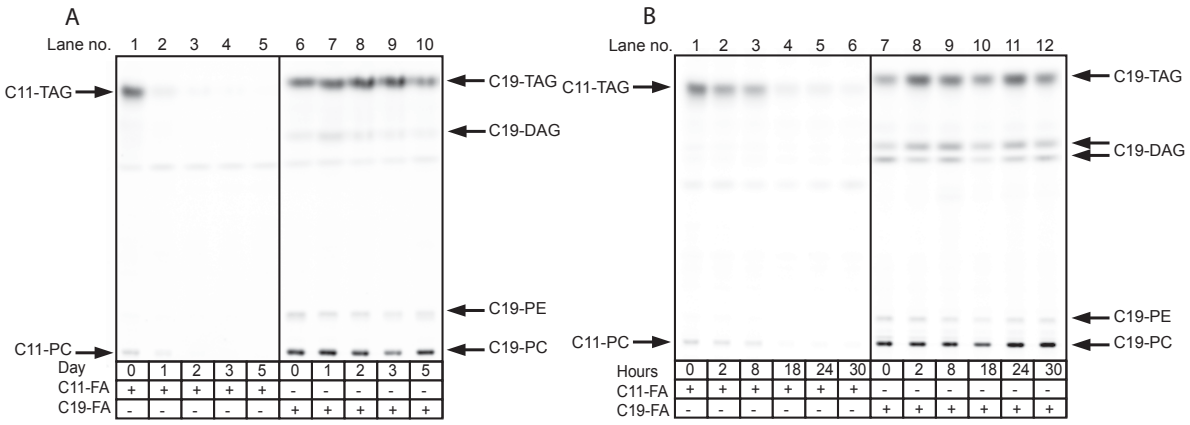

Figure 11. C11 and C19-FA metabolism in dedifferentiating primary mouse hepatocytes.
Panels A and B represent cells dedifferentiated from 0 to 5 days and from 0 to 30 hours, respectively. Primary mouse hepatocytes were isolated from liver and plated on collagen coated 6-well dishes (A) or 6 cm dishes (B). 400.000 cells were used per well (A) or 80.000 cells were used per dish (B). At indicated time points, the medium with 50 µM of either C11 or C19-FA was added to the cells for 1.5 hours. The cells were washed and lipids were extracted from the cells. A click reaction was performed, lipids were separated on a TLC plate and fluorescence was detected by a fluorescence imaging. (A) Day 0 represents the cells where FAs were added on the same day of hepatocyte isolation. (B) Hour 0 represents cells where FAs were added after cell attachment to dishes, i.e. 2 hours after plating. The same rule is applied for other time points. The different lipid classes in which FAs were incorporated are indicated at both sides of the images.

Both in differentiating 3T3-L1 cells and dedifferentiating hepatocytes complex processes presumably take place enabling or disabling C11-TAG synthesis. To better predict and understand mechanisms responsible for these changes it was decided to perform deep mRNA sequencing both with 3T3-L1 cells and primary mouse

hepatocytes.

4.4. mRNA sequencing data

3T3-L1 cells were differentiated for 0, 12, 18, 24, 36, 48 and 60 hours. RNA was isolated from these cells at indicated time points and sequencing was performed. Similarly, primary mouse hepatocytes were kept in cell culture, after isolation and adherence, for 0, 2, 8 and 18 hours. RNA from hepatocytes was likewise isolated and sequencing was done. In both cell lines it was looked at mRNA data for genes coding proteins participating in FA and TAG metabolism. Table 15 summarizes the results of mRNA sequencing. The expression data of genes coding proteins that participate in different processes related to FA and TAG metabolism are grouped and presented for each cell line and specific time point. Table 15 also includes some house keeping genes and quality control genes specific for each cell line.

The sequencing data are rather complex and expression of none of the genes important for FA and TAG metabolism goes drastically down to a negligible amount. So this data do not directly allow us to identify the candidate gene/protein responsible for the differences in C11 metabolism, which was observed in 4.2 and 4.3, but they can help to support or deny certain hypothesis.

4.5. Deeper analysis of the pathway from FA uptake to TAG synthesis

The pathway from free FAs outside the cell to TAG synthesis inside the cell involves a few following steps (Figure 26C). First, FAs need to enter the cell. As discussed in the introduction chapter 1.3 there are a few possible mechanisms for FA entry into the cell. Then, the transport inside the cell and the acyl-CoA synthesis follows. Finally, acyl-CoA enters the TAG synthesis pathway. Additionally, some regulatory mechanisms could be involved, such as channeling specific FAs towards distinct cellular processes like mitochondrial β-oxidation. A closer look at different points of this pathway was taken in order to identify the section, where this pathway fails and in such a way TAG synthesis from MCFAs is disturbed. First, FA entry into the cell was analyzed.

Table 15. mRNA sequencing data for genes participating in FA and TAG metabolism in primary hepatocytes and 3T3-L1 cells.

Data is presented as gene read counts. mRNA sequencing and data analysis was performed by Kristian Händler, Thomas Ulas, Susanne Schmidt, Stefanie Herresthal and Kathrin Klee (AG Schultze).

	Hepatocyte dedifferentiation						3T3-L1 differentiation						
Gene no.	Gene Symbol	0h	2h	8h	18h	Gene Symbol	0h	12h	18h	24h	36h	48h	60h
	FA uptake at plasma membrane												
1	CD36	690.5	597.7	259.1	187.5	Cd36	167.4	112.6	90.5	133.3	789.2	1416.5	3787.7
2	SR-B1	1624.6	1156.5	507.0	464.7	SR-B1	435.4	87.1	109.7	162.4	296.4	305.4	1006.1
3	Got2 (FABPpm)	4203.48	3134.9	2160.36	1719.04	Got2	1206.37	1339.16	1175.1	1066.57	986.63	784.902	732.775
	FA uptake/CoA synthesis												
4	FATP1	16.3	8.7	6.7	16.3	FATP1	193.1	40.3	28.8	44.8	126.4	238.0	547.4
5	FATP2	14149.7	9608.3	3707.0	874.2	FATP2	1.0	1.0	1.0	1.0	1.0	1.0	1.0
6	FATP4	213.4	145.1	222.4	349.5	FATP4	225.3	265.4	285.2	287.0	328.3	315.5	433.7
7	FATP5	7201.7	5371.0	2656.3	1148.9	FATP5	1.0	1.0	1.0	1.0	1.1	1.0	1.0
						FATP3	7.24307	19.7177	34.2795	26.1984	31.3216	39.3644	38.936
	Cytoplasmic FA binding proteins												
8	Fabp1	29919.0	27803.7	13052.2	2468.9								
9	Fabp2	1573.2	1314.6	781.6	360.6								
10	Fabp4	146.9	191.7	174.6	149.1	Fabp4	368.6	330.3	327.7	504.2	8740.4	23621.0	54505.7
11	Fabp5	285.0	296.7	686.0	1567.4	Fabp5	471.6	327.8	479.9	613.0	5221.8	9462.4	12823.9
12	Fabp7	7.5	11.9	2.2	1.0	Fabp7	1.0	1.0	1.0	1.0	1.0	1.0	1.0
	LCFA CoA synthesis (ACSLs)												
13	Acsl1	6153.3	2981.1	460.3	261.7	Acsl1	87.7	635.1	564.9	642.2	4061.7	13419.7	26600.3
14	Acsl3	136.9	92.0	119.0	202.4	Acsl3	263.2	121.6	116.6	164.2	150.5	174.2	274.9
15	Acsl4	1127.5	1343.8	589.3	841.6	Acsl4	553.7	2067.1	1284.8	1163.2	943.6	1263.8	881.5
16	Acsl5	4160.8	3619.0	3516.8	4087.7	Acsl5	927.1	1125.6	976.3	864.0	763.5	495.6	332.5
	Glycerol phosphate synthesis												
17	Gpd1	4113.1	2740.7	1847.9	1369.5	Gpd1	24.1	31.2	49.4	87.9	1105.2	2453.1	4626.4
	GPAT (sn-1 acylation)												
18	GPAT3/ Agpat9	195.9	125.6	72.3	97.0	GPAT3	8.9	64.9	35.7	34.9	294.8	813.5	1064.5
19	GPAT4	1442.6	975.7	518.1	374.9	GPAT4	752.474	1243.04	1080.49	986.807	1120.87	973.375	1347.96
20	GPAT1	1058.4	666.0	1266.4	620.3	GPAT1	268.0	553.7	596.5	525.1	745.0	691.3	1045.8
	LPAAT (sn-2 acylation)												
21	Agpat1	20.1	34.7	57.8	70.3	Agpat1	321.1	401.7	462.1	451.2	514.6	449.7	552.9
22	Agpat2	789.7	376.8	201.2	279.2	Agpat2	199.6	253.9	192.0	196.8	1584.5	3505.2	8808.9
23	Agpat3	1907.1	1324.4	778.3	659.4	Agpat3	576.2	198.0	229.0	266.6	429.0	408.0	570.8
24	Agpat4	12.6	7.6	3.3	1.3	Agpat4	216.5	350.8	222.1	223.6	264.0	214.7	211.8
25	Agpat5	60.3	60.6	112.3	143.9	Agpat5	481.3	839.6	673.2	517.6	594.6	587.5	611.3
	PA Phosphatase (lipins)												
26	Lpin1	634.0	220.9	270.2	120.4	Lpin1	329.2	713.1	643.1	603.1	1440.8	1894.3	3399.1
27	Lpin2	8202.3	6773.3	3281.1	1411.8	Lpin2	214.1	160.2	152.2	210.8	183.5	198.0	282.7
28	Lpin3	38.9	73.6	220.2	267.5	Lpin3	3.2	4.9	8.2	7.6	10.1	3.0	28.0
	DGAT (triglyceride synthesis by sn-3 acylation)												
29	Dgat1	118.0	93.1	85.6	95.0	Dgat1	160.2	253.9	231.7	195.0	591.2	1103.4	1734.2
30	Dgat2	2723.2	1459.7	1295.3	870.9	Dgat2	71.6	136.4	96.0	93.7	431.8	1102.2	3665.4
	MGAT (sn-2 acylation)												
31	Mgat1	438.2	322.7	334.7	538.9	Mgat1	730.7	558.7	541.6	560.6	656.6	510.5	447.8
32	Mgat2	253.6	269.6	394.7	258.4	Mgat2	420.1	388.6	346.9	281.2	285.8	207.0	179.9
33	Mgat4b	212.2	315.1	435.9	482.3	Mgat4b	591.5	248.9	241.3	308.0	576.7	621.5	905.7
34	Mgat5	22.6	18.4	58.9	55.3	Mgat5	132.8	184.0	196.1	179.9	263.4	264.2	454.8
	Cytoplasmic *de novo* FA synthesis												
35	Fasn	4064.1	1843.0	4648.7	772.6	Fasn	2284.8	2444.2	2651.9	2993.6	4227.9	5675.0	24959.5
	LCFA desaturation delta 9												
36	Scd1	136506	93343.2	50973.6	23379.2	Sdc1	1348.8	3616.6	2657.3	1829.2	1372.0	1027.7	851.9
	LCFA elongation												
37	Elovl1	139.4	133.2	206.8	350.8	Elovl1	317.1	370.5	346.9	333.0	399.4	375.2	470.3
38	Elovl2	10086.8	7926.6	3352.3	815.6								
39	Elovl3	1248.0	586.9	70.0	9.8	Elovl3	1.0	1.0	1.0	1.0	1.0	1.2	35.0
40	Elovl5	7136.4	3833.4	1245.3	585.8	Elovl5	590.7	622.8	606.1	646.2	476.5	522.5	1970.9
41	Elovl6	1915.9	2026.1	2297.1	498.6	Elovl6	646.2	725.4	763.7	730.6	444.1	300.0	158.1
42	Elovl7	8.8	58.5	345.8	283.1								

	Hepatocyte dedifferentiation						3T3-L1 differentiation						
Gene no.	Gene Symbol	0h	2h	8h	18h	Gene Symbol	0h	12h	18h	24h	36h	48h	60h
	Mitochondrial carnitine transferases												
43	Crot	6822.5	4666.1	1249.7	900.9	Crot	549.7	259.6	272.9	358.6	337.3	325.7	435.3
44	Crat	339.0	204.7	76.7	117.8	Crat	591.5	258.8	205.7	238.7	569.9	1531.6	6255.5
45	Cpt1a	3673.6	2162.4	702.7	368.4	Cpt1a	1030.9	994.9	1110.6	1187.6	910.0	615.5	413.5
46	Cpt1b	13.8	15.1	1	1	Cpt1b	25.7	23.0	27.0	26.1	28.5	23.0	19.4
47	Cpt2	1027.0	623.7	383.5	251.9	Cpt2	236.6	298.2	300.2	257.3	446.8	532.6	769.3
48	Slc25a20	721.9	463.4	163.4	140.5	Slc25a20	206.8	232.5	222.1	200.8	204.1	215.3	378.4
	Mitochondrial MCFA-CoA synthesis (ACSMs)												
49	Acsm1	2415.6	1957.8	1136.3	402.3								
50	Acsm2	11.3	5.4	3.3	2.0								
51	Acsm3	807.3	649.7	146.8	21.5	Acsm3	1.0	1.0	1.0	2.9	7.3	18.5	271.8
52						Acsm4	31.4	21.4	19.2	23.3	44.7	67.4	110.6
53	Acsm5	675.5	627.0	371.4	52.7	Acsm5	1.0	1.0	1.0	1.0	1.0	1.2	3.9
	Mitochondrial FA β-oxidation												
54	Acadl	1998.8	1609.1	1058.5	984.8	Acadl	590.7	276.9	283.8	354.0	492.8	640.6	1300.5
55	Acadm	3348.5	2577.2	1407.6	882.6	Acadm	684.1	656.4	569.0	604.3	1637.1	2907.6	4142.0
56	Acads	1270.6	906.4	598.2	580.0	Acads	648.7	384.5	392.2	388.9	586.7	632.8	868.3
57	Acadsb	1181.4	1086.1	411.4	267.5	Acadsb	608.4	626.0	554.0	590.9	648.8	804.6	1294.2
58	Acadvl	3555.6	2910.8	1787.9	1060.3	Acadvl	1191.9	1245.5	1203.9	1018.2	1261.3	1722.5	2555.8
59	Hadh	2374.19	1768.32	779.42	448.473	Hadh	857.901	694.229	711.642	671.262	1207.56	1722.49	2670.23
60	Hadha	3553.12	2307.59	1193.03	865.702	Hadha	1891.25	1837.86	1724.94	1589.95	2047.65	2113.75	3267.5
61	Hadhb	1987.49	1678.45	897.278	585.813	Hadhb	396.759	392.712	418.209	388.319	490.519	601.202	912.659
62	Ehhadh	3618.41	2647.61	967.326	238.231	Ehhadh	1	1	1	1	1	1.19286	1.55744
63	Echs1	1825.53	1509.52	799.433	535.694	Echs1	515.867	863.473	739.065	685.816	743.888	971.585	1510.71
64	Acaa2	6567.63	5329.88	2884.19	1273.82	Acaa2	469.995	382.853	372.961	334.175	432.909	351.894	596.499
65	Eci1	1058.4	793.742	430.293	266.22	Eci1	212.463	187.319	145.345	164.759	181.218	219.486	262.428
66	Eci2	1694.95	1413.14	654.891	255.805	Eci2	582.664	475.691	467.572	455.852	536.942	577.941	844.91
	Transcription regulators; protein regulation												
67	Pparγ	106.72	114.784	81.1664	125.624	Pparγ	270.408	224.289	257.782	275.957	767.938	1056.87	1568.34
68	Pparα	672.96	486.208	295.757	82.0139	Pparα	45.068	24.6472	17.8253	27.945	41.3893	57.2573	146.399
69	Pparδ	105.46	168.927	142.319	103.494	Pparδ	203.611	417.359	381.188	480.886	507.857	561.241	612.852
70	Prkaa1	70.309	103.955	135.648	192.017	Prkaa1	719.478	966.17	898.122	943.725	1090.1	973.971	922.782
71	Prkaa2	631.53	845.72	832.789	266.871	Prkaa2	32.9962	28.7551	31.5371	27.945	35.7961	57.8538	90.3314
72	Srebf1	3868.3	2697.42	681.575	352.79	Srebf1	526.33	483.085	571.781	712.597	1773.03	1885.91	2600.14
	TAG hydrolysis												
73	Pnpla2 (ATGL)	618.97	605.323	416.951	225.213	Pnpla2	166.591	332.737	263.266	341.744	1665.08	3122.31	8006.79
74	Lipe (HSL)	139.36	83.3809	34.4679	48.8178	Lipe	255.922	661.366	734.952	702.117	2612.56	3888.73	7119.05
75	Mgll	1887.1	1214.98	420.286	123.672	Mgll	1.60957	1	2.74236	2.32875	14.5422	49.5037	137.055
76	Abhd5	396.74	316.198	366.917	443.916	Abhd5	291.332	972.742	988.62	873.863	1653.89	2712.57	2906.18
77	Lpl	91.653	54.1434	24.4611	31.8943	Lpl	3867.8	9112.06	5993.42	4351.27	7932.19	17442	36194.9
78	Lipc	1642.2	1377.41	816.111	573.446	Lipc	1	1	1.37118	1	1	1	1
79	Pnpla3	25.11	15.1602	46.6985	21.4798	Pnpla3	1	1	1	1	1.67794	11.9286	34.2636
80	Pnpla6	61.52	43.3147	94.5088	90.4756	Pnpla6	257.531	106.804	146.716	135.067	118.575	141.95	147.957
81	Pnpla7	974.28	741.765	500.341	560.428	Pnpla7	148.885	35.3276	72.6725	56.4721	45.3045	42.943	38.1572
82	Pnpla8	1288.2	960.504	585.955	492.083	Pnpla8	371.811	441.185	500.48	593.249	969.292	1470.2	2314.35
	Quality control 1: liver specific genes												
83	Abcb11	4907.8	3104.6	769.4	91.1	Abcb11	5.6	1.0	1.0	1.0	1.0	1.0	3.1
84	Abcg5	1676.1	991.9	283.5	24.1	Abcg5	1.0	1.0	1.0	1.2	1.1	1.0	1.6
85	Abcg8	1387.4	632.4	112.3	14.3	Abcg8	1.0	1.0	1.4	1.0	1.0	1.0	1.0
86	Adh1	10778.6	7345.1	3459.0	810.4	Adh1	7.2	1.0	1.4	14.0	45.3	30.4	31.1
87	Alb	532017	454114.0	250540	143461.0	Alb	1.0	1.0	1.0	1.0	1.0	1.0	1.0
88	F10	2680.5	1826.8	1074.1	491.4								
89	F2	12579.1	9190.3	5571.6	3404.2								
	Quality control 2: adipocyte marker genes												
						Adipoq	8.0	4.1	2.7	1.7	54.8	326.2	951.6
90	G0s2	100.4	41.1	72.3	190.1	G0s2	1.6	1.0	5.5	1.2	119.7	427.0	948.5
	Quality control 3: housekeeping genes												
91	β-actin	7695.1	8565.5	12159.4	23180.0	β-actin	13548.6	9146.6	8855.1	8717.1	5258.7	4574.0	4552.4
92	γ-actin	15666.4	17611.8	14661.1	14418.2	γ-actin	11052.9	5566.2	6901.1	6710.9	3611.5	3114.6	2560.4
93	Akt1	281.2	311.9	610.4	753.1	Akt1	1392.3	1319.5	1283.4	1146.9	1181.8	875.0	626.1
94	Akt2	978.1	776.4	503.7	552.6	Akt2	786.3	649.9	555.3	486.7	690.8	810.5	1445.3
95	Ubb	2213.5	1651.4	1194.2	938.0	Ubb	6869.7	6490.4	6931.3	6518.8	7085.4	6340.1	5723.6
96	Rab5a	726.9	759.1	589.3	360.6	Rab5a	512.6	561.1	485.4	492.5	561.6	707.4	827.0

4.5.1. FA uptake from the medium

4.5.1.1. C11 and C19-FA uptake in hepatocytes

In the previous section it was shown that dedifferentiated hepatocytes are not able to incorporate C11-FA into TAG. Freshly isolated hepatocytes (day 0) and hepatocytes, that were kept in the cell culture for one or three days (day 1 and day 3 respectively) after isolation, were used to examine the FA uptake. The FA uptake was evaluated by measuring the reduction of alkyne-FAs in the medium compared to control sample without cells. As can be seen from Figure 12A lanes 1-7, after overnight feeding C11-FA signal was missing in all samples where cells were present (lanes 1-6), however in control sample without cells signal was present (lane 7). This means that all three cell groups took up C11-FA. However, TAG synthesis was strongly reduced in the day 1 cells (Figure 12A lane 10) and basically not present in the day 3 cells (lane 12). This was not the case when feeding them with C19-FA (Figure 12B) because the TAG amount did not decrease in the day 3 cells compared to the freshly isolated hepatocytes (Figure 12B lanes 8-13). After overnight feeding some of C19-FA was still present in the medium (Figure 12B lanes 1-6). During these experiments very exciting results related to etomoxir treatment was noticed. Etomoxir is an inhibitor of CPT1 (1.6). When day 0 and day 1 cells were fed overnight with C11-FA in the presence of etomoxir, X and Y bands of unknown compounds were identified in the medium (Figure 12A lanes 2 and 4). These bands were not present in the medium of day 0 and day 1 cells without etomoxir treatment (Figure 12A lanes 1 and 3). These bands were also present in day 3 cells with or without etomoxir treatment (Figure 12A lanes 5-6). Furthermore, the cells treated with etomoxir contained much less C11-TAG compared to the untreated cells (Figure 12A lanes 8-13). In the freshly isolated hepatocytes fed with C11-FA without etomoxir or fed with C19-FA with or without etomoxir TAG was detected in the medium (Figure 12A lane 1, Figure 12B lanes 1-2). This indicated a lipoprotein secretion. In day 1 cells no C11-TAG could be identified in the medium (Figure 12A lanes 3-4), though C19-TAG was still secreted (Figure 12B lanes 3-4). Day 3 cells secreted neither C11-TAG nor C19-TAG (Figure 12A lanes 5-6, Figure 12B lanes 5-6) indicating a failing lipoprotein secretion in the dedifferentiating cells. Apparently, etomoxir had no effect on TAG synthesis when feeding cells with C19 (Figure 12B lanes 8-13), nor stimulated it the secretion of unknown compounds into the medium (Figure 12B lanes 1-7).

Because these were very exciting findings, later on, they were analyzed in greater detail with the help of pulse experiments (4.5.2).

But before that it was decided to analyze if other medium or long-chain fatty acids were taken up by freshly isolated hepatocytes and if etomoxir had an effect there as well.

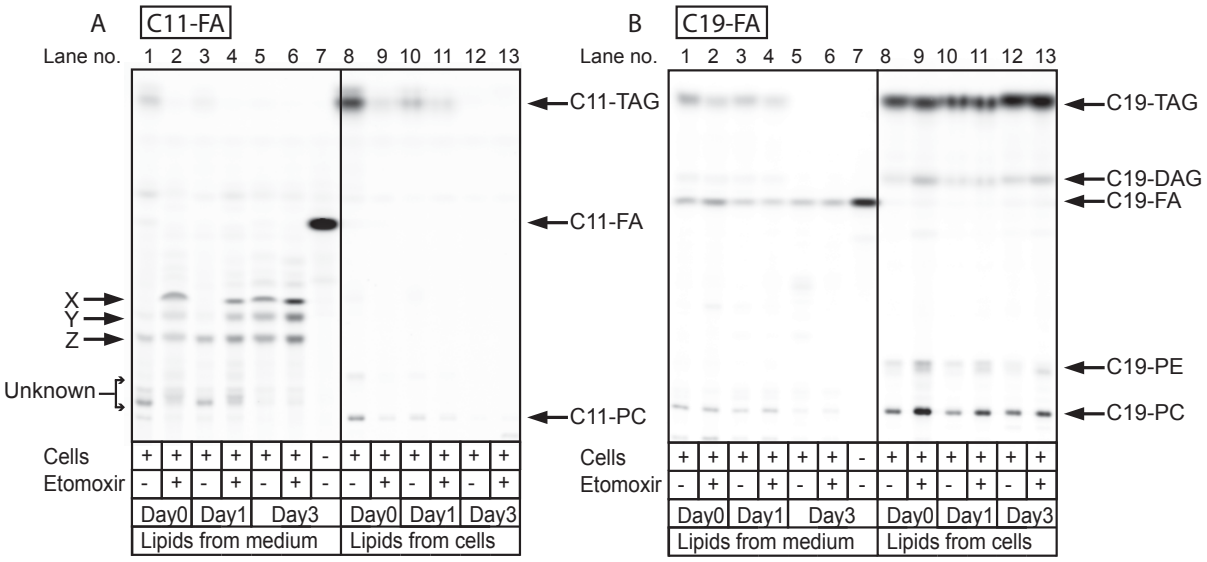

Figure 12. Hepatocyte uptake of C11 or C19-FA from the medium.
Hepatocytes isolated from mouse liver were plated on collagen coated 12-well plates. 150.000 cells were plated per well. The medium with 50 μM of C11-FA (A) or C19-FA (B) was added to cells for overnight feeding (approx. 18 hours). After feeding the medium was collected and 50 μl of it was used for lipid extraction. The cells were washed and lipids were extracted from the cells. Then the click reaction was performed both with lipids from the medium and from the cells. Finally, lipids were separated on a TLC plate and fluorescence was detected by fluorescence imaging. Day 0 represents cells to which C11-FA was added on the same day of hepatocyte isolation. Day 1 represents cells to which C11-FA was added the next day after isolation and day 3 – the third day after isolation. The different lipid classes in which FAs were incorporated and FAs themselves are indicated on the right side of images. Bands X, Y, Z indicate unidentified substances that were secreted into the medium by hepatocytes. Lane 7 represents the control, where the medium with FAs was added to the well without cells. In indicated samples 50 μM of etomoxir was added to the medium with the FA.

4.5.1.2. C9, C13 and C17-FA uptake in hepatocytes

Freshly isolated hepatocytes were fed with C9, C13 and C17-FAs overnight. Then lipids from the medium and from the cells were extracted. When feeding the cells with both C9 and C13-FAs in the presence of etomoxir unknown bands appeared in the medium (Figure 13 lanes 1-2, 4-5) and etomoxir diminished TAG synthesis rate (Figure 13 lanes 10-13). This corresponds with the C11-FA data from Figure 12A. When feeding with C17-FA no intensive unknown bands were detected in the medium (Figure 13 lanes 7 and 8) and the TAG amount did not decrease in the presence of etomoxir (Figure 13 lanes 14-15). This is similar to the results when feeding with C19-FA (Figure 12B).

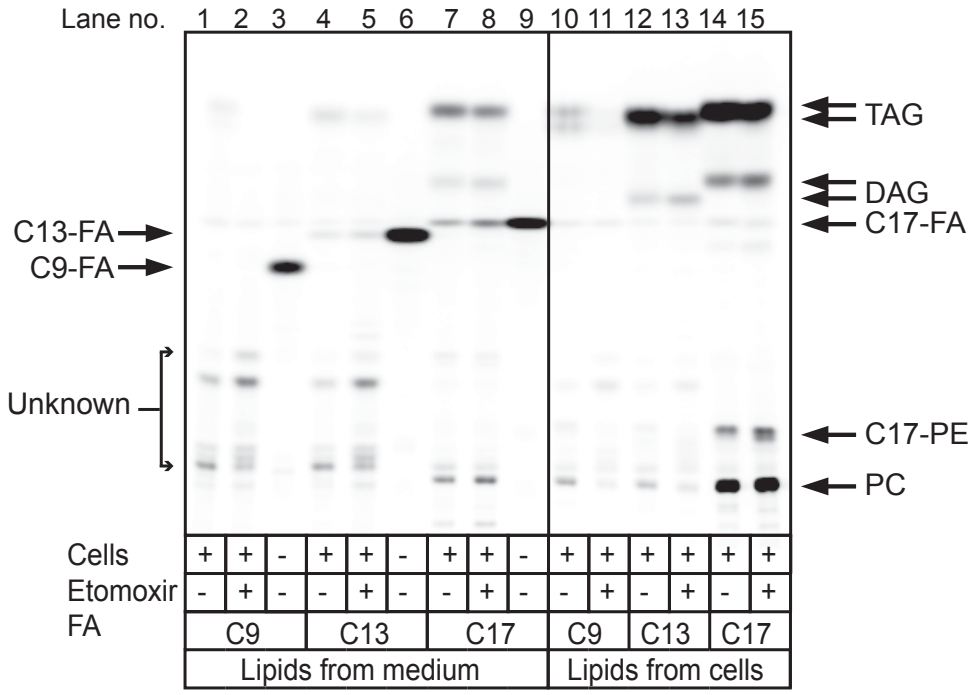

Figure 13. Hepatocyte uptake of C9, C13 and C17-FAs from the medium.
Hepatocytes were isolated from mouse liver and plated on collagen coated 12-well plates. 150.000 cells were plated per well. The medium with 50 μM of either C9 or C13 or C17-FAs was added to the cells for overnight feeding (approx. 18 hours). After feeding the medium was collected and 50 μl of it was used for lipid extraction. The cells were washed and lipids were extracted from the cells. Then click reaction was performed both with lipids from the medium and from the cells. Finally, lipids were separated on a TLC plate and fluorescence was detected by fluorescence imaging. The different lipid classes in which FAs were incorporated and FAs themselves are indicated on both sides of the image. Region "Unknown" indicates unidentified substances that are secreted into the medium by hepatocytes. Lanes 3, 6 and 9 represent controls, where the medium with FA was added to wells without cells. In indicated samples 50 μM of etomoxir was added to the medium with FA.

4.5.1.3. C11 and C19-FA uptake in 3T3-L1 cells

As shown before both freshly isolated and dedifferentiated hepatocytes could take up C11-FA. Following the previous experiments it was decided to verify if undifferentiated (day 0) and differentiated (day 4) 3T3-L1 cells can also take up C11-FA, and if the presence of etomoxir has any effect on the uptake.

Undifferentiated and differentiated 3T3-L1 cells were fed with either C11 or C19-FA overnight. Both cell types did take up C11-FA as it disappeared from the medium compared to control sample (Figure 14, lanes 1-4) and unknown bands were identified in the medium. Since the results with and without etomoxir were the same, no etomoxir effect could be observed (Figure 14, lanes 1-4). In undifferentiated cells one additional band could be seen compared to differentiated cells (Figure 14, lanes 1-4). In differentiated cells treated with etomoxir, the amount of C11-TAG was lower compared

to untreated cells (Figure 14, lanes 13-14). Undifferentiated cells had no C11-TAG at all (Figure 14, lanes 11-12). Apparently, etomoxir had no effect on the C19-TAG amount in both undifferentiated and differentiated cells (Figure 14, lanes 15-18). When feeding differentiated cells with C11-FA the additional TAG band appeared. It ran higher than C11-TAG and at a similar height as C19-TAG (Figure 14, lanes 13-14). A plausible explanation would be that C11-FA was elongated while overnight feeding and that both C11-FA and elongated FA were used for TAG synthesis.

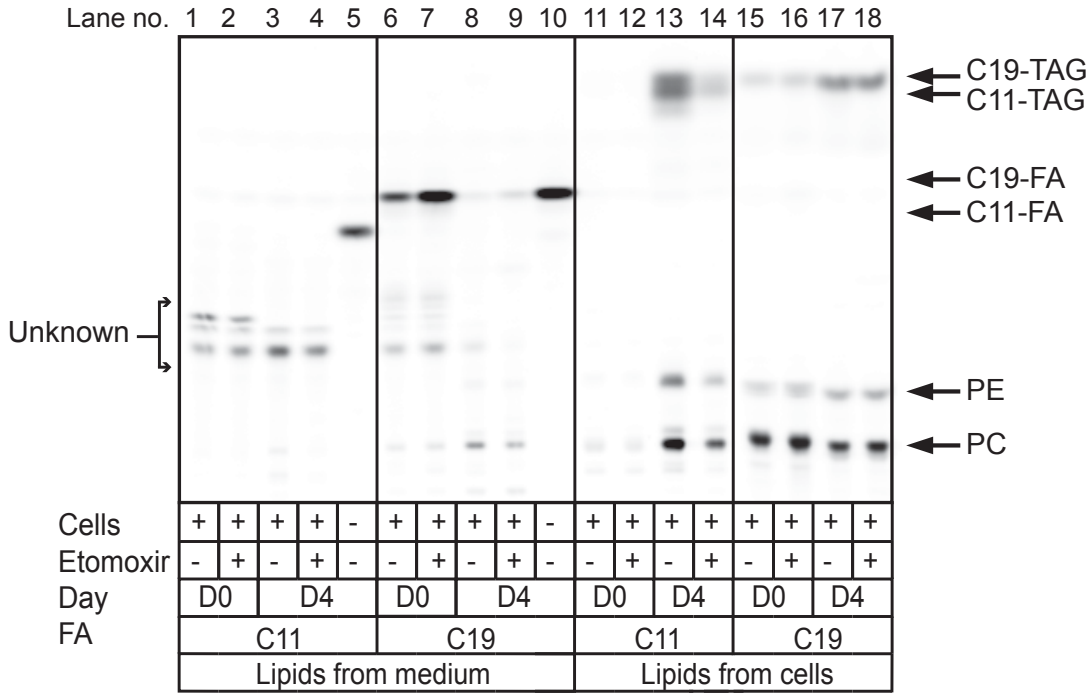

Figure 14. C11 and C19-FA uptake from the medium in 3T3-L1 cells.
3T3-L1 cells were grown in 6-well plates until confluence. The differentiation medium was added to half of the cells for 4 days. After 4 days, the medium with 50 μM of either C11 or C19 fatty acids was added to both differentiated and undifferentiated cells for overnight feeding (approx. 18 hours). After feeding the medium was collected and 50 μl of it was used for lipid extraction. The cells were washed and lipids were extracted from the cells. Then the click reaction was performed both with lipids from the medium and cells. Finally, lipids were separated on a TLC plate and fluorescence was detected by fluorescence imaging. The different lipid classes in which FAs were incorporated and FAs themselves are indicated on the right side of the image. Region "Unknown" indicates unidentified substances that are secreted into the medium by 3T3-L1 cells. Lanes 5 and 10 represent controls, where the medium with FA was added to wells without cells. In indicated samples 50 μM of etomoxir was added to the medium with FA. D0 represents undifferentiated cells. D4 represents cells differentiated for 4 days.

4.5.1.4. C11 and C19-FA uptake in Huh7 cells

As evident from the previous section, undifferentiated 3T3-L1 cells cannot synthesize C11-TAG but take up C11-FA from the medium. To further explore this topic the same experiment as in chapter 4.5.1.3 was made, but with Huh7 cells. Huh7 cells also cannot synthesize C11-TAG (Figure 9 lane 12). From Figure 15A lanes 1-5 and B it can be seen that Huh7 cells did not take up C11-FA as C11-FA amount in the medium was the same both in samples with and without cells. However, Huh7 cells did take up C19-FA as C19-FA amount in the medium after incubation with cells decreased significantly (Figure 15A lanes 6-10 and B). These cells did not incorporate C11-FA in TAG and they did not use it for other metabolic processes as C11-FA did not disappear from the medium.

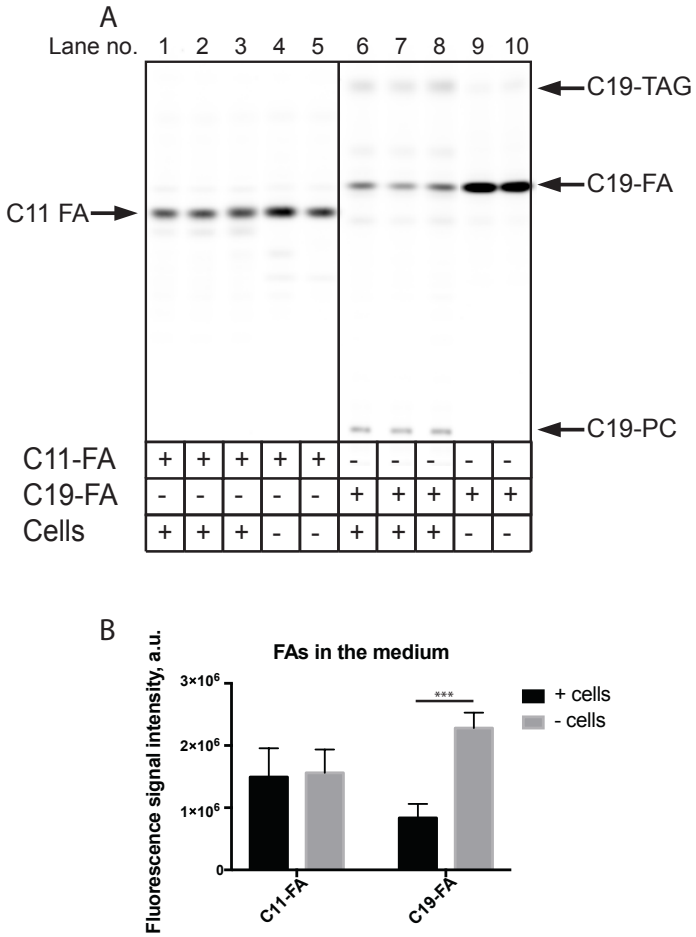

Figure 15. Huh7 uptake of C19 and C11-FAs from the medium.
(A) 150.000 cells were seeded per well in a 24-well plate. Next day the medium with either 50 µM of C11-FA or C19-FA was added to the cells for overnight feeding (approx. 18 hours). After feeding the medium was collected and 50 µl of it was used for lipid extraction. Then click reaction was performed, lipids were separated on a TLC plate and fluorescence was detected by fluorescence imaging. FAs and lipids secreted by cells to the medium are indicated on both sides of the image. The lanes 4, 5, 9 and 10 represent the controls, where the medium with FA was added to wells without cells. (B) Quantification of data from panel A. The values represent fluorescence intensity of C11 and C19-FA bands. The data represent mean +SD, n=5. *** stands for p≤0.001.

4.5.1.5. Protease treatment of hepatocytes

To see if C11 and C19-FAs need a transport protein to get inside the cell freshly isolated hepatocytes were treated with different proteases. By doing this putative FA transport proteins located at the outer side of the plasma membrane theoretically could be removed. However, there was no significant difference between control cells and cells treated with different proteases while feeding with C11 and C19-FAs (Figure 16). It should be mentioned that no positive control for protease treatment was used in this experiment, therefore the data should be interpreted carefully. However, with proper controls, e.g., performing Western Blot for well known outer membrane proteins, this could be a nice method for FA transport experiments.

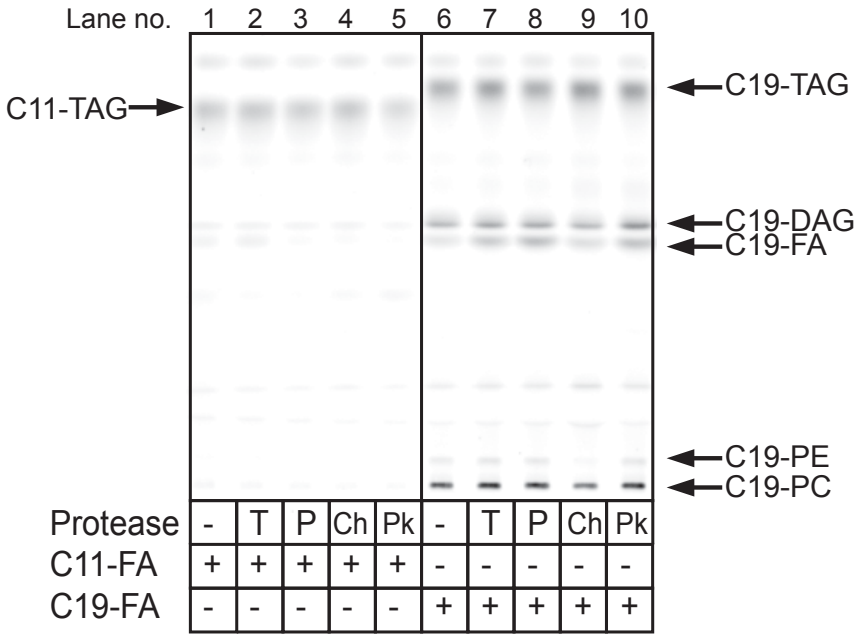

Figure 16. Treatment of hepatocytes with different proteases.
Hepatocytes were isolated from mouse liver and plated on collagen coated 6-well dishes. 400.000 cells were used per well. Different proteases were added to cells for 15 min at 37˚C in the absence of FBS. Digestion was inhibited by adding William's E medium supplemented with FBS. Cells from each digestion were divided into two equal parts. One part was used for feeding with 50 µM of C11-FA and the second part for feeding with 50 µM of C19-FA. The cells were incubated with FAs for 15 min and washed. Then lipids were extracted from the cells and the click reaction was performed. Finally, lipids were separated on a TLC plate and fluorescence was detected by fluorescence imaging. C19-FA and the different lipid classes in which FAs were incorporated are indicated on both sides of the image. "T" stands for trypsin, "P" for papain, "Ch" – chymotrypsin, "Pk" – proteinase K.

4.5.1.6. Huh7 in differentiation medium

Cells, used in previous experiments, got in contact with different substances as C11-TAG synthesis was investigated. There was a reasonable need to determine if the ability to synthesize C11-TAG was not influenced by having a contact with these substances. Upon differentiation 3T3-L1 cells were treated with insulin, IBMX and dexamethasone. The analyzed slices came from mouse organs that also had contact with insulin from the blood. It was reasoned that these substances might affect the C11-TAG synthesis. To verify this Huh7 cells were treated with insulin, IBMX and dexamethasone either by each of them separately or in different combinations for 3 days. Afterward, cells were fed with a mixture of C11 and C19-FAs. Different serum conditions were also tested. However, none of these conditions facilitated C11-FA incorporation into TAG and only C19-TAG bands could be detected (Figure 17).

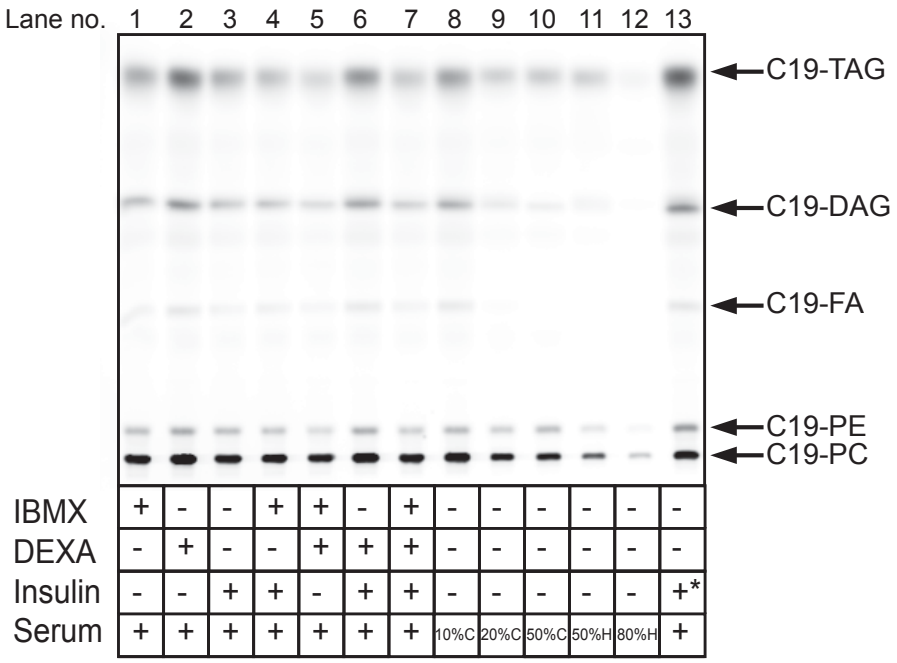

Figure 17. C11 and C19-FA metabolism in Huh7 cells grown in different differentiation medium conditions.
60.000 of Huh7 cells were seeded per one well of a 24-well plate. When cells were attached, the medium and different additional components, used for differentiation of 3T3-L1 cells, was added for 3 days. The components were added either on their own or in different combinations. Additional components were: 0.5 mM IBMX, 10 µM dexamethasone (DEXA), and 5 µg/ml insulin. In these conditions the medium contained 10% FBS. The effect of serum was also tested as indicated in the figure. C stands for FBS and H for horse serum. * indicates insulin concentration of 15 µg/ml. After 3 days of incubation a mixture of 50 µM C11 and 50 µM C19-FAs was added to cells for 1.5 hours. The cells were washed and lipids were extracted from the cells. The click reaction was performed, lipids were separated on a TLC plate and fluorescence was detected by fluorescence imaging.

4.5.2. Pulse experiments and the etomoxir effect

In order to better understand the etomoxir effect observed in hepatocytes and differentiated 3T3-L1 cells pulse experiments were carried out with C11 and C19-FAs and lipids from the medium and the cells were analyzed.

4.5.2.1. Initial C11-FA pulse experiments in hepatocytes

Freshly isolated hepatocytes were fed with C11-FA for indicated time periods in medium with or without etomoxir. Lipids from both the medium and the cells were analyzed. As evident from Figure 18A, during short pulse times (up to 90 min) unknown bands were detected when analyzing the medium from both etomoxir-treated and untreated cells. In the medium from etomoxir-treated cells, these bands were more intense. Etomoxir also had an effect on the C11-TAG amount in cells. Already after 20 min of incubation, a decrease in C11-TAG amount was observed in etomoxir-treated cells compared to untreated cells (Figure 18B, lanes 3 and 9). In experiments with longer pulse times (Figure 18C, D) it can be seen that in the time period between 2 and 4 hours the unknown bands disappeared from the medium of the untreated cells (Figure 18C, lanes 1 and 2), whereas in the medium from etomoxir-treated cells the bands were quite intense (Figure 18C, lanes 8 and 9), but diminished with time. One could wonder why after overnight feeding these “unknown” bands (Figure 18, lane 14) were less intense as in Figure 12A lane 2. In experiment described in this chapter (Figure 18, lane 14) cells were fed with C11-FA directly after isolation and adherence to plates, so the total overnight feeding time was approx. 24 hours. However, in the previous experiment (Figure 12A lane 2) overnight feeding lasted approximately 18 hours. Moreover, at the start of the feeding the cells from the previous experiment (Figure 12A) were 6-7 hours older than the cells in this experiment (Figure 18). In chapter 4.3 it was already demonstrated the influence of the time, which cells spend in the 2D cell culture after isolation, on hepatocyte metabolism. Hepatocytes incorporated C11-FA not only in TAG but also in PC (Figure 18B, D).

The most interesting time points from experiments described in this chapter were selected for further pulse experiments.

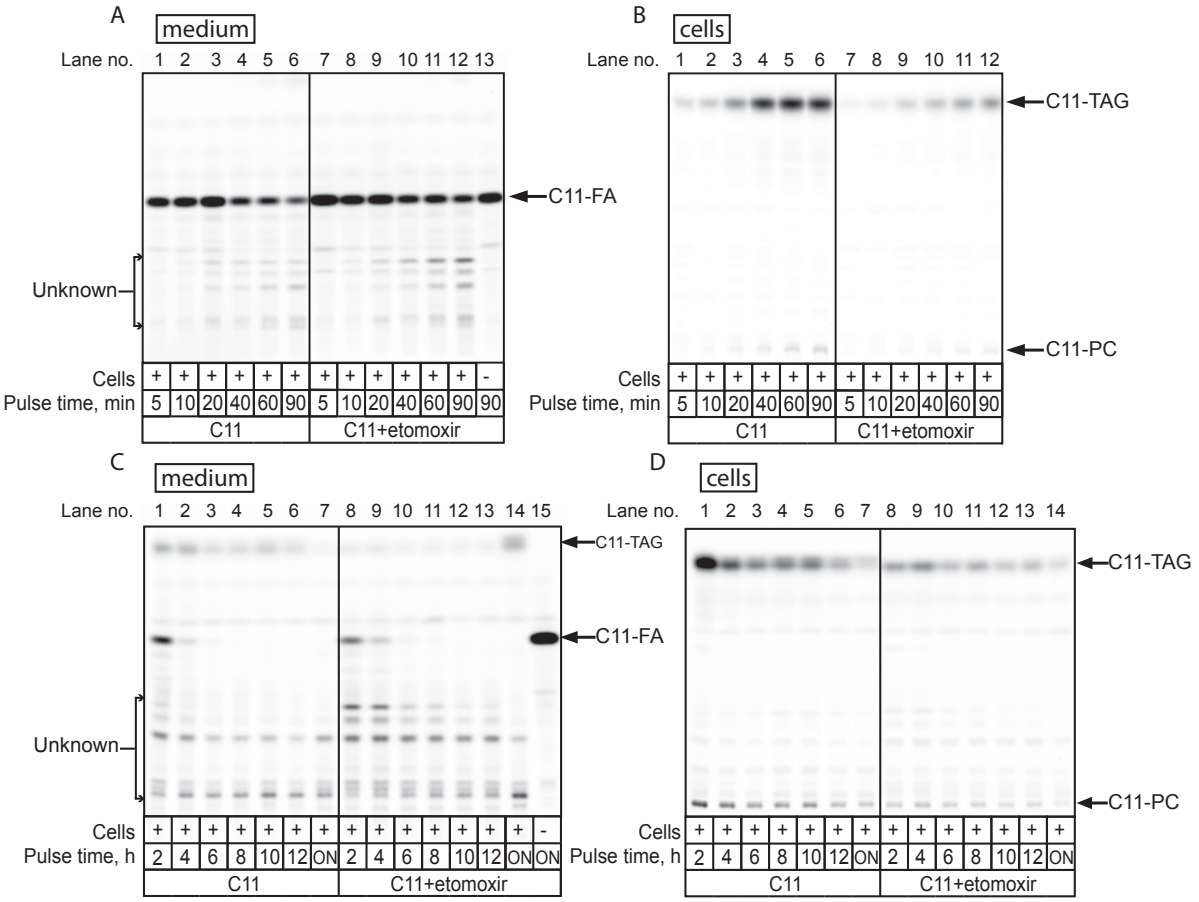

Figure 18. Initial C11-FA pulse experiments in hepatocytes.
After isolation from mouse liver hepatocytes were plated on collagen coated 3.5 cm dishes. 200.000 cells were plated per one dish. 50 µM of C11-FA was added for shorter intervals (A, B) or longer intervals (C, D). The medium was collected and 50 µl of it was used for lipid extraction. The cells were washed and lipids were extracted from the cells. Then click reaction was performed both with lipids from the medium (A, C) and the cells (B, D). Finally, lipids were separated on a TLC plate and fluorescence was detected by fluorescence imaging. In the indicated samples (+ etomoxir) 50 µM of etomoxir was added to the medium with FA. Lane 13 in panel A and lane 15 in panel C represent controls, where the medium with FA was added to the well without cells. ON stands for overnight (approx. 24 hours).

4.5.2.2. Detailed C11-FA pulse experiments in hepatocytes

Freshly isolated hepatocytes were fed with C11-FA for 5 and 20 minutes and for 1, 2, 6 and 10 hours. Cells were fed with FA either in the presence or absence of etomoxir. Lipids from both the medium and the cells were analyzed.

Already after 20 min of the incubation time a significant decrease in the TAG amount in etomoxir-treated hepatocytes could be detected (Figure 19A lanes 2, 8 and Figure 19C). This decrease stayed constant over the time. The PC amount also decreased in

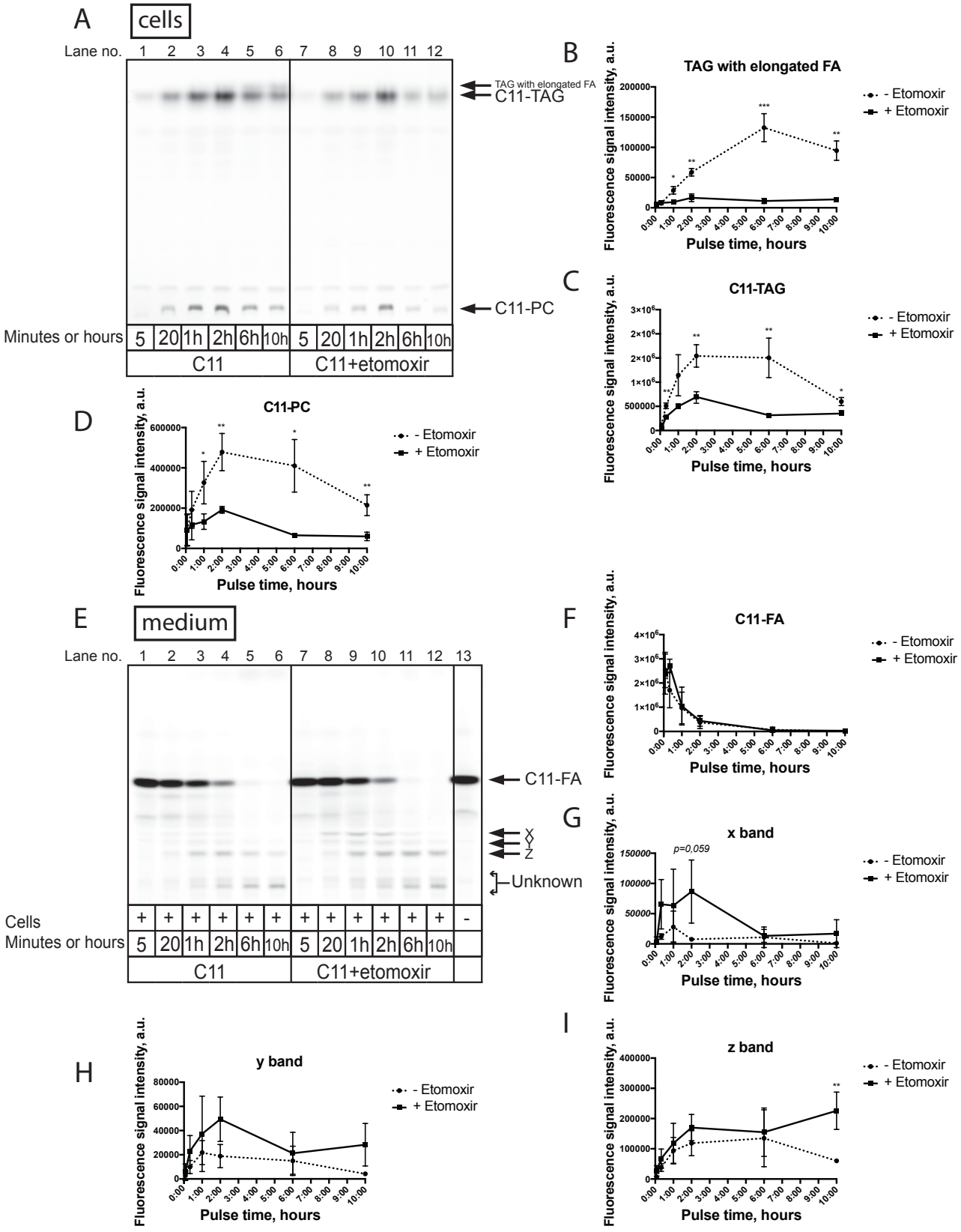

Figure 19. C11-FA pulse experiments in hepatocytes.
After isolation from mouse liver hepatocytes were plated on collagen coated 3.5 cm dishes. 200.000 cells were plated per one dish. 50 μM of C11-FA was added for a pulse time indicated in panels A and E. After this time period the medium was collected and 50 μl of it was used for lipid extraction. Cells were washed and lipids were extracted. Then the click reaction was performed both with lipids from the medium (E) and cells (A). Finally, the lipids were separated on a TLC plate and fluorescence was detected by fluorescence imaging. In the indicated samples (+ etomoxir) 50 μM of etomoxir was added to the medium with FA. Lane 13 in panel E represents a control, where the medium with FA was added to the well without cells. Graphs B, C and D illustrate quantifications of bands indicated at the right side of the panel A (TAG with elongated FA, C11-TAG and C11-PC). Graphs F, G, H and I illustrate the quantifications of C11-FA bands and the unknown bands X, Y, Z indicated in panel E. The data represent mean ±SD, n=3. * stands for p≤0.05; ** p≤0.01; *** p≤0.001.

etomoxir-treated cells (Figure 19D). Another exciting result is that during the pulse time an additional upper TAG band appeared in cells not treated with etomoxir (Figure 19A and B). This upper TAG band likely represents TAG synthesized from elongated C11-FA. After 6 hours of incubation, this band reached its peak (Figure 19B). In cells treated with etomoxir upper TAG band was barely present (Figure 19A lanes 7-12, B). Experiments with lipid extraction from the medium showed that etomoxir had no significant effect on the residual C11-FA amount (Figure 19E, F). After 2 hours of feeding, less than 20 % of C11-FA was left in the medium. In the time window between 2 and 6 hours, C11-FA was completely used up (Figure 19F). Once the C11-FA was nearly depleted from the medium, the amount of C11-TAG in the cells started decreasing as well (Figure 19C).

As in the previous experiment (Figure 12A) the unknown bands X, Y and Z appeared in both etomoxir-treated and untreated cells (Figure 19E). The Z-band was more intensive in etomoxir-treated cells (Figure 19E, I). Furthermore, it was also the most intensive band out of the three. In the cells not treated with etomoxir the intensity of the X-band increased slightly in the first hour but then disappeared with time (Figure 19G). In etomoxir-treated cells the X-band was more intense after a short pulse, but its intensity declined when incubating longer than 2 hours. The Y-band behaved similarly over time but was, in general, less intense than the X-band (Figure 19H).

4.5.2.3. C19-FA pulse experiments in hepatocytes

Freshly isolated hepatocytes were fed with C19-FA for 5 and 20 minutes and for 1, 2, 6 and 10 hours. The cells were fed with the FA either in the presence or absence of etomoxir. Lipids from both the medium and the cells were analyzed.

As illustrated by Figure 20A and Figure 20B the TAG amount was barely affected by etomoxir in hepatocytes fed with C19-FA. The PC and PE amounts increased slightly in etomoxir-treated cells (Figure 20C, D). The C19-FA amount was not affected by etomoxir and there were no additional bands appearing in the medium (Figure 20E, F). During the pulse time of 10 hours, the TAG amount in the presence and in the absence of etomoxir increased steadily or remained unchanged (Figure 20A, B). The C19-FA could still be detected in the medium after six hours of feeding (Figure 20E lanes 5 and 11, F).

Further pulse experiments were conducted with differentiated 3T3-L1 cells.

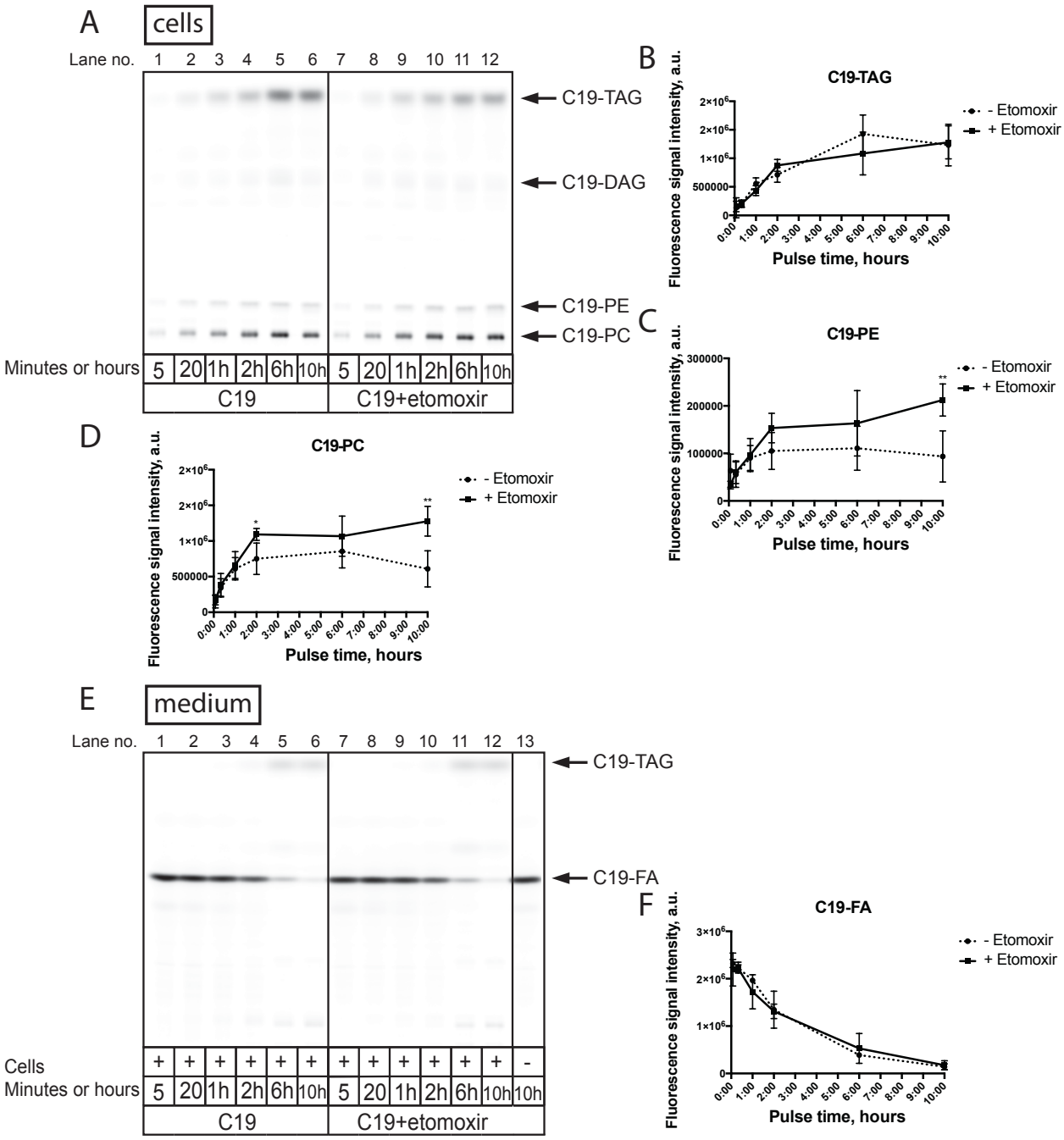

Figure 20. C19-FA pulse experiments in hepatocytes
After isolation from mouse liver, hepatocytes were plated on collagen coated 3.5 cm dishes. 200.000 cells were plated per one dish. 50 μM of C19-FA was added for a pulse time indicated in panels A and E. After this time period the medium was collected and 50 μl of it was used for lipid extraction. The cells were washed and lipids were extracted. Then the click reaction was performed both with lipids from the medium (E) and cells (A). Finally, lipids were separated on a TLC plate and fluorescence was detected by fluorescence imaging. In the indicated samples (+ etomoxir) 50 μM of etomoxir was added to the medium with FA. Lane 13 in panel E represents the control, where the medium with FA was added to the well without cells. Graphs B, C and D illustrate the quantifications of the bands indicated at the right side of the panel A. Graph F illustrates the quantification of FA bands indicated in panel E. The data represent mean ±SD, n=4. * stands for p≤0.05; ** p≤0.01.

4.5.2.4. C11 and C19-FA pulse experiments in 3T3-L1 cells

Similarly as hepatocytes, 3T3-L1 cells were fed with C11 or C19-FAs for 10 minutes and for 1 and 4 hours. The effect of etomoxir was analyzed. Experiments showed that cells treated with etomoxir incorporated less C11-FA into C11-TAG and into C11-PC (Figure 21A lanes 1-6, B, C). In a time window between 1 and 4 hours, the C11-TAG amount started to decrease in both conditions (Figure 21B). This correlated with the C11-FA decrease in the medium (Figure 21D). After 4 hours of feeding, approximately only 5% of C11-FA was left in the medium. Etomoxir did not have a significant effect on C11-FA amount in the medium (Figure 21A lanes 7-12, D). Unknown bands marked with X, Y, Z appeared in the medium from 3T3-L1 cells. When incubated for up to 1 hour the intensity of Y and Z bands was not affected by the presence of etomoxir (Figure 21F, G). After 4 hours with etomoxir treatment, the intensity of the Y band increased significantly (Figure 21F). The signal of the X-band was consistently weaker in the cells not treated with etomoxir (Figure 21E).

The treatment with etomoxir had no significant effect on the amount of TAG, DAG, PE and PC in 3T3-L1 cells fed with C19-FA (Figure 22A lanes 1-6, B, C, D, E). The etomoxir treatment also virtually did not change the amount of C19-FA in the medium (Figure 22A lanes 7-12, F). In both conditions the C19-TAG amount constantly increased (Figure 22B). After a 4 hour pulse there was still more than 30% of C19-FA left in the medium (Figure 22F).

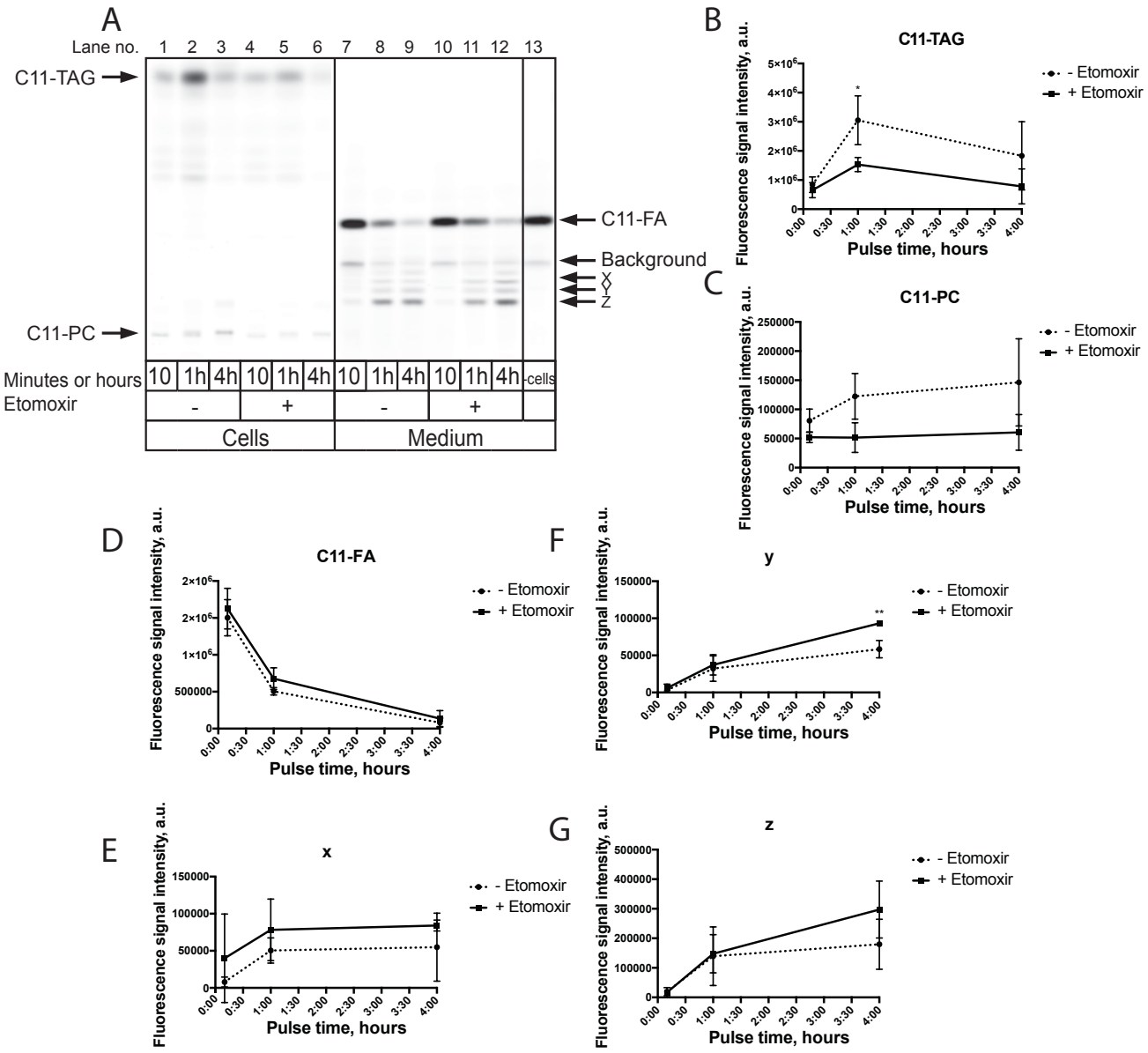

Figure 21. C11-FA pulse experiments in 3T3-L1 cells.
3T3-L1 cells were grown in 12-well plates until confluence. After two more days, differentiation medium was added for 4 days. After 4 days, the medium with 50 µM of C11-FA was added for a pulse time indicated in panel A. After this time period the medium was collected and 50 µl of it was used for lipid extraction. The cells were washed and lipids were extracted. Then the click reaction was performed both with lipids from the medium and the cells. Finally, lipids were separated on a TLC plate and fluorescence was detected by fluorescence imaging (A). In the indicated samples 50 µM of etomoxir was added to the medium with FA. Lane 13 in panel A represents the control, where the medium with C11-FA was added to the well without cells. Graphs B and C illustrate quantifications of the bands indicated at the left side of the panel A (C11-TAG, C11-PC). Graphs D, E, F and G illustrate quantifications of C11-FA bands and the unknown bands X, Y and Z indicated at the right side of the panel A. The data represent mean ±SD, n=3. * stands for $p \leq 0.05$.

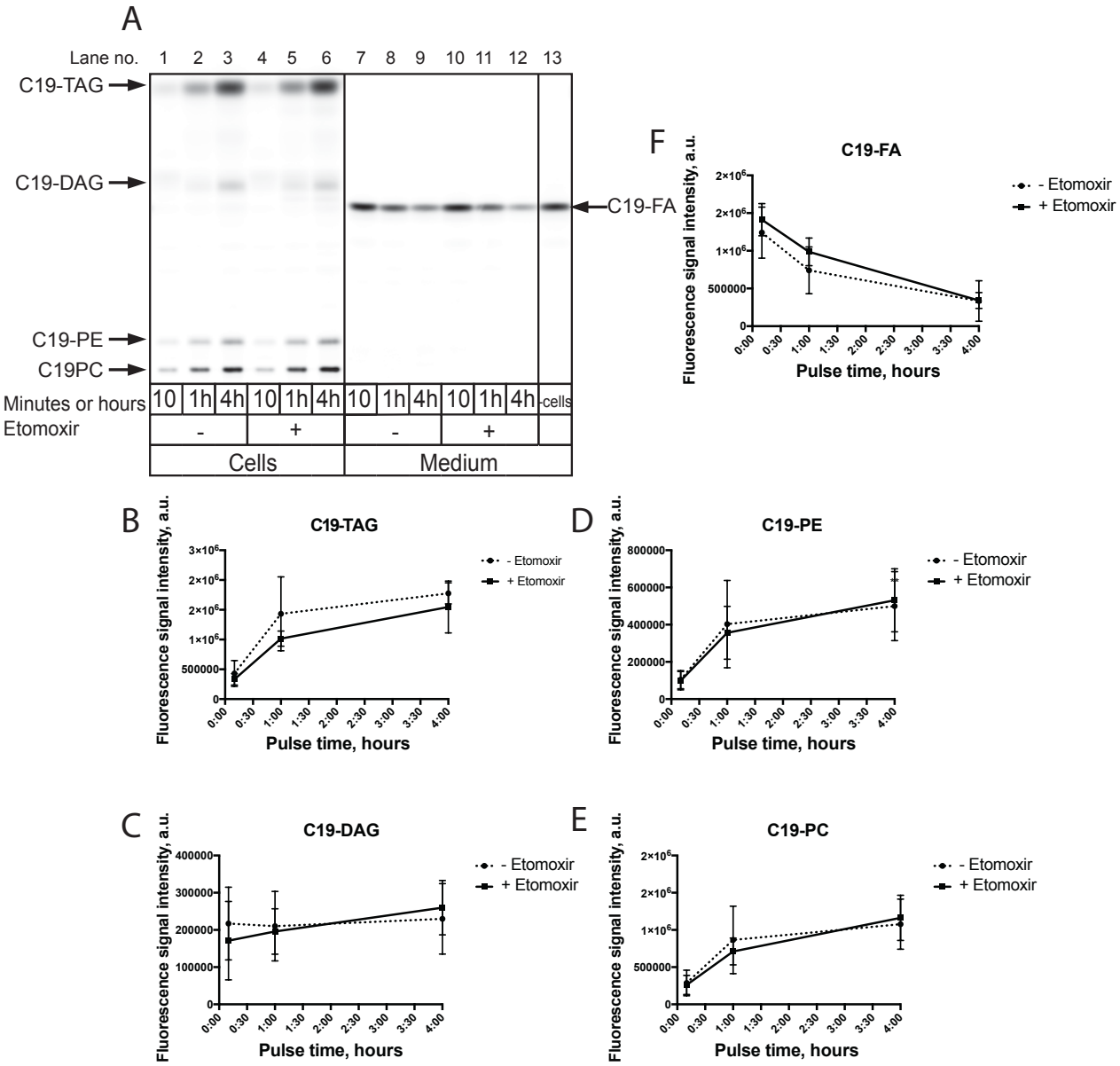

Figure 22. C19-FA pulse experiments in 3T3-L1 cells.
3T3-L1 cells were grown in 12-well plates until confluence. After two more days, a differentiation medium was added for 4 days. After 4 days, the medium with 50 μM of C19-FA was added for a pulse time indicated in panel A. After this time period the medium was collected and 50 μl of it was used for lipid extraction. The cells were washed and lipids were extracted. Then click reaction was performed both with lipids from the medium and the cells. Finally, lipids were separated on a TLC plate and fluorescence was detected by fluorescence imaging (A). In indicated samples 50 μM of etomoxir was added to the medium with FA. Lane 13 in panel A represents control, where the medium with C19-FA was added to the well without cells. Graphs B, C, D and E illustrate quantifications of bands indicated at the left side of the panel A (C19-TAG, C19-DAG, C19-PE and C19-PC). Graph F illustrates quantification of C19-FA bands indicated at the right side of the panel A. The data represent mean ±SD, n=3.

4.5.2.5. C11 and C19 pulse-chase experiments in 3T3-L1 cells

This experiment was carried out to determine what happens with C11 and C19-TAG after one-hour pulse and then a longer chase lasting up to 24 hours. When 3T3-L1 cells were pulsed with C11-FA for 1 hour and then chased, the intensity of the C11-TAG band decreased with increasing chase times (Figure 23A lanes 1-3, C). C11-TAG and C11-PC bands were less intense in cells treated with etomoxir (Figure 23A lanes 1-6, C, D). When 3T3-L1 cells were pulsed with C19-FA for 1 hour and then chased, the amount of C19-TAG stayed relatively constant over time (Figure 23A lanes 7-12, E). The intensity of C19-TAG and C19-PC bands in cells treated with etomoxir was higher. However, the measured difference was not significant (Figure 23E, F).

An interesting result was the appearance of an additional TAG band in the pulse-chase experiment with C11-FA (probably indicating C11-FA elongation), which was much more intense in etomoxir untreated cells and increased over the time (Figure 23A lanes 1-6 and B).

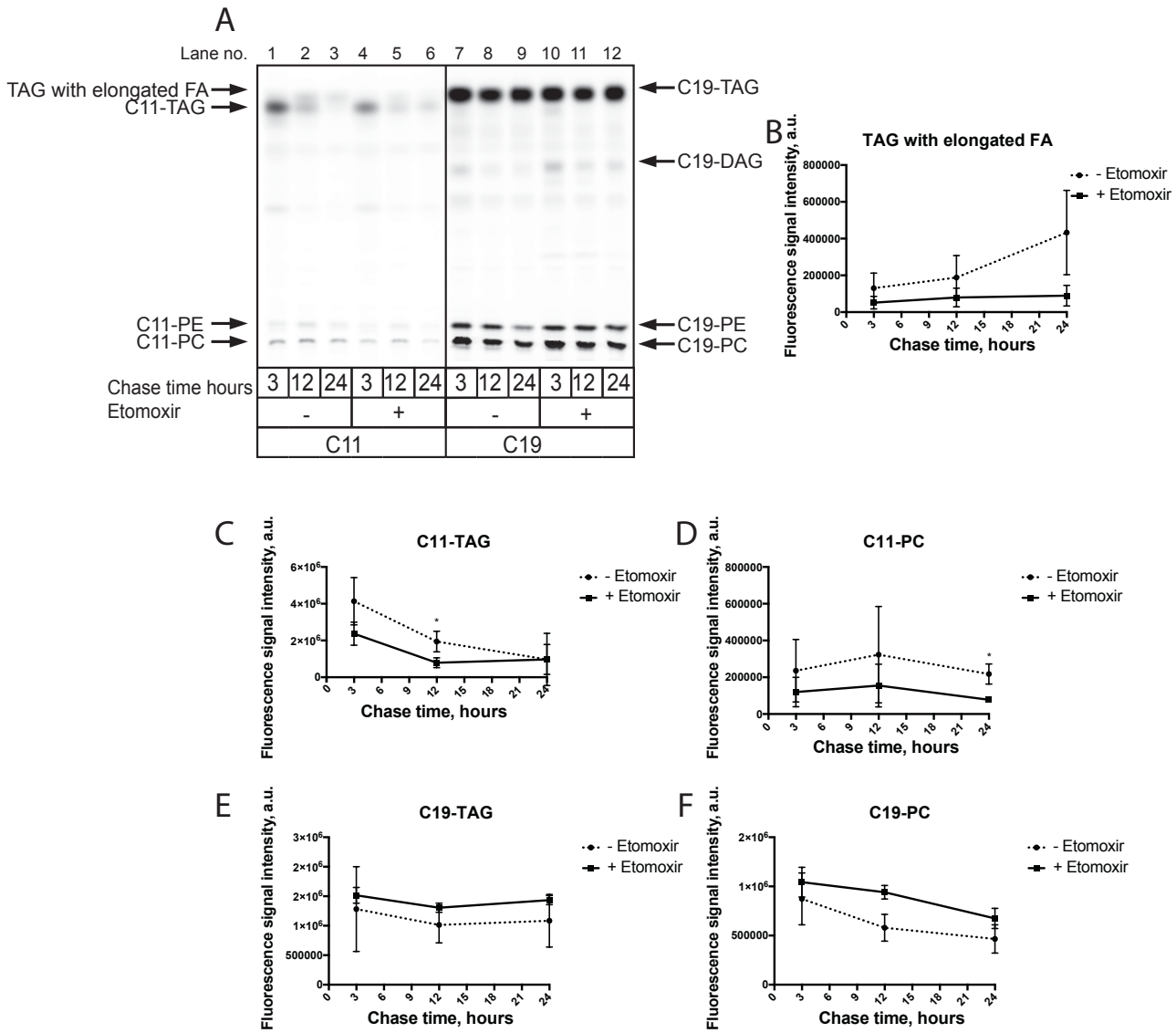

Figure 23. C11 and C19-FA pulse-chase experiments in 3T3-L1 cells.
3T3-L1 cells were grown in 12-well plates until confluence. After two more days, a differentiation medium was added for 4 days. After 4 days, the medium with 50 μM of C11-FA or C19-FA in the presence or in the absence of 50 μM etomoxir was added for 1 hour. After this pulse period, the medium was removed and fresh chase medium with or without etomoxir was added for chase times indicated in panel A. After this time period, the cells were washed and lipids were extracted. Then the click reaction was performed. Finally, lipids were separated on a TLC plate and fluorescence was detected by fluorescence imaging. Graphs B, C and D illustrate quantifications of bands from panel A lanes 1-6 (TAG with elongated FA, C11-TAG and C11-PC bands). Graphs E and F illustrate quantifications of bands from panel A lanes 7-12 (C19-TAG and C19-PC bands). The data represent mean ±SD, n=3 for C11 feeding and n=2 for C19 feeding.

4.5.2.6. Extraction and alkaline hydrolysis experiment with lipids from the medium

In order to find out more about the nature of the unknown bands appearing in the medium of dedifferentiated hepatocytes fed with C11-FA (Figure 12A lane 5), different lipid extractions were performed and extracted lipids were hydrolyzed under alkaline conditions. When the lipids were extracted from the medium using water, no signal of unknown bands could be detected on the TLC plate (Figure 24 lane 2). Substances representing unknown bands could only be extracted with a 1% acetic acid (Figure 24 lane 1). This indicates a hydrophilic nature of these substances and the most probable existence of least one carboxyl group. With an alkaline hydrolysis experiment, it was shown that at least X and Y bands were not hydrolyzed. The Z-band was either partially hydrolyzed or was lost during the extraction procedure. The most intensive of the "unknown" bands was hydrolyzed (Figure 24 lane 3). The only additional hydrolysis product could be detected at the height of C19-FA (Figure 24, lane 3). However, the click reaction mixture background band, which could be seen in Figure 24, lanes 1 and 2 also runs at this height. It is difficult to say if this band is actually a product of hydrolysis or just a background band. It is also not clear where the clickable hydrolysis product disappeared.

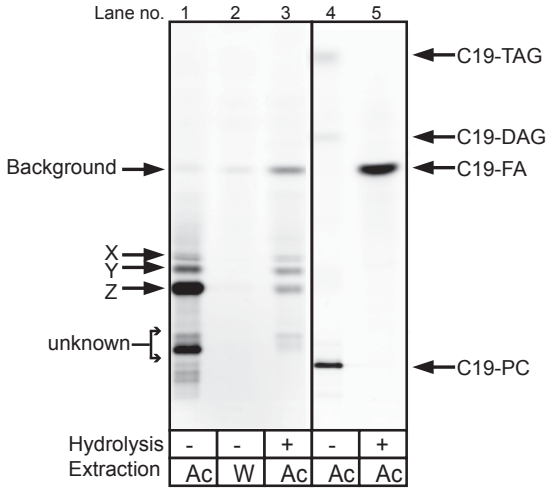

Figure 24. Extraction and alkaline hydrolysis experiment with the medium from dedifferentiated hepatocytes fed with C11-FA overnight.
After isolation from mouse liver hepatocytes were plated on collagen coated 10 cm dishes. 3.2 million cells were plated per one dish. The cells were grown in the incubator for 3 days. Then 50 µM of C11-FA was added to the cells for overnight feeding. After feeding the medium was collected. 150 µl of the medium was used for lipid extraction with water (W) or with 1 % acetic acid (Ac). One probe of acetic acid extraction was used for alkaline hydrolysis. C19-TAG, C19-DAG and C19-PC, used as controls for hydrolysis efficiency, were completely hydrolyzed to C19-FA (lanes 4 – 5). X, Y and Z indicate unknown hydrophilic substances.

4.5.3. TAG synthesis

If we now take a look at the pathway from FA outside the cell to TAG synthesis inside the cell, introduced in chapter 4.5, it can be excluded that a defect of C11-FA entry into the cell was the reason for the absence of C11-TAG synthesis in hepatocytes and in 3T3-L1 cells (4.5.1.1; 4.5.1.3). Acyl-CoA and TAG synthesis are the most interesting parts of this pathway and therefore they were investigated in the next step. At the initial screening of sequencing data of differentiating 3T3-L1 cells, several acyl-CoA and TAG synthesis related hit proteins were identified, of which the mRNA expression increased in the time period between 24 and 48 hours. Among these hits were ACSL1, GPAT3 (AGPAT9) and DGAT2 (Table 15, rows 13, 18 and 30). This was consistent with results obtained by Mikkelsen et al., 2010. They have shown that mRNA levels of these proteins extremely increase on day 2 of 3T3-L1 cell differentiation. In order to see a possible effect of these proteins on C11-FA metabolism they were overexpressed either alone or in different combinations in Hek293 cells; a cell line that cannot incorporate C11-FA into TAG. Original idea was to overexpress these proteins in undifferentiated 3T3-L1 cells and Huh7 cells, but as their overexpression was not efficient (data not shown) it was decided to take another cell line, namely Hek293, which is good at transfection and cannot synthesize C11-TAG, see chapter 4.1.3

4.5.3.1. Overexpression of DGAT2, AGPAT9 and ACSL1 in Hek293 cells

DGAT2, AGPAT9, and ACSL1 were overexpressed in Hek293 cells either alone or in different combinations. Overexpression of flag-tagged DGAT2 worked very efficiently (Figure 25B lanes 6, 7, 8, 10; FLAG row). Overexpression of the other plasmids especially in the triple combinations was weaker (Figure 25B). Nevertheless, none of the overexpressions affected the metabolic fate of C11-FA as no C11-TAG could be detected at all (Figure 25A). The amount of C19-TAG increased in all conditions where DGAT2 flag plasmid was present compared to GFP control (Figure 25A lanes 5, 7, 13, 15, 17 and 21; C). It could be that the overexpression of proteins was too weak to cause a significant metabolic effect on C11-FA metabolism. For this reason it was later decided to study the enzymatic activities of proteins participating in TAG synthesis more thoroughly.

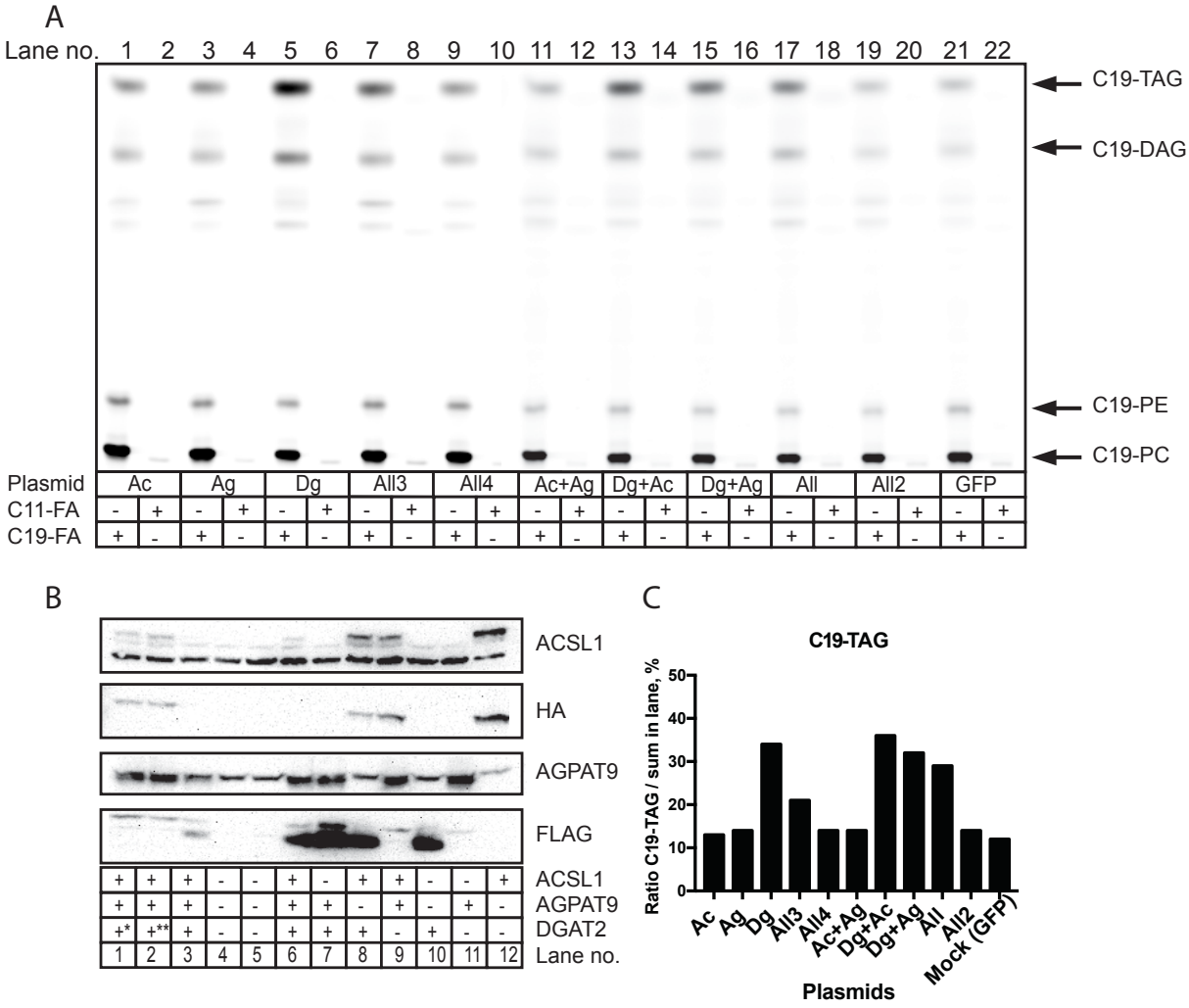

Figure 25. Overexpression of ACSL1, AGPAT9 and DGAT2 in Hek293 cells.
(A) Hek293 cells were grown up to 60-70% confluence and transfected with plasmids containing sequences for ACSL1, AGPAT9 and DGAT2 either alone or in different combinations. 24 hours after transfection the cells were fed with 50 μM of C11 or C19-FAs for 1.5 hours. The cells were washed and lipids were extracted from the cells. Then the click reaction was performed both with lipids from the medium and from the cells. Finally, lipids were separated on a TLC plate and the fluorescence was detected by fluorescence imaging. The different lipid classes, in which FAs were incorporated, are indicated on the right side of the image. AC stands for ACSL1 with HA tag, Ag – AGPAT9 with flag tag, Dg – DGAT2 with flag tag, All – all three plasmids together. In "All2" different DGAT2 plasmids, which had HA tag instead of flag tag were used. In "All4" different DGAT2 plasmids, which had no tag at all were used. In "All3" different transfection reagent was used. In GFP – cells were transfected with GFP plasmid. (B) Western blot showing the overexpression. The table shows which plasmids were overexpressed. * marks that DGAT2 had an HA tag instead of Flag (lane 1). ** marks that DGAT2 had no tag at all (lane 2). Lane 4 represents untransfected cells, lane 5 represents a GFP transfection. The row with ACSL1 antibody shows a native ACSL1 protein (lower band) and an HA-tagged protein (higher band). The row with the HA antibody shows the HA-tagged ACSL1 protein. The AGPAT9 row shows native and transfected proteins. In the row for Flag antibody, flag-tagged AGPAT9 (higher band) and flag-tagged DGAT2 (lower band) can be seen. (C) Quantification of data in panel A. Values represent the fluorescence intensity of C19-TAG divided by the sum of fluorescence intensity of C19-TAG, C19-TAG, C19-PE and C19-PC.

4.5.3.2. Acyl-CoA synthesis assay with lysates from Huh7 cells and primary mouse hepatocytes

The acyl-CoA synthesis, GPAT, LPAAT and DGAT activities are important steps in the cellular TAG synthesis pathway, see chapter 1.4. A simplified TAG synthesis scheme is presented in Figure 26C. An interesting question was if any of these activities are disrupted in cells that cannot synthesize C11-TAG. To test this, lysates from Huh7 cells and primary mouse hepatocytes were prepared for activity assays. Both cell types are of liver origin, but Huh7 cells cannot convert C11-FA into TAG while hepatocytes can. In order to determine if both lysates are able to synthesize C11-CoA, an acyl-CoA synthesis assay was performed (Figure 26C step 2):

alkyne-FA + CoA + ATP ➔ alkyne-FA-CoA + AMP + PPi.

Unfortunately, it was not possible to perform a direct acyl-CoA synthesis assay, because during the extraction the acyl-CoA remained in the water phase and the click reaction, which followed afterward, was not compatible with salts present in the water phase. Different reaction buffers and click reaction conditions were tested. However, the click reaction did not work (data not shown). Therefore coupled acyl-CoA/LPCAT and acyl-CoA/LPAAT reactions were performed, where the additional substrates LPC (for LPCAT assay) or LPA (for LPAAT assay) were added. These substrates could react with forming acyl-CoA:

alkyne-FA + CoA + ATP ➔ alkyne-FA-CoA + AMP + PPi (acyl-CoA synthesis assay part);
alkyne-FA-CoA + LPA/LPC ➔ alkyne-PA/PC + CoA (LPAAT/LPCAT assay part).

The products from these coupled reactions (PA or PC) could be extracted in the chloroform phase and the click reaction could be performed. As can be seen from Figure 26A lanes 7 and 8 in a purple boxed area, both lysates could synthesize C11-CoA, as C11-PC was detected in the coupled assay. When LPA was the additional substrate, no C11-PA was detected in the samples with both lysates (Figure 26A lanes 3 and 4 in a purple boxed area). However, C11-TAG (a final product of the glycerol phosphate pathway) was detected upon a longer exposure of the TLC plate (Figure 26A, lanes 3 and 4, in “longer explosion” part). The ability of both lysates to synthesize C11-TAG was later confirmed by a DGAT assay (Figure 27).

An LPCAT assay was performed as an additional control to determine if the PC synthesis from acyl-CoA and LPC could influence the result of the acyl-CoA synthesis assay (Figure 26B):

alkyne-FA-CoA + LPC ➔ alkyne-PC + CoA.

This turned out not to be the case as both Huh7 and hepatocyte lysates were comparably effective in the LPCAT assay, i.e. the amount of C11-PC was similar in assays with both lysates (Figure 26B lanes 1 and 2 in the orange boxed area). It is evident from these results that both lysates had active enzymes for acyl-CoA synthesis from the C11-FA. Later on it was analyzed if the ability to synthesize LPA, PA and TAG from C11-acyl-CoA was impaired in Huh7 lysates.

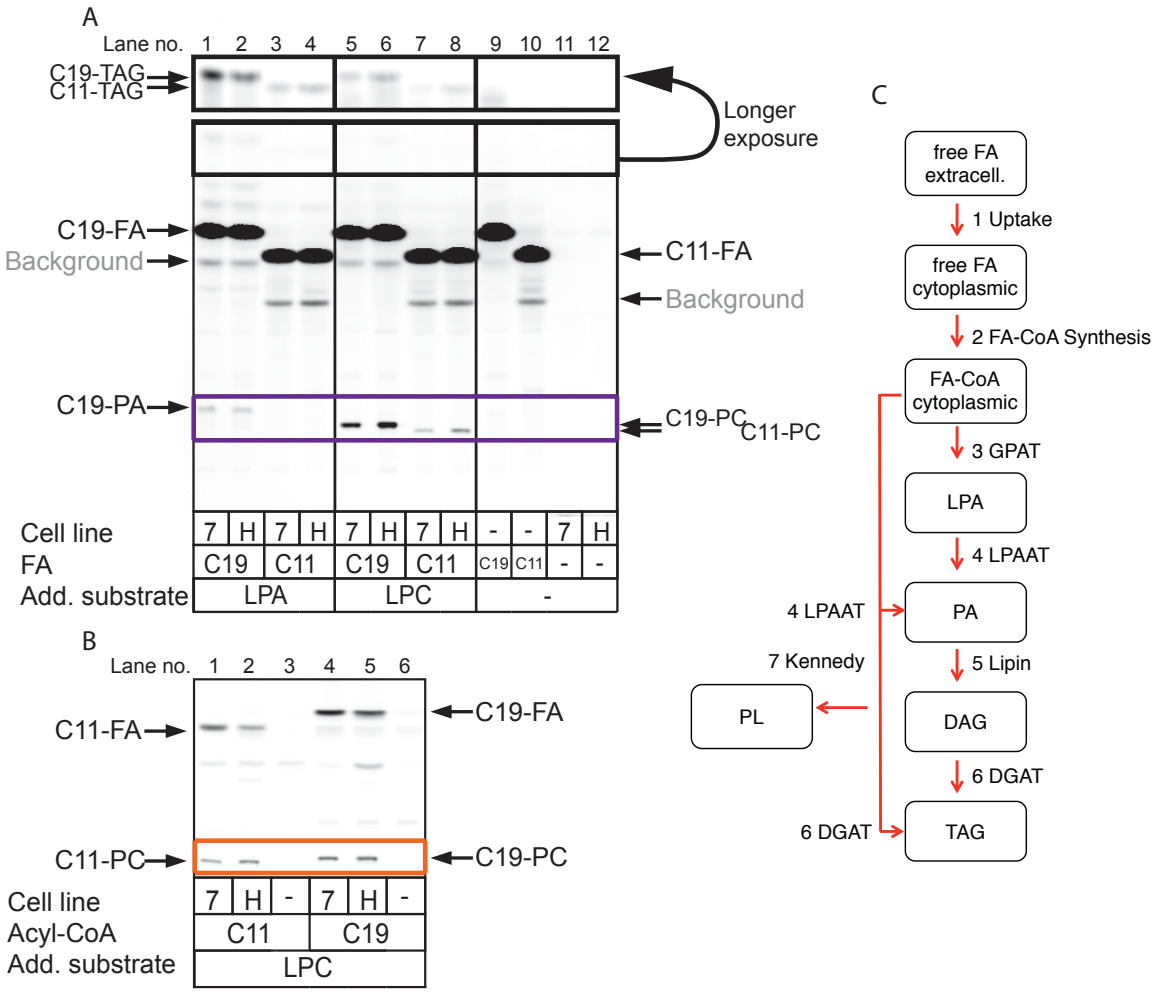

Figure 26. Coupled acyl-CoA synthesis assays with lysates from Huh7 cells and primary mouse hepatocytes.
(A) C11 or C19-FAs and LPA or LPC were added to a reaction tube and chloroform and ethanol were evaporated. Then 13 µl of delipidated BSA was added and the tube was vortexed. The reaction mixture containing CoA and ATP was added. Finally, a lysate containing 200 µg of total protein was added and the mixture was incubated at 30°C for 30 min while shaking at 800 rpm. The reaction was stopped by adding a mixture of chloroform and methanol. Lipids were extracted and the click reaction was performed. Finally, lipids were separated on a TLC plate and fluorescence was detected by fluorescence imaging. "7" indicates the lysate from Huh7 cells and "H" indicates the lysate from primary mouse hepatocytes. "Add. Substrate" indicates the additional substrate, which was added to the reaction mixture. The upper part of the plate is additionally showed as a longer exposition image to make TAG visible. (B) LPCAT assay. First, the reaction buffer containing CoAs (C11 or C19), HSLi and LPC was added. Then the lysate containing 200 µg of total protein was added and the mixture was incubated at 30°C for 30 min with shaking at 800 rpm. Finally, the same extraction procedure followed as described in panel A. (C) Graphical representation of the pathway from FA outside the cell to TAG synthesis inside the cell.

4.5.3.3. DGAT, LPAAT and GPAT assays with lysates from Huh7 cells and primary mouse hepatocytes

In the DGAT assay alkyne-CoAs react with DAG to form TAG (Figure 26C step 6):

alkyne-FA-CoA + DAG ➔ alkyne-TAG + CoA.

For the DGAT assay four different DAGs were used to find out the best conditions for the reaction. As can be seen from Figure 27A lanes 5-16 in the purple boxed area and Figure 27C lanes 9-12 in the purple boxed area, the best substrates for an *in vitro* assays were DAGs with C10:0 and C8:0 FAs. With these DAGs reasonable amounts of both C11 and C19-TAGs were produced. In C12:0 and C18:1 DAG conditions (Figure 27A lanes 5-8 in the purple boxed area and Figure 27C lanes 9-12 in the purple boxed area) TAG bands were slightly more intense than in the assay with only alkyne-FA-CoA (Figure 27A lanes 1-4 in the purple boxed area). Both Huh7 and hepatocyte lysates could convert C11-CoA and DAG into TAG. The ratio C11-TAG/C19-TAG was similar for both cell lysates (Figure 27B).

This was also nicely confirmed by the LPAAT assay (Figure 26C step 4):

alkyne-FA-CoA + LPA ➔ alkyne-PA + CoA.

When LPA and C11-CoA were present in the assay mixture, C11-PA (Figure 27C lanes 7-8 in the green boxed area), C11-DAG (Figure 27C lanes 7-8 in the blue boxed area) and even traces of C11-TAG (Figure 27C lanes 7-8 in the purple boxed area) could be identified in samples with each lysate. Moreover, the ratio of C11-PA/C19-PA was the same in lysates from Huh7 cells and hepatocytes (Figure 27D).

Unfortunately, the GPAT assay (Figure 26C step 3) did not work for C11-CoA as no C11-LPA or C11-PA could be identified (Figure 27C, lanes 3 and 4 in the orange boxed area).

GPAT assay:

G3P + alkyne-FA-CoA ➔ alkyne-LPA + CoA.

Generally speaking, as both lysates from Huh7 cells and hepatocytes could synthesize acyl-CoA, PA and TAG from C11-FA the reason for the absence of C11-TAG synthesis in intact Huh7 cells most probably was caused by other mechanisms than the absence of metabolizing proteins.

Although Huh7 and hepatocytes both derive from the liver, they are different cells. Huh7 originates from human carcinoma, while hepatocytes are primary mouse cells. In order to compare the ability to synthesize C11-CoA, C11-LPA, C11-PA and C11-TAG in more related cells, assays were performed with lysates from: freshly isolated hepatocytes and dedifferentiated hepatocytes kept in the medium for four days; undifferentiated 3T3-L1 cells and 3T3-L1 cells differentiated for 10 days.

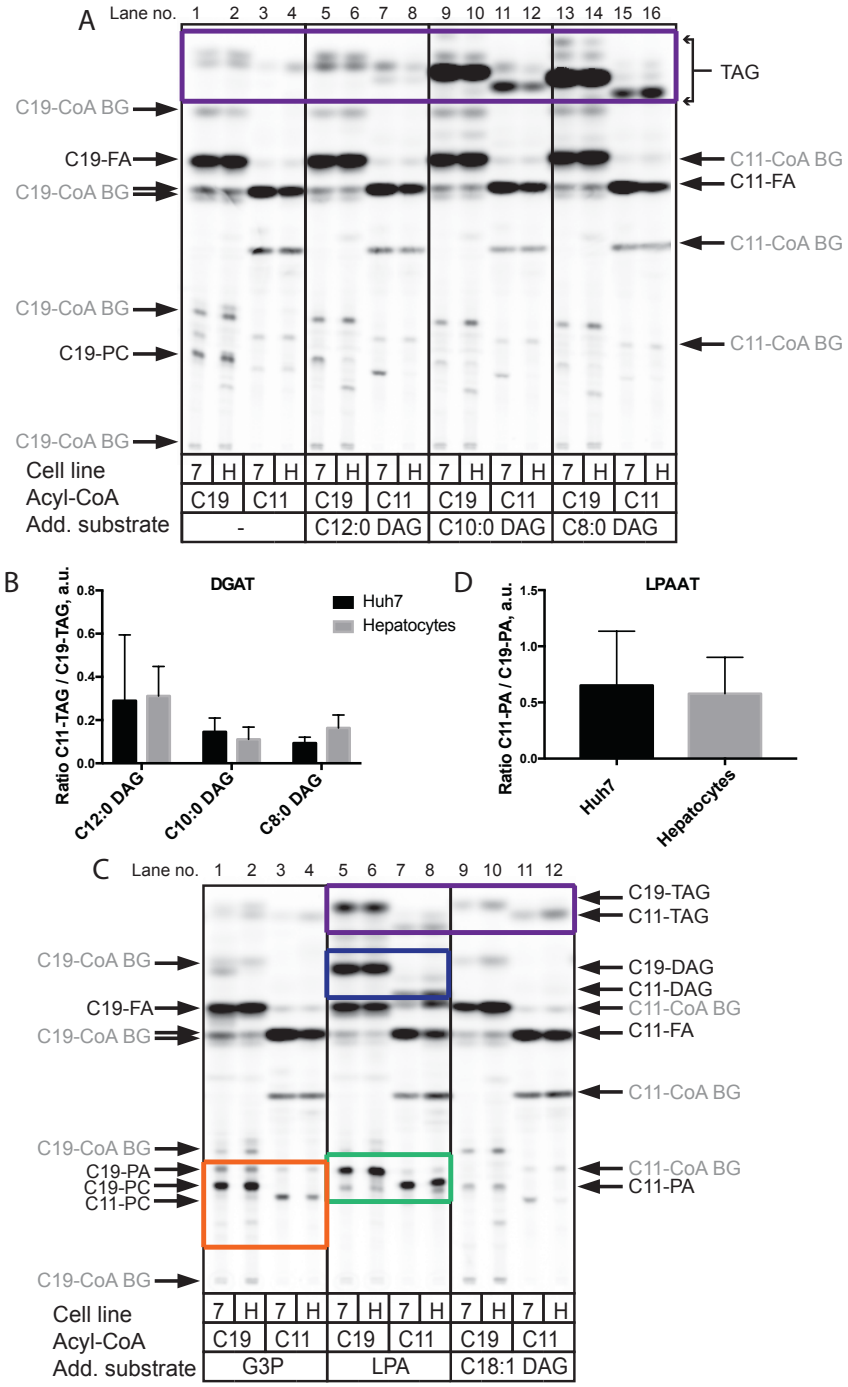

Figure 27. DGAT, GPAT and LPAAT assays with lysates from Huh7 cells and primary mouse hepatocytes.

For the DGAT assays (A, C) DAG (C12:0, C10:0, C8:0 or C18:1) was added to the reaction tube and chloroform was evaporated. Then PC and reaction buffer with CoAs (C11 or C19) and HSLi were added. For the GPAT and LPAAT assays (C) the reaction buffer containing CoAs (C11 or C19), HSLi and either G3P or LPA respectively was added to the reaction tube. Finally, lysate containing 30 µg of total protein was added to all types of assays and the mixture was incubated at 30°C for 30 min with shaking at 800 rpm. The reactions were stopped by adding a mixture of chloroform and methanol. Lipids were extracted and the click reaction was performed. Finally, lipids were separated on a TLC plate and fluorescence was detected by fluorescence imaging. "7" indicates a lysate from Huh7 cells and "H" a lysate from primary mouse hepatocytes. "Add. Substrate" indicates the additional substrate, which was added to the reaction mixture. C11-CoA has three unspecific background (BG) bands shown in grey color while C19-CoA has four unspecific BG bands. Graph B illustrates quantification of data in panel A. Values represent fluorescence intensity of C11-TAG divided by fluorescence intensity of C19-TAG (purple boxed areas). Graph D illustrates quantifications of the data in panel C lanes 5-8 (green boxed area). Values represent fluorescence intensity of C11-PA divided by fluorescence intensity of C19-PA. The data represent mean +SD, n=3.

4.5.3.4. Acyl-CoA synthesis assay with lysates from 3T3-L1 cells and primary mouse hepatocytes

It was shown that undifferentiated 3T3-L1 cells and dedifferentiated hepatocytes cannot synthesize C11-TAG from C11-FAs (see Figure 9 and Figure 11). The gain of function feature of differentiating 3T3-L1 cells and the loss of function feature of dedifferentiating hepatocytes was used for activity assays. First, lysates from freshly isolated hepatocytes and from hepatocytes kept in the medium for four days as well as from undifferentiated 3T3-L1 cells and from 3T3-L1 cells differentiated for 10 days were prepared. As in the previous experiment (4.5.3.2) an acyl-CoA synthesis assay coupled with LPCAT assay was performed. From the coupled acyl-CoA synthesis assay it could be seen that both hepatocyte lysates had similar acyl-CoA activities towards C11-CoA synthesis (Figure 28A, lanes 1-4 in the purple boxed area, Figure 28B). The activities in the control LPCAT assay were also similar (Figure 28C, lanes 1-4 in the orange boxed area, Figure 28D). On the other hand, the lysate from differentiated 3T3L1 cells was much more effective in C11-CoA synthesis compared to the undifferentiated cells (Figure 28A, lanes 5-8 in the purple boxed area, Figure 28B). This difference is even more pronounced as undifferentiated cells had more activity in the control LPCAT assay (Figure 28C, lanes 5-8 in the orange boxed area, Figure 28D). Next, hydrolysis experiment with pancreatic lipase was done. This experiment should help to see at which position of TAG molecule C11-FA is incorporated in order to better understand, which enzymatic activity contributes to C11-TAG synthesis in 3T3-L1 cells and primary mouse hepatocytes.

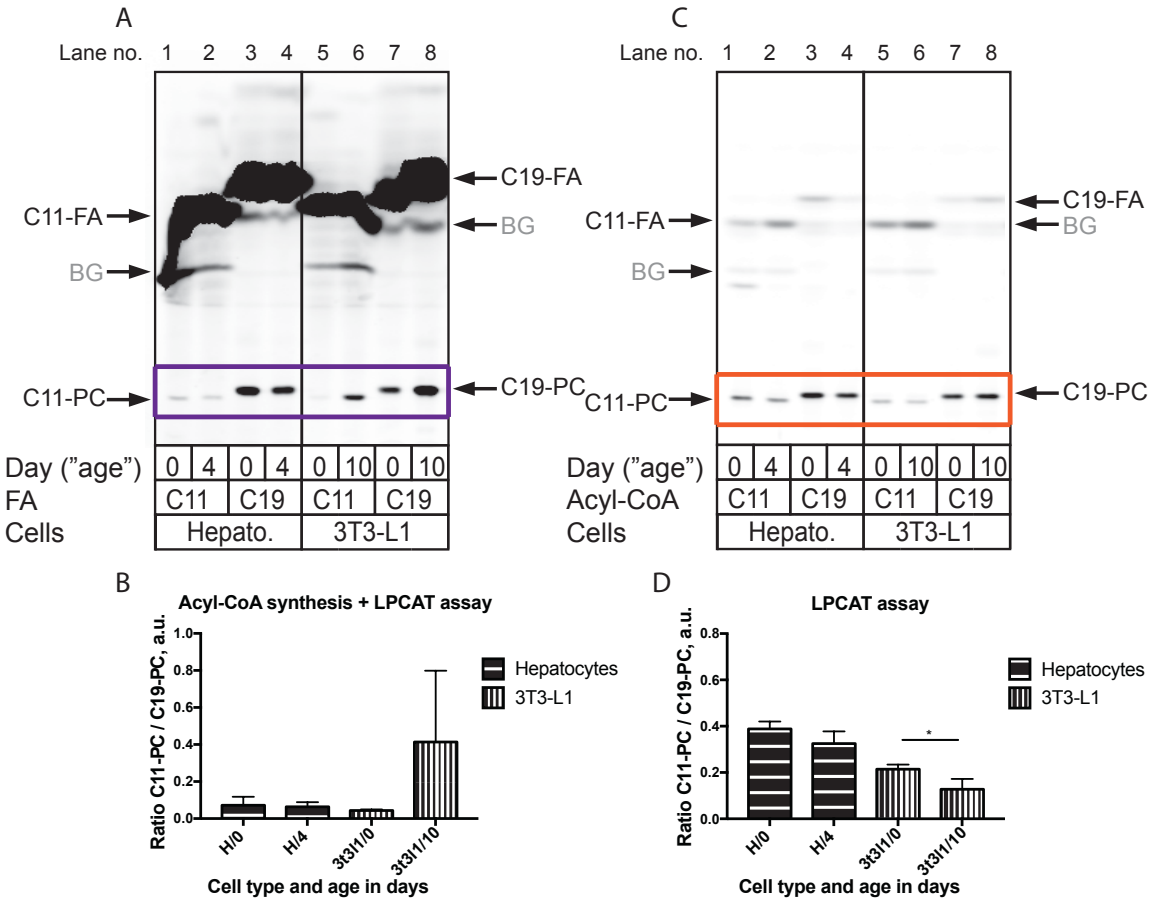

Figure 28. Coupled acyl-CoA synthesis assays with lysates from primary mouse hepatocytes and 3T3-L1 cells.
In A and C lysates from freshly isolated hepatocytes (day 0) or hepatocytes kept in culture for 4 days (day 4) after isolation were used as well as lysates from undifferentiated 3T3-L1 cells (day 0) or 3T3-L1 cells that were differentiated for 10 days (day 10). (A) First, C11 or C19-FAs and LPC were added to the reaction tubes and chloroform and ethanol were evaporated. Then 13 µl of DL-BSA was added and the tube was vortexed and the reaction mixture containing CoA and ATP was added. Finally, the lysate containing 200 µg of total protein was added and the mixture was incubated at 30°C for 30 min while shaking at 800 rpm. The reaction was stopped by adding a mixture of chloroform and methanol. Lipids were extracted and the click reaction was performed. Finally, lipids were separated on a TLC plate and fluorescence was detected by fluorescence imaging. (C) LPCAT assay. Same conditions as in Figure 26, panel B. Graph B illustrates quantifications of data in panel A. The values represent fluorescence intensity of C11-PC (detected in lanes 1, 2, 5, 6 in purple boxed area) divided by fluorescence intensity of C19-PC (detected in lanes 3, 4, 7, 8 in purple boxed area). Graph D illustrates quantifications of data in panel C. Values represent fluorescence intensity of C11-PC (detected in lanes 1, 2, 5, 6 in orange boxed area) divided by fluorescence intensity of C19-PC (detected in lanes 3, 4, 7, 8 in orange boxed area). The data represent mean +SD, n=3. * stands for $p \leq 0.05$.

4.5.3.5. Lipase treatment

The experiment described in this chapter was performed to determine at which stereospecific position of the TAG molecule C11-FA was incorporated. A pancreatic lipase treatment was performed with TAGs from both differentiated 3T3-L1 cells and freshly isolated hepatocytes fed with C11-FA. During the lipolysis process, the pancreatic lipase hydrolyzes TAG at *sn1* and *sn3* positions. Using this method it is possible to show if the FA of interest is at the *sn1*/*sn3* or at the *sn2* position, see Figure 29B. As evident from Figure 29A lanes 1-4, when standard TAG with C11-FA at the *sn2* position was hydrolyzed, the main clickable product of hydrolysis was C11-MAG (lane 2). On the other hand, during the hydrolysis of *sn3* labeled C11-TAG, the main clickable product was C11-FA (lane 4).

Later the cellular lipids from differentiated 3T3-L1 cells and hepatocytes both fed with C11-FA were analyzed. First of all, neutral lipids were separated from all other lipids by applying chromatography. Then a lipase treatment was performed and the main product, which was identified on a TLC plate for both 3T3-L1 cells and hepatocytes, was C11-FA (Figure 29A, lanes 6 and 8). This indicates that in both cases C11-FA was incorporated mainly at *sn1* or *sn3* position. In the glycerol-3-phosphate pathway, GPATs are responsible for the incorporation of FA at the *sn1* position and DGATs incorporate FAs at the *sn3* position, see chapters 1.4.2 and 1.4.5. As the GPAT activity in the glycerol-3-phosphate pathway is rate limiting (Wendel et al., 2009) it is most likely, that C11-FAs get directly incorporated into already existing DAGs to form TAG molecules via DGAT activity. In the next section LPAAT, DGAT and GPAT assays with lysates from 3T3-L1 cells and primary hepatocytes are analyzed.

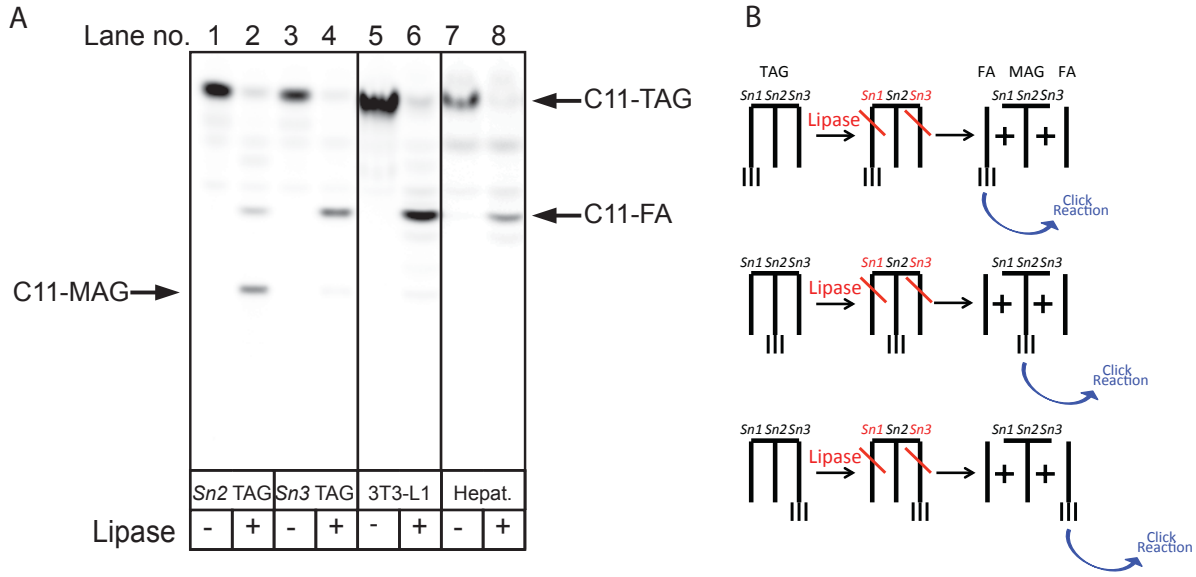

Figure 29. TAG treatment with a pancreatic lipase.
(A) TAG standards having C11-FA at either *Sn2* or *Sn3* positions and TAGs isolated from cellular lipids from differentiated 3T3-L1 cells and primary mouse hepatocytes fed with 50 µM C11-FA for 1.5 hours were treated with a pancreatic lipase. After treatment lipids were extracted and the click reaction was performed. Finally, lipids were separated on a TLC plate and fluorescence was detected by fluorescence imaging. (B) Principal scheme illustrating hydrolysis of *Sn1* or *Sn2* or *Sn3* alkyne-labeled TAG. Pancreatic lipase hydrolyzes TAG molecule both at *Sn1* and *Sn3* positions. Products of hydrolysis are used for the click reaction. If alkyne-FA is detected on TLC plate, then it means that alkyne-FA was at either *Sn1* or *Sn3* position. If alkyne-MAG is detected on TLC plate, then alkyne-FA was at *Sn2* position.

4.5.3.6. LPAAT synthesis assay with lysates from 3T3-L1 cells and primary mouse hepatocytes

The LPAAT assay was performed in a similar way as in 4.5.3.3. The lysates from freshly isolated hepatocytes and from hepatocytes, which were kept in the medium for four days, as well as from undifferentiated 3T3-L1 cells and from 3T3-L1 cells differentiated for 10 days were used. Moreover, two types of LPA and acyl-CoA were used. In the first LPAAT assay, alkyne-acyl-CoAs and normal LPA were used. In the second assay, normal acyl-CoAs and alkyne-LPA were used.

In both LPAAT assays the ratio C11-PA/C19-PA (Figure 30A lanes 1-8 in green boxed area, Figure 30C) and the ratio C10-PA/C18-PA (Figure 30B in green boxed area, Figure 30D) was lower in lysates from day 4 hepatocytes and undifferentiated 3T3-L1 compared to day 0 hepatocytes and day 10 3T3-L1 cells, respectively. This indicates a lower LPAAT activity towards medium-chain acyl CoAs in these lysates. However, this decrease in the ratio was not extremely high just in the range of 30-40%. The

sequencing data show that the expression of two AGPAT proteins (AGPAT2 and AGPAT3 also known as LPAAT2 and LPAAT3, see chapter 1.4.3) decrease during hepatocyte dedifferentiation (Table 15, gene no. 22 and 23). Similarly, the expression of AGPAT2 in 3T3-L1 cells increases upon differentiation (Table 15, gene no. 22). A feasible explanation would be that these AGPAT proteins are more specific for C11-PA synthesis than other members of the AGPAT family and therefore the LPAAT activity decreases when there is less of these proteins (in dedifferentiated hepatocytes and undifferentiated 3T3-L1 cells). Similarly as in LPAAT assay, described in chapter 4.5.3.3, DAG and TAG bands (Figure 30A lanes 1-8 in the purple boxed area and Figure 30B lanes 1-8 in the purple boxed area) and DAG bands (Figure 30A lanes 1-8 in the blue boxed area and Figure 30B lanes 1-8 in the blue boxed area) were detected.

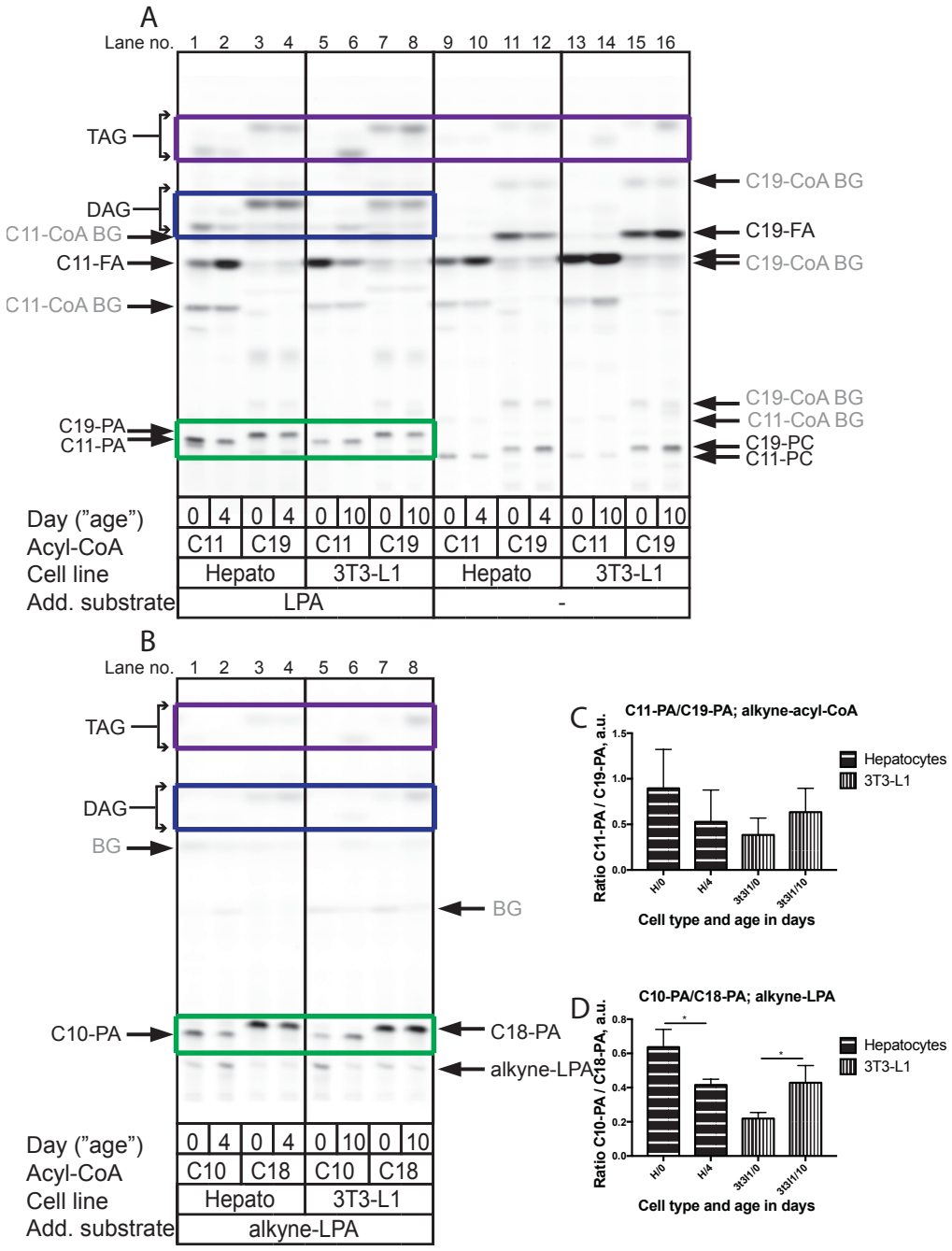

Figure 30. LPAAT assays with lysates from primary mouse hepatocytes and 3T3-L1 cells.
In A and B lysates from freshly isolated hepatocytes (day 0) or hepatocytes kept in culture for 4 days (day 4) after isolation were used as well as lysates from undifferentiated 3T3-L1 cells (day 0) or 3T3-L1 cells that were differentiated for 10 days (day 10). First, the reaction buffer was added, which contained HSLi, C11 or C19-CoAs (A), C10 or C18 CoAs (B) and LPA (A) or alkyne-LPA (B). Finally, the lysate containing 30 µg of total protein was added to all types of assays and the mixture was incubated at 30°C for 30 min with shaking at 800 rpm. Reactions were stopped by adding a mixture of chloroform and methanol. Lipids were extracted and the click reaction was performed. Finally, lipids were separated on a TLC plate and fluorescence was detected by fluorescence imaging. In panel A both C11-CoA and C19-CoA have three unspecific background bands (BG) each shown in grey color. Graph C illustrates quantifications of data in panel A. Values represent the fluorescence intensity of C11-PA (detected in lanes 1, 2, 5 6 in green boxed area) divided by the fluorescence intensity of C19-PA (detected in lanes 3, 4, 7 8 in green boxed area). Graph D illustrates the quantifications of the data in panel B. Values represent fluorescence intensity of C10-PA (detected in lanes 1, 2, 5, 6 in green boxed area) divided by fluorescence intensity of C18-PA (detected in lanes 3, 4, 7, 8 in green boxed area). The data represent mean +SD, n=4 (A), n=3 (B). * stands for p≤0.05.

4.5.3.7. DGAT and GPAT synthesis assays with lysates from 3T3-L1 cells and primary mouse hepatocytes

DGAT and GPAT assays were performed in a similar way as in chapter 4.5.3.3. Lysates from freshly isolated hepatocytes and from hepatocytes kept in the medium for four days as well as from undifferentiated 3T3-L1 cells and from cells differentiated for 10 days were used. C10-DAG was used as a DAG source. It was shown that the ratio between C11 and C19-TAG stayed the same in assays with lysates from both fresh and dedifferentiated hepatocytes (Figure 31A lanes 9-12 in the purple boxed area, Figure 31B). This indicates that although dedifferentiated hepatocytes cannot synthesize C11-TAG when fed with C11-FA, lysates from these cells have enzymes for C11-TAG synthesis from C11-acyl-CoA.

Figure 31B shows that the ratio between C11 and C19-TAG was lower in the lysate from undifferentiated 3T3-L1 cells compared to the lysate from differentiated cells (Figure 31A lanes 13-16 in the purple boxed area, Figure 31B). This suggests that the lysate from undifferentiated cells is not as effective in C11-TAG synthesis as a lysate from differentiated cells.

Unfortunately, the GPAT assay did not work for C11-CoA as no C11-LPA or C11-PA could be identified (Figure 31A lanes 1, 2, 5 and 6 in the orange boxed area). On the other hand, C19-PA was identified (Figure 31A lanes 3, 4, 7 and 8 in the orange boxed area).

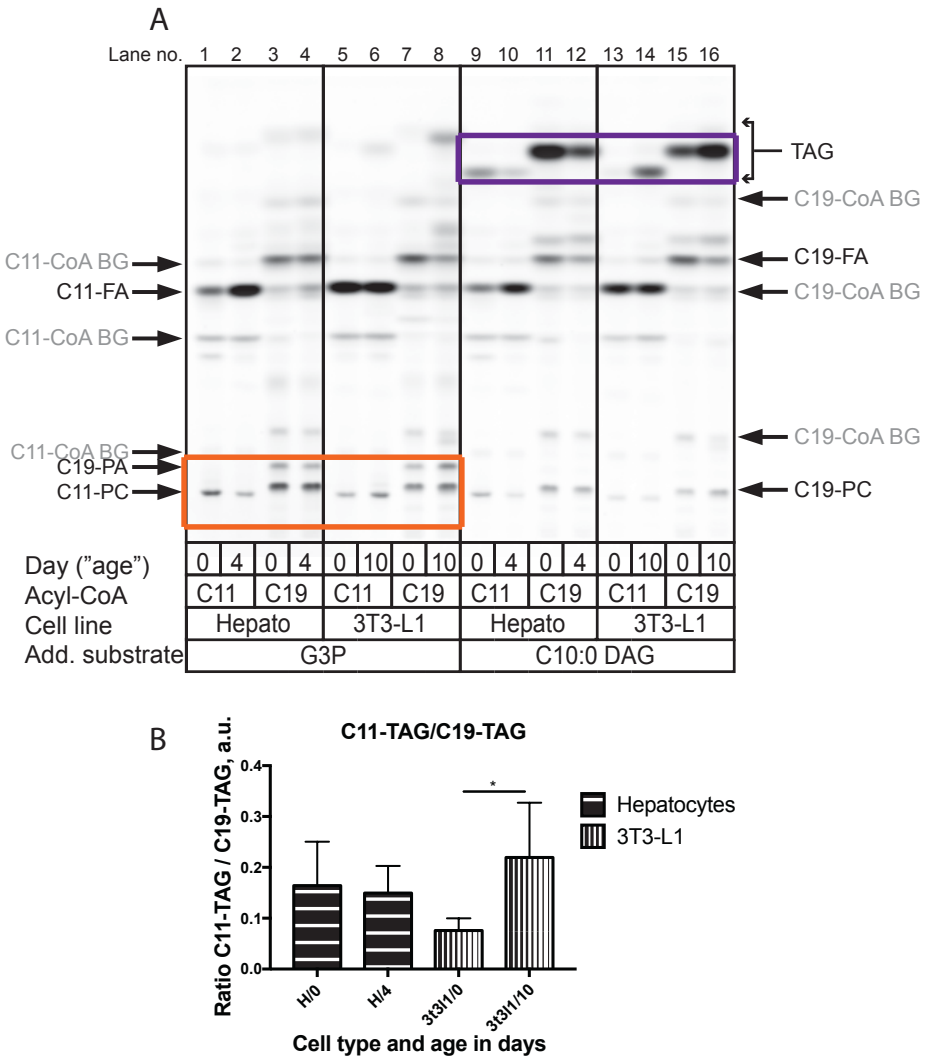

Figure 31. DGAT and GPAT assay with lysates from primary mouse hepatocytes and 3T3-L1 cells.

(A) Lysates from freshly isolated hepatocytes (day 0) or hepatocytes kept in culture for 4 days (day 4) after isolation were used as well as lysates from undifferentiated 3T3-L1 cells (day 0) or 3T3-L1 cells that were differentiated for 10 days (day 10). For DGAT assays first C10:0 DAG was added to the reaction tube and chloroform was evaporated. Then PC and reaction buffer with CoAs (C11 or C19) and HSLi were added. For the GPAT assay the reaction buffer containing CoAs (C11 or C19), HSLi and G3P was added to the reaction tube. Finally, the lysate containing 30 µg of total protein was added to both assays and the mixture was incubated at 30°C for 30 min with shaking at 800 rpm. Reactions were stopped by adding a mixture of chloroform and methanol. Lipids were extracted and the click reaction was performed. Finally, lipids were separated on a TLC plate and fluorescence was detected by fluorescence imaging. Both C11-CoA and C19-CoA have three unspecific background bands (BG) each shown in grey color. Graph B illustrates quantification of data in panel A. Values represent fluorescence intensity of C11-TAG (detected in lanes 1, 2, 5, 6 in purple boxed area) divided by fluorescence intensity of C19-TAG (detected in lanes 3, 4, 7, 8 in purple boxed area). The data represent mean +SD, n=5.

4.5.3.8. Competition assay in hepatocytes

In the experiments described in this chapter cells were incubated in the presence of multiple FAs. The purpose was to determine if C11-FA and C19-FA influence the metabolism of each other. It was also important to verify if and at which concentrations C11-FA competes with C10:0 FA or C18:1 FA and weather C19-FA competes with C18:1 FA or C10:0 FA. For this a competition assay with different combinations of C11-FA, C19-FA, C10:0 and C18:1 FAs was performed.

Figure 32A, B shows that at concentrations up to 50 μM neither C10-FA nor C18-FA nor C19-FA competed with C11-FA as no decrease in C11-TAG synthesis was detected. Moreover, the amount of C11-TAG increased significantly after adding C10:0 FA (Figure 32A lane 2 compared to lane 4; B), while the addition of C18:1 did not cause such an effect (Figure 32B lane 1 compared to lane 4, B). This could be explained by sparing C11-FA from β-oxidation. As at smaller concentrations C10:0 and C18:1 FAs didn't compete with C11-FA, the amount of these FAs was raised up to 500 μM. The amount of C11-TAG increased slightly after raising C10-FA concentration up to 100 μM (Figure 32C lanes 9-11, E dark bars). By raising the concentration of C10-FA to 500 μM the amount of C11-TAG decreased and additional two lower TAG bands appeared (Figure 32C lane 12, E dark bars). These additional bands indicated the presence of TAGs with two and with three MCFAs. Similarly, three TAG bands appeared in C19-FA fed cells, when the competitor was C10-FA at concentration of 500 μM (Figure 32C lane 4). These three bands indicated the presence of TAGs with none, one or two MCFAs. Native lipids in hepatocytes mostly have LCFAs. The resulting TAG, which is observed in C11-FA experiments with up to 100 μM of competitor FAs had two LCFAs and one MCFA (C11-FA). When 500 μM of C10-FA was added two additional types of TAG were synthesized, namely TAG having two MCFAs and one LCFA as well as TAG having three MCFAs. TAG that includes one C11-FA, one C10-FA and one LCFA runs lower on the TLC plate as TAG that includes only one C11-FA and two LCFAs. Furthermore, TAG with one C11-FAs and two C10-FAs would run even lower than the one containing one C11-FA, one C10-FA and one LCFA. When 500 μM of C10-FA was added together with C19-FA, two additional types of TAG were synthesized, namely TAG having two LCFAs and one C10-FA as well as TAG having one LCFA and two C10-FAs. TAG that includes two LCFAs and one C10-FA runs lower on the TLC plate as TAG that includes three LCFAs. Furthermore, TAG with

one C19-FAs and two C10-FAs would run even lower than the one containing two LCFAs and one C10-FA. After 500 µM of C18:1 FA was added to the cells the amount of C11-TAG increased significantly (Figure 32C lane 16, E light bars). In this experiment neither the addition of C11-FA (Figure 32A lanes 9-12, B) nor C10:0 (Figure 32C lanes 1-4, D dark bars) nor C18:1 (Figure 32C lanes 5-8, D light bars) significantly changed the C19-TAG amount.

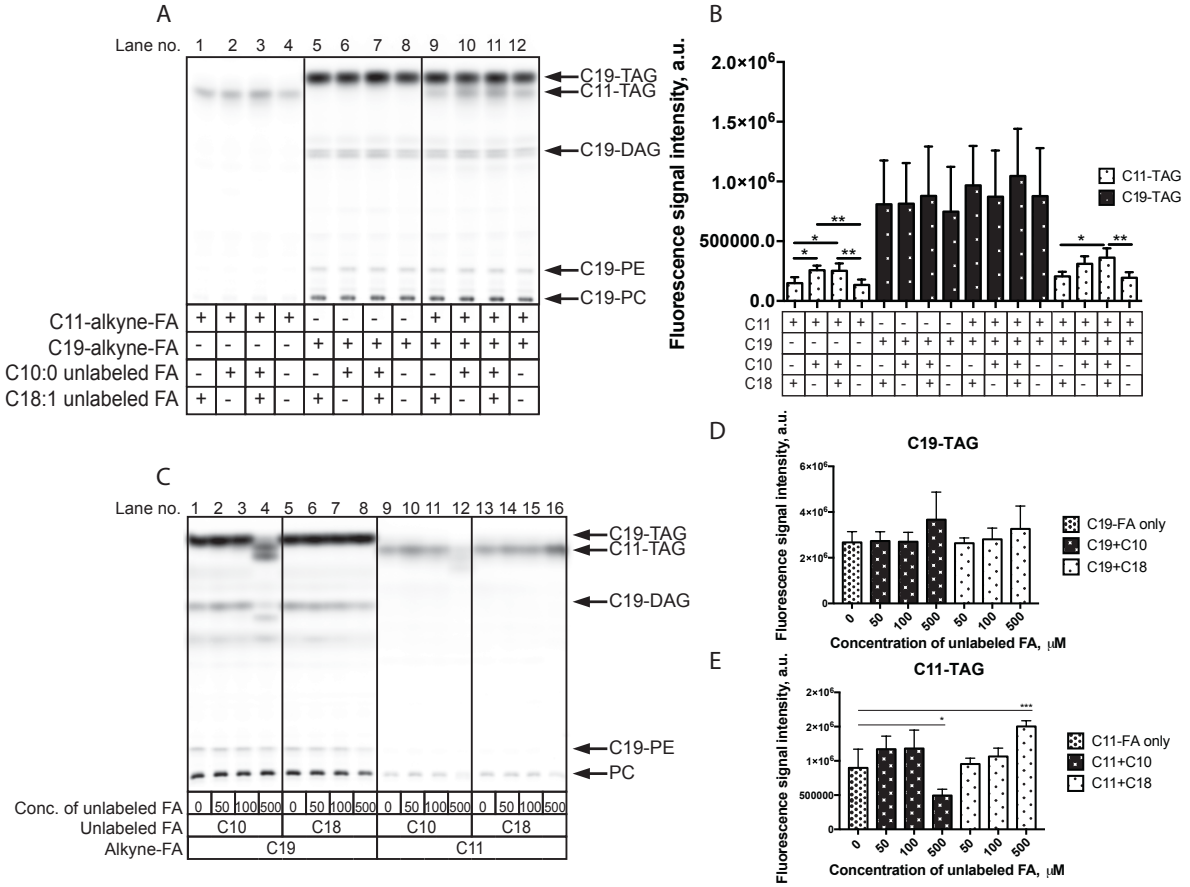

Figure 32. Medium and long-chain FA competition experiment in primary mouse hepatocytes.
After isolation from the liver, primary mouse hepatocytes were plated on collagen coated 12-well dishes. 150.000 cells were plated per well. (A) Different combinations of C11-FA, C19-FA, C10-FA (C10:0, decanoate) and C18-FA (C18:1, oleate) were added to cells for 1.5 hours. 20 µM of C11-FA, 20 µM of C19-FA, 50 µM of C10-FA and 50 µM of C18-FA were used. (C) cells were fed with 50 µM of C11-FA or C19-FAs for 1.5 hours. Additionally, 50, 100 or 500 µM of C10-FA or C18-FA was added for competition. After incubation with FAs cells were washed and lipids were extracted from cells. Then the click reaction was performed, lipids were separated on a TLC plate and fluorescence was detected by fluorescence imaging. Graph B represents quantifications of data from panel A. Values represent the fluorescence intensity of C11 and C19-TAG bands. D and E represent quantifications of data from C. Values represent fluorescence intensity of C19-TAG bands and C11-TAG bands respectively. The data represent mean +SD, n=4. * stands for p≤0.05; ** p≤0.01; *** p≤0.001.

5. Discussion

Although MCFAs are not the main constituents of lipids consumed with food, they are still an important part of our modern human diet. However, data concerning MCFAs are still relatively sparse and controversial. In this work several important aspects of MCFA metabolism such as the uptake and the TAG synthesis are analyzed. This study is based on two very important cell types participating in cellular metabolism, namely hepatocytes and adipocytes. In this chapter the most important findings described in this thesis will be discussed in relation to the data obtained by other scientists. The discussion is concluded by presenting a new hypothetical model for MCFA metabolism.

5.1. Metabolism of C11-FA in different cell lines and mouse organs

C11-FA metabolism in different cell lines, primary cells and mouse organs was investigated. It was found that different cancer cell lines (e.g. Huh7, HepG2, A431), the fibroblast line 3T3-L1 and some other lines cannot incorporate C11-FA into TAG (Figure 9). On the other hand, the organs (e.g. liver), from which these cells (e. g. Huh7, HepG2) originate, possess this particular ability (Figure 8). This allows us to draw two important conclusions.

First, cell lines used in experiments as representatives of certain organs do not necessarily have the same features or metabolic capabilities as these organs. Good examples illustrating this are hepatoma cell lines such as Huh7 and HepG2. Compared to primary hepatocytes these cells have very low levels of cytochrome P450 enzymes participating in the drug biotransformation process and therefore are of limited use in drug metabolism studies (Castell et al., 2006; Rodríguez-Antona et al., 2002). It seems that in these cells not only the drug metabolism but also the lipid (at least MCFA) metabolism is affected. In agreement with this data was the finding that HepG2 cells did not esterify MCFA octanoate into TAG (Wen et al., 2000). All in all, Huh7 and HepG2 cells cannot be used in MCFA research as liver representatives.

Second, the metabolism of MCFAs and LCFAs in cultured cells is different. Though not being able to synthesize TAG from MCFAs, hepatoma cell lines produce TAG from LCFAs. This was a very interesting finding, which encouraged us to investigate the metabolism of MCFAs in more detail.

The high efficiency of C11-TAG production in the gut and in the liver (Figure 8) is related to the function of these organs: the intestine resynthesizes digested TAGs coming from the diet and the liver synthesizes TAGs, which are either stored in lipid droplets or secreted in a form of lipoproteins. The ability to synthesize TAGs from MCFAs in liver cells was already shown earlier with radioactivity experiments (Mayorek and Bar-Tana, 1983). In these experiments octanoate and decanoate were almost exclusively incorporated into TAG and not in other lipid classes. In experiments with the intestine, MCFAs showed a higher potential to be incorporated into TAG than LCFAs (Figure 8). This result was unexpected. According to the literature, most of the generated MCFAs leave the intestine in the form of FAs after lipid digestion and not in the form of TAGs (Bach and Babayan, 1982). However, there is literature showing that MCFAs are also found in the lymph (Bloom et al., 1951; Nancy You et al., 2008). Data presented in this thesis suggest that the intestine is capable of synthesizing a decent amount of MCTs, which then could be incorporated into chylomicrons.

5.2. Differentiation of adipocytes and dedifferentiation of hepatocytes: gain and loss of function in MCT synthesis

Our experiment with cell lines (Figure 9) showed that undifferentiated 3T3-L1 cells did not incorporate C11-FA into TAG, however, from Figure 7 it could be seen that differentiated cells can synthesize C11-TAG. Differentiation of 3T3-L1 cells from fibroblast-like cells into adipocyte-like cells is a complex process determined by changing expression of multiple transcription factors, cell cycle regulators, structural proteins or proteins participating in cellular metabolism (Farmer, 2006; Mikkelsen et al., 2010). During differentiation 3T3-L1 cells gain the function of TAG synthesis from MCFAs. The C11-TAG synthesis can be observed after 42 hours from the beginning of differentiation (Figure 10). The inability to synthesize TAG from MCFA [1-^{13}C] octanoate in undifferentiated 3T3-L1 cells was also demonstrated in the study of Wen et al. (Wen

et al., 2000). The potential of adipocytes to incorporate MCFAs into TAGs was confirmed by many other studies (Brandes et al., 1985; Bugaut, 1989; Sarda et al., 1987; Wen et al., 2000).

The dedifferentiation of primary hepatocytes, which starts directly after plating cells on the collagen layer (Baker et al., 2001), makes the work with primary cells more complicated and also can distort the results. This encouraged the development of three-dimensional culture techniques, which protect primary hepatocytes from dedifferentiation (Bell et al., 2016; Brophy et al., 2009; Godoy et al., 2013; van Zijl and Mikulits, 2010). In this thesis it was examined how dedifferentiation affects the LCFA and MCFA metabolism (Figure 11). A striking finding was that the dedifferentiating cells lost the ability to synthesize TAG from C11-FA, but continued to synthesize C19-TAG. Hepatocytes that spent one day in culture almost completely lost the ability to synthesize C11-TAG (Figure 11A). In addition to adipocytes this gives us one more cell type, this time with a loss of function, for the investigation of the MCFA metabolism. To the best of the author's knowledge, this work is the first to show that the dedifferentiation of hepatocytes changes the metabolism of lipids, particularly the metabolism of MCFAs.

RNA sequencing of differentiating adipocytes and dedifferentiating hepatocytes delivered a broad spectrum of data from which changes in the expression of genes belonging to different classes and having a broad variety of functions could be determined. Genes participating in lipid metabolism are of particular relevance for this work. The expression level of the majority of the genes related to lipid metabolism increased in differentiating adipocytes and decreased in dedifferentiating hepatocytes (Table 15). Similar trends were observed in proteomic or mRNA analyses from other studies (Mikkelsen et al., 2010; Rowe et al., 2010). Nevertheless, because of the immense complexity of biological processes of differentiation and dedifferentiation and the numerous changes in the expression of different genes, it was not possible to identify genes directly responsible for changes in C11-TAG synthesis. Still, these data can support the hypothesis related to C11-TAG synthesis in hepatocytes and 3T3-L1 adipocytes and suggest candidates for further studies.

In general, two cell models for work with MCFAs: a loss of function hepatocyte model and a gain of function adipocyte model were established.

5.3. MCFA uptake

It is possible to follow the FA uptake by detecting alkyne-FAs in the medium using a click labeling method. The FA amount from the samples with cells is compared to a control medium samples without cells. Using pulse experiments it was shown that the uptake of C11-FA is faster than the uptake of C19-FA in both hepatocytes and 3T3-L1 cells (4.5.2). The FA uptake was evaluated by measuring the reduction of alkyne-FAs in the medium. FAs that cells take up from the medium could be used for lipid synthesis or/and degraded in catabolic processes. In experiments with undifferentiated 3T3-L1 cells and dedifferentiated hepatocytes C11-FA was used up from the medium (Figure 13, Figure 12A), which was an interesting finding. As previously mentioned these cells do not use C11-FA for lipid synthesis. Apart from being incorporated in cellular lipid structure, there are other known ways for FA to be used up by the cells, such as mitochondrial β-oxidation, peroxisomal β-oxidation, microsomal ω-oxidation and peroxisomal α-oxidation. ω-oxidation is not possible with alkyne-FAs as the ω carbon atom is incorporated in an alkyne structure and is not susceptible to ω-oxidation. Peroxisomal α-oxidation is a minor pathway used for the degradation of FAs that have a methyl group at the β-carbon atom and therefore it is not relevant for the C11-FA. It is believed that the main oxidation type for MCFAs is the mitochondrial β-oxidation (Bach and Babayan, 1982). Yet some scientists suggest that MCFAs could be β-oxidized to a large extent in peroxisomes (Bian et al., 2005; Christensen et al., 1989). Compared to palmitate treatment, increased amounts of hydrogen peroxide, which is an indicator for peroxisomal β-oxidation, were found in the liver perfused with octanoate and decanoate (Foerster et al., 1981) and also in hepatocytes fed with different MCFAs (Leighton et al., 1982).

Data from the experiments with dedifferentiated hepatocytes and undifferentiated 3T3-L1 cells (Figure 11A, Figure 12A, Figure 9 and Figure 13) imply that although C11-FAs can be transferred into the cells, they are not incorporated into TAG. Huh7 cells, in contrary, do not metabolize C11-FA at all as C11-FA remains in the medium. This implies that MCFAs either cannot get inside the Huh7 cells or they do get inside, but cannot be metabolized and are secreted back into the medium. The assumption that Huh7 cells may lack enzymes for MCFA metabolism is supported by earlier studies showing that the expression level of mitochondrial ACSMs in Huh7 cells was much lower compared to liver samples (Boomgaarden et al., 2009). However, from enzymatic assays with lysates

it can be seen that Huh7 cells have enzymatic activities for the synthesis of MCFA-CoAs and MCTs (Figure 26, Figure 27). This question remains unclear and needs further investigation.

5.4. The etomoxir effect

Etomoxir is known as an inhibitor of the mitochondrial LCFA β-oxidation (Jew et al., 1997). LCFA-CoAs can get inside mitochondria only in a form of acylcarnitine. To participate in mitochondrial β-oxidation LCFA-CoAs have first to be converted to acylcarnitines by the enzyme CPT1. Etomoxir can be used to prevent LCFA conversion to acylcarnitine. Once inside the cell etomoxir is converted into etomoxir-CoA, which irreversibly binds to the active site of CPT1 and in such a way inhibits its enzymatic activity (Kiorpes et al., 1984). Malonyl-CoA is a physiological reversible inhibitor of CPT1 (McGarry et al., 1977, 1978).

It is known from the literature that etomoxir can protect the heart from a FA-induced ischemic injury (Lopaschuk et al., 1988). Moreover, with the growing evidence of the role of FA metabolism in tumor growth (Carracedo et al., 2013), CPT1 and its inhibitors attracted attention in cancer research (Qu et al., 2016). It was shown that etomoxir can induce cancer cell death by inhibiting FA oxidation (Pike et al., 2011; Samudio et al., 2010; Schlaepfer et al., 2014). However, the treatment with etomoxir proved to have some serious adverse effects related to the induction of oxidative stress (Merrill et al., 2002) and activation of transcription factors such as peroxisome proliferator-activated receptor alpha (PPARα) and nuclear factor-kappaB (NF-κB) (Cabrero et al., 2003; Forman et al., 1997). As a consequence, its usage as a drug was not approved (Carracedo et al., 2013).

The mitochondrial β-oxidation of MCFAs was studied in various studies. In contrast to LCFAs, CPT1 is not required for the oxidation of MCFAs (Bach and Babayan, 1982; Papamandjaris et al., 1998). It is generally accepted that MCFAs can cross the inner mitochondrial membrane without having to be converted into acylcarnitine. This concept is supported by studies showing that the inhibition of CPT1 does not decrease the oxidation rate of octanoate (Abdel-aleem et al., 1994; Guo et al., 2006). It is worth mentioning that the plasma concentrations of free carnitine were lower and the concentrations of carnitine derivatives were higher in healthy humans infused with a

mixture of LCT and MCT compared to a mere LCT infusion (Rössle et al., 1990). This suggests the role of carnitine in the metabolism of MCT.

In this work the term "etomoxir effect" is used to describe a distinctive cell response to etomoxir treatment. This response has the following two characteristics. The first one is the appearance of unknown substances in the medium after etomoxir treatment of C11-FA fed hepatocytes. The second is a decrease of the C11-TAG amount in cells treated with etomoxir. The etomoxir effect was evident in hepatocytes, whereas in 3T3-L1 cells this effect was expressed to a lesser extent. Therefore, the further etomoxir related discussion will focus mainly on hepatocytes.

Treatment with etomoxir enhanced the appearance of unknown substances in the medium of C11-FA fed hepatocytes. With an increasing pulse time, some of these substances disappeared from the medium, showing that they were taken up again by the cells and were metabolized (Figure 19E, G, F). Furthermore, these substances also appeared in control cells without etomoxir treatment, but the amount was significantly lower and they disappeared faster (Figure 19E, G, F). No such substances could be detected in the C19 feeding condition (Figure 20E, F). These substances are quite hydrophilic as they could only be extracted from the medium by addition of acetic acid, but not with water (Figure 24).

Studies of FA oxidation also mention the development of acid-soluble products (ASPs) in the medium of cells incubated with [1-^{14}C] labeled FAs. Indeed $^{14}CO_2$, which is most often measured to determine the β-oxidation rate, represents only 5-40% of the FA degradation products whereas the rest (60-95%) is found in the medium as ASPs (1988). The appropriate way to evaluate the β-oxidation rate would be to sum the fractions of both $^{14}CO_2$ and radioactive ASPs as it was shown that measuring only $^{14}CO_2$ is inaccurate (van Hinsbergh et al., 1978; Veerkamp et al., 1986).

A greater amount of ASPs was found in the medium while feeding cells with MCFAs compared to LCFAs. (Christensen et al., 1989, 1991). The composition of ASPs was partially identified. They primarily include acetate, ketone bodies, succinate and citrate (Kawamura and Kishimoto, 1981; Lin et al., 1996).

When an alkyne-FA with an odd number of carbon atoms undergoes a full process of β-oxidation, propiolyl-CoA is generated as the end product. This substance is unstable and in several reactions it is converted to an enoyl-CoA derivative (Patel and Walt, 1988). As a result the alkyne label is lost and the click reaction cannot take place. Therefore with alkyne labeling it is not possible to detect ketone bodies or intermediates of the citric

acid cycle. Unknown substances that were found in the medium during experiments with C11-FA fed cells most probably are forms of shortened or modified FAs such as acylcarnitines, 3-hydroxy acyl-CoAs, 3-oxoacyl-CoAs or their carnitine intermediates. A preliminary lipid mass spectrometry analysis performed in collaboration with Gerhard Liebisch from Regensburg allowed to identify hydroxy FA with 7 carbon atoms in the medium of day 3 hepatocytes incubated overnight with C11-FA, data not shown. A more detailed analysis would be required to identify other unknown substances present in the medium.

In order to follow the β-oxidation of FAs using the click labeling method oxa-alkyne-FA based methodology was developed by Christoph Thiele. In oxa-FAs one carbon atom is replaced with an oxygen atom, so a full β-oxidation cannot take place. It stops at the point where oxygen is at the β position of the FA chain (Figure 33). As a consequence, an alkyne group of shortened oxa-FA is not degraded and can be labeled with the click reaction. Therefore the amount of oxa-FA used for the β-oxidation can be quantified. Medium and long-chain oxa-FAs were synthesized by Maria Fiedler and Jennifer Saam and were fed to hepatocytes and adipocytes. Preliminary data indicate that the C11 oxa-FA was more efficiently β-oxidized than the C17 oxa-FA (data not shown) and that etomoxir did not influence the β-oxidation rate of C11 oxa-FA, because the amount of C9 oxa-FA in the medium was the same in etomoxir treated and untreated cells (Figure 34, lanes 7-9 and 11-13). Similarly as in the C11-FA experiments etomoxir significantly reduced the C11 oxa-TAG amount (Figure 34, lanes 1-6).

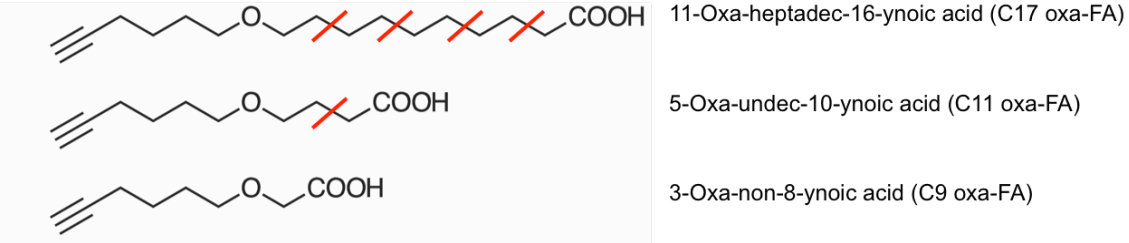

Figure 33. Structures of oxa-FAs.
Red lines mark in how many cycles of β-oxidation C17 oxa-FA and C11 oxa-FA can participate. The final β-oxidation product of both FAs is C9 oxa-FA, which cannot be further β-oxidized. Oxa-FAs were synthesized by Maria Fiedler and Jennifer Saam.

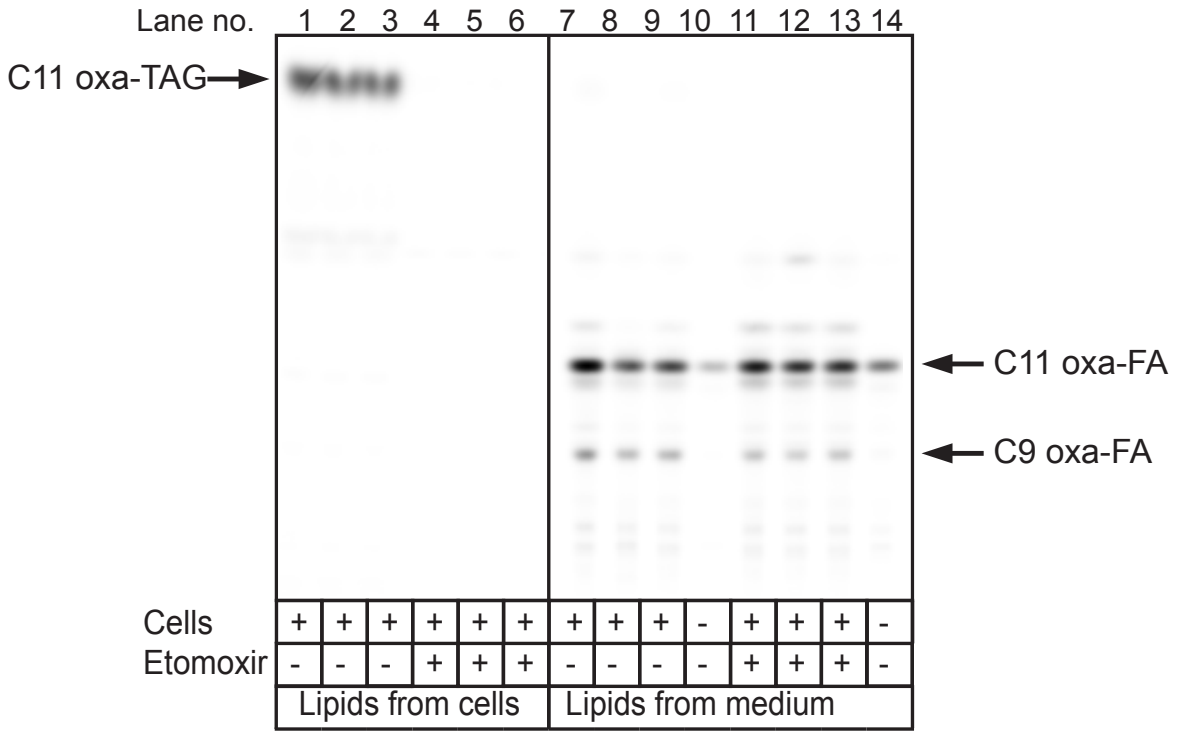

Figure 34. C11 oxa-FA metabolism in hepatocytes.
Hepatocytes isolated from a mouse liver were plated on collagen coated 12-well plates. 150.000 cells were plated per well. First, cells were incubated with 50 µM etomoxir for 2 hours. Then 1 hour incubation with 50 µM of C11 oxa-FA followed. The medium was collected and 50 µl of it was used for lipid extraction. Cells were washed and lipids were extracted from cells. Then click reaction was performed both with lipids from the medium and cells. Finally, lipids were separated on a TLC plate and the fluorescence was detected by fluorescence imaging. In the indicated samples 50 µM of etomoxir was added to the medium with FA. Lanes 10 and 14 represent controls, where the medium with FA was added to the well without cells. Data taken from Bachelor thesis of Maria Fiedler, submitted 2016.

As already mentioned, there were two characteristics of the etomoxir effect in C11-FA fed hepatocytes. The first one, i.e. the appearance of unknown substances in the medium, was already discussed. The second one, the decrease of the C11-TAG amount, will be analyzed in this paragraph. To the best of the author's knowledge, this work is the first to describe that a CPT1 inhibitor hinders the C11-FA incorporation into TAG in hepatocytes and to some extent in adipocytes. The decrease in TAG synthesis is observed in minutes after adding etomoxir (Figure 19A and C). This hints to a direct inhibition of a protein participating in the processes of the C11-TAG synthesis and not to an effect related to changes in the gene transcription. Some studies indeed hint to a role of etomoxir in the activation of the transcription regulators PPARα and NF-κB (Cabrero et al., 2003; Forman et al., 1997). The fact that etomoxir affects the C11-TAG synthesis points to the role of CPT1 in the MCT synthesis. Theoretically, MCFAs could be converted to acyl-CoAs in the cytosol by ACSLs as these enzymes possess the activity both towards

LCFAs and MCFAs (Normann et al., 1981). If this were the case, the inhibition of CPT1 would not have an effect on the MCT amount. This leads to an assumption that C11-FA is converted to C11-CoA in mitochondria and then transported from the mitochondria to the cytosol in a C11-carnitine form. CPT1 is needed for the conversion of C11-carnitine back into C11-CoA, which is then used for the C11-TAG synthesis. This hypothesis suggests the role of mitochondrial MCFA-CoA formation in the C11-TAG synthesis pathway. The mRNA data in Table 15 indicate that in dedifferentiating hepatocytes the amount of CPT1 diminishes. In 3T3-L1 adipocytes, however, CPT1 declines with the differentiation, and most probably C11-TAG synthesis is enabled by a different mechanism than in hepatocytes.

In pulse experiments with C11-FA fed hepatocytes the TAG band of higher mobility, probably containing elongated FA could be identified on a TLC plate. This band was significantly weaker in etomoxir-treated cells (Figure 19A, B). Presumably, in etomoxir-treated cells the FA elongation process was disturbed. Inside the cells FAs can be elongated in mitochondria, in microsomes or in the cytosol, as a part of the *de novo* FA synthesis (Jump, 2009). The microsomal FA elongation is considered to be the dominant pathway for the FA elongation (Jakobsson et al., 2006). The lack of C11-CoAs in microsomes is a possible reason for the failed C11-FA elongation. According to the recently introduced assumption, C11-CoAs are synthesized in mitochondria and their accumulation in the cytosol and subsequently in microsomes is inhibited by etomoxir.

The etomoxir treatment does not cause the development of the previously mentioned unknown substances in C19-FA fed hepatocytes and also does not change the amount of C19-TAG, however, it causes a slight increase in the amount of PC and PE (Figure 20A, C, D). LCFAs need CPT1 to get inside the mitochondria to be able to participate in β-oxidation. By inhibiting CPT1 with etomoxir, this pathway of LCFAs is blocked. FAs that are spared from β-oxidation are channeled to other metabolic pathways. It was shown that etomoxir increased oleate incorporation into TAG (Boren and Brindle, 2012). The data from experiments presented in this thesis suggest that a C19-FA is rather channeled to the phospholipid synthesis. In general, the minimum effect of etomoxir on the LCFA metabolism was likely predetermined by the circumstance that in all experiments described in this work a high glucose medium was used. However, the LCFA oxidation, which is the target of etomoxir, is normally activated under fasting conditions when the level of glucose is low (Guo et al., 2006).

5.5. TAG synthesis from MCFAs

Experiment, where C11-TAG was hydrolyzed with a pancreatic lipase, showed that C11-FA was incorporated at the *sn1* or *sn3* position of a TAG molecule (Figure 29). This accounts for either GPAT (*sn1*) or DGAT (*sn3*) enzymatic activities in the glycerol phosphate pathway, see chapters 1.4.2 and 1.4.5. Experimental studies have shown that MCFAs are poor substrates for the esterification of G3P both in hepatocytes and adipocytes and that they are good substrates for the DAG esterification (Brandes et al., 1985; Mayorek and Bar-Tana, 1983). This implies that C11-TAG was produced by DGAT enzymes in experiments with C11-FA fed cells. The expression of DGAT2 extremely increases during the differentiation of 3T3-L1 cells (Table 15, gene no. 30), however, the increase in DGAT1 expression is much smaller (Table 15 gene no. 29). This indicated a possible role of DGAT2 in C11-TAG synthesis. Experiments with an *in vitro* DGAT assays showed that both day 0 and day 4 hepatocyte lysates can synthesize C11-TAG (Figure 31). For the DGAT reaction acyl-CoA and DAG are needed and they both need to be accessible for the DGAT enzymes. The data from an *in vitro* acyl-CoA synthesis assay show that both hepatocyte lysates (day 0 and day 4) are able to synthesize similar amounts of C11-CoA (Figure 28). This acyl-CoA synthesis assay was not direct (i.e. coupled), therefore the comparison of the activities in lysates is questionable. Still this assay can show if there was any acyl-CoA synthesis activity at all. Experimental data from acyl-CoA synthesis leads to the conclusion that dedifferentiated hepatocytes have a potential to synthesize C11-CoA. The DAG amount in cells is also not a limiting factor for the DGAT reaction. This was confirmed using a control assay with only C11-CoA added to the lysates (Figure 30A lanes 9-12 in purple boxed area). This control assays with both hepatocyte lysates contained small amounts of C11-TAG and C19-TAG, which had been produced from added C11-CoA and C19-CoA and endogenous DAG residing in cellular lysates. If dedifferentiated cells can synthesize C11-CoA and have sufficient reserves of DAG, then it could be that the C11-CoA does not reach the TAG synthesis site, see the upcoming chapter.

A different trend was observed in assays with lysates from undifferentiated and differentiated 3T3-L1 cells. The difference in C11-CoA production efficiency was very high between these two cell types (Figure 28A). This raises the question if enough C11-

CoA is produced in undifferentiated cells for effective C11-TAG synthesis. Moreover, data from the DGAT assay implies that undifferentiated 3T3-L1 cells synthesized much less C11-TAG than differentiated cells (Figure 31). These results suggest that dedifferentiated hepatocytes and undifferentiated 3T3-L1 cells do not synthesize C11-TAG due to different mechanisms involved. This will be discussed in the upcoming chapter.

The data from the competition experiments suggest that C11-FA is spared from β-oxidation by adding 50 or 100 µM of C10-FA. As a result, more C11-TAG can be synthesized (Figure 32). In general β-oxidation of MCFAs was shown to be very active (Christensen et al., 1989; Metges and Wolfram, 1991; Pégorier et al., 1988). When the concentration of C10-FA reaches a physiologically very high level of 500 µM, the C10-FA starts to compete with C11-FA and the amount of the C11-TAG decreases. In the previous paragraph, it was mentioned that cells have relatively high reserves of DAG, which can be used for TAG synthesis after supplementing cells with FAs. However, when the amount of C10-FA increased to very high levels, presumably C10-FA was channeled to other enzymatic steps of the glycerol phosphate pathway, such as the esterification of G3P to produce LPA and the esterification of LPA to produce PA followed by DAG synthesis (Figure 26C). No PA and DAG intermediates were detected on the TLC plate because C11-FA was not used in reactions generating these lipids. C11-FA was used only for the final DGAT reaction, involving either endogenous DAGs or DAGs synthesized from supplemented C10-FAs. Three C11-TAG bands were identified on the TLC plate as TAGs having one, two or three MCFAs run differently (Figure 32C lane 12). It is most likely that at very high concentration C10-FA competes with C11-FA for DGAT enzymes. When 500 µM of oleate (C18:1) was added, the C11-TAG amount increased. This could be explained by the fact that oleate is a relatively good substrate for GPAT and LPAAT enzymes and that at high concentrations oleate was very efficiently used for the synthesis of LPA followed by the synthesis of PA and DAG. This newly synthesized DAG could then be used by DGAT enzymes for C11-TAG synthesis. Brandes et al., 1985 showed that when adipocytes were fed with 600 µM of octanoate (C8:0), the addition of up to 200 µM of palmitate (C16:0) slightly increased the C8-TAG amount. However, with higher concentrations of palmitate, the C8-TAG amount started to decrease. In future experiments the concentrations of FAs would have to be increased deliberately for oleate to compete with C11-FA for DGAT activity.

5.6. The concluding hypothesis

Based on experimental data analysis and literature research a concluding hypothesis for the MCFA metabolism in hepatocytes and 3T3-L1 adipocytes is presented. Figure 35 shows a generally accepted metabolism scheme of LCFAs and MCFAs. According to this model under normal physiological conditions LCFAs (red arrows) are used for cellular lipid synthesis and MCFAs (blue arrows) are used for mitochondrial β-oxidation.

For hepatocytes a slightly different model is proposed where MCFAs can also be incorporated into TAG, Figure 36A (blue arrows). In hepatocytes MCFAs first get inside mitochondria and are activated there by ACSMs. A part of these FAs is used for β-oxidation. Remaining FAs are transported as FA-carnitines via the carnitine shuttle to the cytosol, where they are converted to acyl-CoAs by CPT1. These acyl-CoAs can then be used by DGAT enzymes for the TAG synthesis.

In dedifferentiated hepatocytes (Figure 36A red arrows) CPT1 level is decreased (Table 15, gene no. 45). It is likely that the conversion of acylcarnitines into acyl-CoAs is affected by the low amount of CPT1. Consequently, the amount of MCFA-CoAs in the cytosol is not sufficient for TAG synthesis. As MCFAs cannot be utilized for the TAG synthesis, they are oxidized to a larger extent. As a result, various shortened and modified forms of C11-FA are secreted into the medium. The oxidation process of C11-FA most likely takes place in mitochondria, but peroxisomes and the cytosol could also contribute.

In differentiated 3T3-L1 cells (Figure 36A blue arrows) the expression level of ACSL1 is very high (Table 15, gene no. 13). Therefore it is possible that MCFA-CoAs are synthesized not only in mitochondria but also in the cytosol, which is the main source of the MCFA-CoA synthesis. A part of mitochondrial MCFA-CoAs is channeled to β-oxidation and a part to the TAG synthesis.

In undifferentiated cells (Figure 36A red arrows), the expression levels of ACSMs are extremely low (Table 15, gene no. 51-53), hence mitochondria hardly play a big role in the MCFAs metabolism. The amount of ACSL1 is also much lower in undifferentiated cells than in differentiated cells (Table 15, gene no. 13) and is hardly sufficient for efficient MCFA-CoA and subsequent TAG synthesis. C11-FAs disappeared from the

medium of undifferentiated 3T3-L1 cells fed with C11-FAs overnight (Figure 14), what happened with these FAs is unclear.

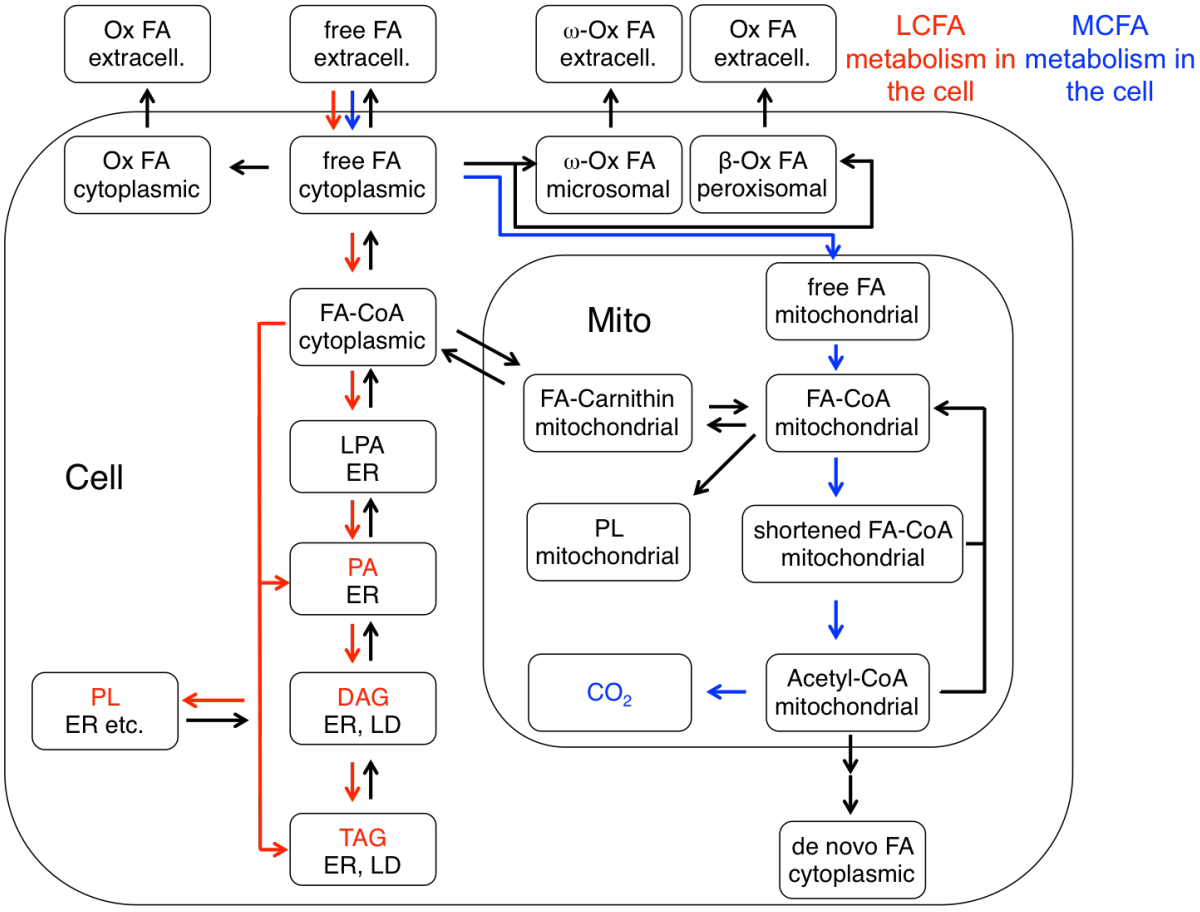

Figure 35. LCFA and MCFA metabolism, conventional model.
According to the conventional model, LCFAs (red arrows) are mainly used for TAG, DAG and phospholipid synthesis. MCFAs (blue arrows) are metabolized in mitochondria via β-oxidation and the final metabolite is CO_2. Ox – oxidized.

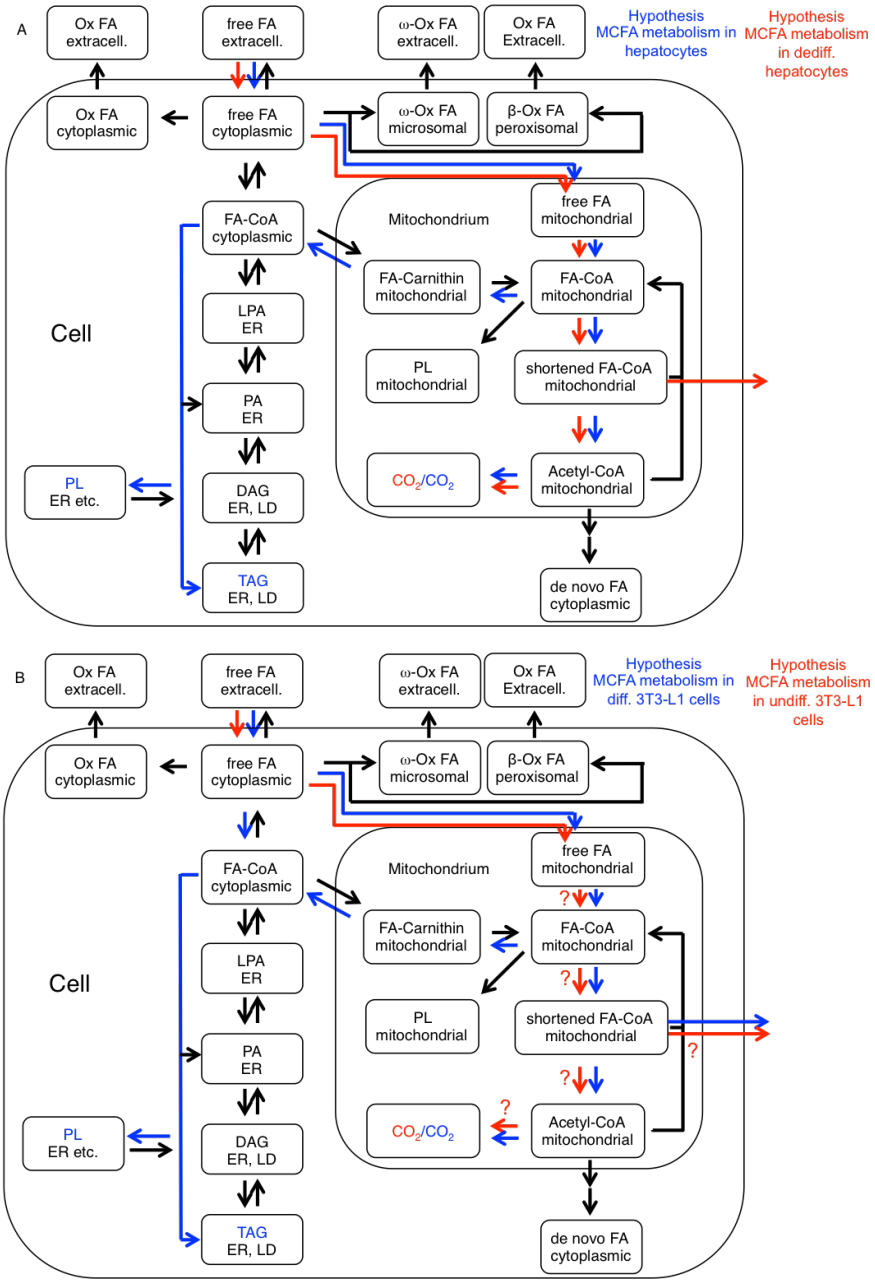

Figure 36. Hypothetical model of MCFA metabolism in hepatocytes and 3T3-L1 adipocytes.

A) In hepatocytes (blue arrows) MCFAs are used for both mitochondrial β-oxidation and TAG synthesis and to some extent for PL synthesis. MCFA-CoAs are synthesized in the mitochondria and transported via carnitine transport system to the cytosol, where they are used for TAG synthesis. In dedifferentiated hepatocytes (red arrows) the acyl-carnitine conversion to acyl-CoA is disturbed. Shortened and oxidized FA derivatives, formed in the mitochondria, are released into the medium. B) In differentiated 3T3-L1 cells (blue arrows) MCFA-CoAs synthesized both in mitochondria and in the cytosol are used for TAG and to some extent for PL synthesis. Some of FAs are oxidized and secreted as a modified substance into the cytosol. In undifferentiated 3T3-L1 cells (red arrows) the expression of ACSMs is extremely low. Therefore the role of the mitochondria in the MCFA metabolism is unclear. Not enough of cytoplasmic MCFA-CoA is synthesized for the MCT synthesis. Ox – oxidized.

6. Outlook

In order to support or deny the hypothesis, which was raised in the discussion chapter, there are several important experiments, which should be addressed in future studies. For hepatocytes it was hypothesized that MCFA-CoA is synthesized in mitochondria and that CPT1 is involved in the conversion of MCFA-carnitine to MCFA-CoA. However, in etomoxir-treated cells and in dedifferentiated hepatocytes this conversion is disturbed. In future experiments it is important to determine MCFA-CoA and MCFA-carnitine amounts in different cellular compartments, e.g. mitochondria, cytosol and microsomes. Moreover, the role of carnitine in MCFA metabolism is an interesting aspect and should be investigated.

In general, it is important to make some control experiments by feeding cells with natural MCFAs such as decanoate and measure MCTs in cells as well as metabolites in the medium applying MS. In such way a possible effect of alkyne group on MCFA metabolism could be excluded.

The other question to clarify is what happens with MCFAs when they cannot efficiently be incorporated into TAG but still disappear from the medium. This was observed with dedifferentiated hepatocytes, hepatocytes treated with etomoxir and undifferentiated 3T3-L1 cells. To answer this question, oxidative processes could be investigated. To get a better understanding, which oxidative processes are involved in the MCFA metabolism, it is important to analyze metabolites that are secreted into the medium. For this lipid MS should be applied. Moreover, oxa-FAs could be used to quantify the potential of β-oxidation both in hepatocytes and 3T3-L1 cells. Furthermore, the role of peroxisomal β-oxidation could also be evaluated.

The finding that the gut can very effectively synthesize C11-TAG is promising and therefore should be further investigated by performing similar experiments as were did with hepatocytes and adipocytes.

Future work could also include animal experiments such as feeding mice with C11-FA or decanoate and examining lipids from the blood and from different organs by using click method and MS.

References

Abdel-aleem, S., Li, X., Anstadt, M.P., Perez-Tamayo, R.A., and Lowe, J.E. (1994). Regulation of glucose utilization during the inhibition of fatty acid oxidation in rat myocytes. Horm. Metab. Res. Horm. Stoffwechselforschung Horm. Metab. *26*, 88–91.

Aon, M.A., Bhatt, N., and Cortassa, S.C. (2014). Mitochondrial and cellular mechanisms for managing lipid excess. Front. Physiol. *5*.

Bach, A.C., and Babayan, V.K. (1982). Medium-chain triglycerides: an update. Am. J. Clin. Nutr. *36*, 950–962.

Bahrami, G., and Rahimi, Z. (2005). Fatty acid composition of human milk in Western Iran. Eur. J. Clin. Nutr. *59*, 494–497.

Baker, T.K., Carfagna, M.A., Gao, H., Dow, E.R., Li, Q., Searfoss, G.H., and Ryan, T.P. (2001). Temporal Gene Expression Analysis of Monolayer Cultured Rat Hepatocytes. Chem. Res. Toxicol. *14*, 1218–1231.

Bell, C.C., Hendriks, D.F.G., Moro, S.M.L., Ellis, E., Walsh, J., Renblom, A., Puigvert, L.F., Dankers, A.C.A., Jacobs, F., Snoeys, J., et al. (2016). Characterization of primary human hepatocyte spheroids as a model system for drug-induced liver injury, liver function and disease. Sci. Rep. *6*, 25187.

Bian, F., Kasumov, T., Thomas, K.R., Jobbins, K.A., David, F., Minkler, P.E., Hoppel, C.L., and Brunengraber, H. (2005). Peroxisomal and Mitochondrial Oxidation of Fatty Acids in the Heart, Assessed from the 13C Labeling of Malonyl-CoA and the Acetyl Moiety of Citrate. J. Biol. Chem. *280*, 9265–9271.

Bloom, B., Chaikoff, I.L., and Reinhardt, W.O. (1951). Intestinal lymph as pathway for transport of absorbed fatty acids of different chain lengths. Am. J. Physiol. Content *166*, 451–455.

Boomgaarden, I., Vock, C., Klapper, M., and Döring, F. (2009). Comparative Analyses of Disease Risk Genes Belonging to the Acyl-CoA Synthetase Medium-Chain (ACSM) Family in Human Liver and Cell Lines. Biochem. Genet. *47*, 739–748.

Boren, J., and Brindle, K.M. (2012). Apoptosis-induced mitochondrial dysfunction causes cytoplasmic lipid droplet formation. Cell Death Differ. *19*, 1561–1570.

Brandes, R., Mayorek, N., Berry, E., Arad, R., and Bar-Tana, J. (1985). The specificity of triacylglycerol synthesis for medium-chain fatty acids in rat and human adipose preparations. Biochim. Biophys. Acta BBA - Lipids Lipid Metab. *836*, 63–66.

Brandt, C., McFie, P.J., and Stone, S.J. (2016). Biochemical characterization of human acyl coenzyme A: 2-monoacylglycerol acyltransferase-3 (MGAT3). Biochem. Biophys. Res. Commun. *475*, 264–270.

Brophy, C.M., Luebke-Wheeler, J.L., Amiot, B.P., Khan, H., Remmel, R.P., Rinaldo, P., and Nyberg, S.L. (2009). Rat hepatocyte spheroids formed by rocked technique maintain differentiated hepatocyte gene expression and function. Hepatology *49*, 578–586.

Bugaut, M. (1989). In vivo incorporation of lauric acid into rat adipose tissue triacylglycerols. Lipids *24*, 193–203.

Cabrero, À., Merlos, M., Laguna, J.C., and Carrera, M.V. (2003). Down-regulation of acyl-CoA oxidase gene expression and increased NF-κB activity in etomoxir-induced cardiac hypertrophy. J. Lipid Res. *44*, 388–398.

Cao, J., Cheng, L., and Shi, Y. (2007). Catalytic properties of MGAT3, a putative triacylgycerol synthase. J. Lipid Res. *48*, 583–591.

Carracedo, A., Cantley, L.C., and Pandolfi, P.P. (2013). Cancer metabolism: fatty acid oxidation in the limelight. Nat. Rev. Cancer *13*, 227–232.

Castell, J.V., Jover, R., Martnez-Jimnez, C.P., and Gmez-Lechn, M.J. (2006). Hepatocyte cell lines: their use, scope and limitations in drug metabolism studies. Expert Opin. Drug Metab. Toxicol. *2*, 183–212.

Christensen, E., Hagve, T.-A., Grønn, M., and Christophersen, B.O. (1989). β-oxidation of medium chain (C8C14) fatty acids studied in isolated liver cells. Biochim. Biophys. Acta BBA - Lipids Lipid Metab. *1004*, 187–195.

Christensen, E., Grønn, M., Hagve, T.A., and Christophersen, B.O. (1991). Omega-oxidation of fatty acids studied in isolated liver cells. Biochim. Biophys. Acta *1081*, 167–173.

Cohen, J.C., Horton, J.D., and Hobbs, H.H. (2011). Human Fatty Liver Disease: Old Questions and New Insights. Science *332*, 1519–1523.

Coleman, R. (2004). Enzymes of triacylglycerol synthesis and their regulation. Prog. Lipid Res. *43*, 134–176.

Coleman, R.A., and Mashek, D.G. (2011). Mammalian Triacylglycerol Metabolism: Synthesis, Lipolysis, and Signaling. Chem. Rev. *111*, 6359–6386.

Dieterich, D.C., Link, A.J., Graumann, J., Tirrell, D.A., and Schuman, E.M. (2006). Selective identification of newly synthesized proteins in mammalian cells using bioorthogonal noncanonical amino acid tagging (BONCAT). Proc. Natl. Acad. Sci. *103*, 9482–9487.

Doege, H., Baillie, R.A., Ortegon, A.M., Tsang, B., Wu, Q., Punreddy, S., Hirsch, D., Watson, N., Gimeno, R.E., and Stahl, A. (2006). Targeted Deletion of FATP5 Reveals Multiple Functions in Liver Metabolism: Alterations in Hepatic Lipid Homeostasis. Gastroenterology *130*, 1245–1258.

Donkor, J., Sariahmetoglu, M., Dewald, J., Brindley, D.N., and Reue, K. (2007). Three Mammalian Lipins Act as Phosphatidate Phosphatases with Distinct Tissue Expression Patterns. J. Biol. Chem. *282*, 3450–3457.

Eberhardt, C., Gray, P.W., and Tjoelker, L.W. (1999). cDNA cloning, expression and chromosomal localization of two human lysophosphatidic acid acyltransferases. Adv. Exp. Med. Biol. *469*, 351–356.

Eichmann, T.O., Kumari, M., Haas, J.T., Farese, R.V., Zimmermann, R., Lass, A., and Zechner, R. (2012). Studies on the Substrate and Stereo/Regioselectivity of Adipose Triglyceride Lipase, Hormone-sensitive Lipase, and Diacylglycerol-O-acyltransferases. J. Biol. Chem. *287*, 41446–41457.

Elaut, G., Henkens, T., Papeleu, P., Snykers, S., Vinken, M., Vanhaecke, T., and Rogiers, V. (2006). Molecular mechanisms underlying the dedifferentiation process of isolated hepatocytes and their cultures. Curr. Drug Metab. *7*, 629–660.

Eto, M., Shindou, H., and Shimizu, T. (2014). A novel lysophosphatidic acid acyltransferase enzyme (LPAAT4) with a possible role for incorporating docosahexaenoic acid into brain glycerophospholipids. Biochem. Biophys. Res. Commun. *443*, 718–724.

Fabbrini, E., Sullivan, S., and Klein, S. (2010). Obesity and Nonalcoholic Fatty Liver Disease: Biochemical, Metabolic and Clinical Implications. Hepatol. Baltim. Md *51*, 679.

Farmer, S.R. (2006). Transcriptional control of adipocyte formation. Cell Metab. *4*, 263–273.

Foerster, E.C., Fährenkemper, T., Rabe, U., Graf, P., and Sies, H. (1981). Peroxisomal fatty acid oxidation as detected by H2O2 production in intact perfused rat liver. Biochem. J. *196*, 705–712.

Forman, B.M., Chen, J., and Evans, R.M. (1997). Hypolipidemic drugs, polyunsaturated fatty acids, and eicosanoids are ligands for peroxisome proliferator-activated receptors α and δ. Proc. Natl. Acad. Sci. *94*, 4312–4317.

Fredrikson, G., Strålfors, P., Nilsson, N.O., and Belfrage, P. (1981). Hormone-sensitive lipase of rat adipose tissue. Purification and some properties. J. Biol. Chem. *256*, 6311–6320.

Friedman, J. (2002). Diabetes: Fat in all the wrong places. Nature *415*, 268–269.

Gaebler, A., Milan, R., Straub, L., Hoelper, D., Kuerschner, L., and Thiele, C. (2013). Alkyne lipids as substrates for click chemistry-based in vitro enzymatic assays. J. Lipid Res. *54*, 2282–2290.

Godoy, P., Hewitt, N.J., Albrecht, U., Andersen, M.E., Ansari, N., Bhattacharya, S., Bode, J.G., Bolleyn, J., Borner, C., Böttger, J., et al. (2013). Recent advances in 2D and 3D in vitro systems using primary hepatocytes, alternative hepatocyte sources and non-parenchymal liver cells and their use in investigating mechanisms of hepatotoxicity, cell signaling and ADME. Arch. Toxicol. *87*, 1315–1530.

Goldberg, I.J. (1996). Lipoprotein lipase and lipolysis: central roles in lipoprotein metabolism and atherogenesis. J. Lipid Res. *37*, 693–707.

Gomez-Muñoz, A., Hamza, E.H., and Brindley, D.N. (1992). Effects of sphingosine, albumin and unsaturated fatty acids on the activation and translocation of phosphatidate phosphohydrolases in rat hepatocytes. Biochim. Biophys. Acta BBA - Lipids Lipid Metab. *1127*, 49–56.

Grevengoed, T.J., Klett, E.L., and Coleman, R.A. (2014). Acyl-CoA Metabolism and Partitioning. Annu. Rev. Nutr. *34*, 1–30.

Guo, W., Xie, W., and Han, J. (2006). Modulation of adipocyte lipogenesis by octanoate: involvement of reactive oxygen species. Nutr. Metab. *3*, 30.

Haemmerle, G., Lass, A., Zimmermann, R., Gorkiewicz, G., Meyer, C., Rozman, J., Heldmaier, G., Maier, R., Theussl, C., Eder, S., et al. (2006). Defective Lipolysis and Altered Energy Metabolism in Mice Lacking Adipose Triglyceride Lipase. Science *312*, 734–737.

Hamilton, J.A., Johnson, R.A., Corkey, B., and Kamp, F. (2001). Fatty acid transport. J. Mol. Neurosci. *16*, 99–108.

Hamilton, J.A., Guo, W., and Kamp, F. (2002). Mechanism of cellular uptake of long-chain fatty acids: Do we need cellular proteins? Mol. Cell. Biochem. *239*, 17–23.

Haunerland, N.H., and Spener, F. (2004). Fatty acid-binding proteins – insights from genetic manipulations. Prog. Lipid Res. *43*, 328–349.

van Hinsbergh, V.W.M., Veerkamp, J.H., and van Moerkerk, H.T.B. (1978). An accurate and sensitive assay of long-chain fatty acid oxidation in human skeletal muscle. Biochem. Med. *20*, 256–266.

Houten, S.M., and Wanders, R.J.A. (2010). A general introduction to the biochemistry of mitochondrial fatty acid β-oxidation. J. Inherit. Metab. Dis. *33*, 469–477.

Hsu, T.-L., Hanson, S.R., Kishikawa, K., Wang, S.-K., Sawa, M., and Wong, C.-H. (2007). Alkynyl sugar analogs for the labeling and visualization of glycoconjugates in cells. Proc. Natl. Acad. Sci. *104*, 2614–2619.

Huisgen, R. (1963). Kinetics and Mechanism of 1,3-Dipolar Cycloadditions. Angew. Chem. Int. Ed. Engl. *2*, 633–645.

Jakobsson, A., Westerberg, R., and Jacobsson, A. (2006). Fatty acid elongases in mammals: Their regulation and roles in metabolism. Prog. Lipid Res. *45*, 237–249.

Jensen, R.G. (2002). The Composition of Bovine Milk Lipids: January 1995 to December 2000. J. Dairy Sci. *85*, 295–350.

Jew, S., Kim, H., Jeong, B., and Park, H. (1997). Asymmetric synthesis of (R)-(+)-etomoxir. Tetrahedron Asymmetry *8*, 1187–1192.

Jump, D.B. (2009). Mammalian Fatty Acid Elongases. Methods Mol. Biol. Clifton NJ *579*, 375–389.

Kalhan, S.C., Mahajan, S., Burkett, E., Reshef, L., and Hanson, R.W. (2001). Glyceroneogenesis and the Source of Glycerol for Hepatic Triacylglycerol Synthesis in Humans. J. Biol. Chem. *276*, 12928–12931.

Kamp, F., Guo, W., Souto, R., Pilch, P.F., Corkey, B.E., and Hamilton, J.A. (2003). Rapid Flip-flop of Oleic Acid across the Plasma Membrane of Adipocytes. J. Biol. Chem. *278*, 7988–7995.

Kawamura, N., and Kishimoto, Y. (1981). Characterization of Water-Soluble Products of Palmitic Acid β-Oxidation by a Rat Brain Preparation. J. Neurochem. *36*, 1786–1791.

Kiorpes, T.C., Hoerr, D., Ho, W., Weaner, L.E., Inman, M.G., and Tutwiler, G.F. (1984). Identification of 2-tetradecylglycidyl coenzyme A as the active form of methyl 2-tetradecylglycidate (methyl palmoxirate) and its characterization as an irreversible, active site-directed inhibitor of carnitine palmitoyltransferase A in isolated rat liver mitochondria. J. Biol. Chem. *259*, 9750–9755.

Kraemer, F.B., and Shen, W.-J. (2002). Hormone-sensitive lipase control of intracellular tri-(di-)acylglycerol and cholesteryl ester hydrolysis. J. Lipid Res. *43*, 1585–1594.

Kuerschner, L., Moessinger, C., and Thiele, C. (2008). Imaging of Lipid Biosynthesis: How a Neutral Lipid Enters Lipid Droplets. Traffic *9*, 338–352.

Lass, A., Zimmermann, R., Oberer, M., and Zechner, R. (2011). Lipolysis – A highly regulated multi-enzyme complex mediates the catabolism of cellular fat stores. Prog. Lipid Res. *50*, 14–27.

Lehner, R., and Kuksis, A. (1993). Triacylglycerol synthesis by an sn-1,2(2,3)-diacylglycerol transacylase from rat intestinal microsomes. J. Biol. Chem. *268*, 8781–8786.

Leighton, F., Brandan, E., Lazo, O., and Bronfman, M. (1982). Subcellular Fractionation Studies on the Organization of Fatty Acid Oxidation by Liver Peroxisomes*. Ann. N. Y. Acad. Sci. *386*, 62–80.

Lemarié, F., Beauchamp, E., Legrand, P., and Rioux, V. (2016). Revisiting the metabolism and physiological functions of caprylic acid (C8:0) with special focus on ghrelin octanoylation. Biochimie *120*, 40–48.

Lin, X., Adams, S.H., and Odle, J. (1996). Acetate represents a major product of heptanoate and octanoate β-oxidation in hepatocytes isolated from neonatal piglets. Biochem. J. *318*, 235–240.

Lopaschuk, G.D., Wall, S.R., Olley, P.M., and Davies, N.J. (1988). Etomoxir, a carnitine palmitoyltransferase I inhibitor, protects hearts from fatty acid-induced ischemic injury independent of changes in long chain acylcarnitine. Circ. Res. *63*, 1036–1043.

Mansbach, C.M., and Gorelick, F. (2007). Development and Physiological Regulation of Intestinal Lipid Absorption. II. Dietary lipid absorption, complex lipid synthesis, and the intracellular packaging and secretion of chylomicrons. Am. J. Physiol. - Gastrointest. Liver Physiol. *293*, G645–G650.

Marten, B., Pfeuffer, M., and Schrezenmeir, J. (2006). Medium-chain triglycerides. Int. Dairy J. *16*, 1374–1382.

Mayorek, N., and Bar-Tana, J. (1983). Medium chain fatty acids as specific substrates for diglyceride acyltransferase in cultured hepatocytes. J. Biol. Chem. *258*, 6789–6792.

McGarry, J.D., Mannaerts, G.P., and Foster, D.W. (1977). A possible role for malonyl-CoA in the regulation of hepatic fatty acid oxidation and ketogenesis. J. Clin. Invest. *60*, 265–270.

McGarry, J.D., Leatherman, G.F., and Foster, D.W. (1978). Carnitine palmitoyltransferase I. The site of inhibition of hepatic fatty acid oxidation by malonyl-CoA. J. Biol. Chem. *253*, 4128–4136.

Merrill, C.L., Ni, H., Yoon, L.W., Tirmenstein, M.A., Narayanan, P., Benavides, G.R., Easton, M.J., Creech, D.R., Hu, C.X., McFarland, D.C., et al. (2002). Etomoxir-Induced Oxidative Stress in HepG2 Cells Detected by Differential Gene Expression Is Confirmed Biochemically. Toxicol. Sci. *68*, 93–101.

Metges, C.C., and Wolfram, G. (1991). Medium- and long-chain triglycerides labeled with 13C: a comparison of oxidation after oral or parenteral administration in humans. J. Nutr. *121*, 31–36.

Mikkelsen, T.S., Xu, Z., Zhang, X., Wang, L., Gimble, J.M., Lander, E.S., and Rosen, E.D. (2010). Comparative Epigenomic Analysis of Murine and Human Adipogenesis. Cell *143*, 156–169.

Nancy You, Y.-Q., Ling, P.-R., Qu, J.Z., and Bistrian, B.R. (2008). Effects of Medium-Chain Triglycerides, Long-Chain Triglycerides, or 2-Monododecanoin on Fatty Acid Composition in the Portal Vein, Intestinal Lymph, and Systemic Circulation in Rats. JPEN J. Parenter. Enteral Nutr. *32*, 169–175.

Normann, P.T., Thomassen, M.S., Christiansen, E.N., and Flatmark, T. (1981). Acyl-CoA synthetase activity of rat liver microsomes substrate specificity with special reference to very-long-chain and isomeric fatty acids. Biochim. Biophys. Acta BBA - Lipids Lipid Metab. *664*, 416–427.

Papamandjaris, A.A., Macdougall, D.E., and Jones, P.J.H. (1998). Medium chain fatty acid metabolism and energy expenditure: Obesity treatment implications. Life Sci. *62*, 1203–1215.

Patel, S.S., and Walt, D.R. (1988). Acetyl coenzyme A synthetase catalyzed reactions of coenzyme A with α,β-unsaturated carboxylic acids. Anal. Biochem. *170*, 355–360.

Pégorier, J.-P., Duée, P.-H., Herbin, C., Laulan, P.-Y., Bladé, C., Peret, J., and Girard, J. (1988). Fatty acid metabolism in hepatocytes isolated from rats adapted to high-fat diets containing long-or medium-chain triacylglycerols. Biochem. J. *249*, 801–806.

Péterfy, M., Phan, J., Xu, P., and Reue, K. (2001). Lipodystrophy in the fld mouse results from mutation of a new gene encoding a nuclear protein, lipin. Nat. Genet. *27*, 121–124.

Pike, L.S., Smift, A.L., Croteau, N.J., Ferrick, D.A., and Wu, M. (2011). Inhibition of fatty acid oxidation by etomoxir impairs NADPH production and increases reactive oxygen species resulting in ATP depletion and cell death in human glioblastoma cells. Biochim. Biophys. Acta *1807*, 726–734.

Pillutla, P., Hwang, Y.C., Augustus, A., Yokoyama, M., Yagyu, H., Johnston, T.P., Kaneko, M., Ramasamy, R., and Goldberg, I.J. (2005). Perfusion of hearts with triglyceride-rich particles reproduces the metabolic abnormalities in lipotoxic cardiomyopathy. Am. J. Physiol. - Endocrinol. Metab. *288*, E1229–E1235.

Prasad, S.S., Garg, A., and Agarwal, A.K. (2011). Enzymatic activities of the human AGPAT isoform 3 and isoform 5: localization of AGPAT5 to mitochondria. J. Lipid Res. *52*, 451–462.

Pulinilkunnil, T., Kienesberger, P.C., Nagendran, J., Sharma, N., Young, M.E., and Dyck, J.R.B. (2014). Cardiac-specific adipose triglyceride lipase overexpression protects from cardiac steatosis and dilated cardiomyopathy following diet-induced obesity. Int. J. Obes. *38*, 205–215.

Qu, Q., Zeng, F., Liu, X., Wang, Q.J., and Deng, F. (2016). Fatty acid oxidation and carnitine palmitoyltransferase I: emerging therapeutic targets in cancer. Cell Death Dis. *7*, e2226.

Rodríguez-Antona, C., Donato, M.T., Boobis, A., Edwards, R.J., Watts, P.S., Castell, J.V., and Gómez-Lechón, M.-J. (2002). Cytochrome P450 expression in human hepatocytes and hepatoma cell lines: molecular mechanisms that determine lower expression in cultured cells. Xenobiotica *32*, 505–520.

Rössle, C., Carpentier, Y.A., Richelle, M., Dahlan, W., D'Attellis, N.P., Fürst, P., and Elwyn, D.H. (1990). Medium-chain triglycerides induce alterations in carnitine metabolism. Am. J. Physiol. *258*, E944-947.

Rostovtsev, V.V., Green, L.G., Fokin, V.V., and Sharpless, K.B. (2002). A Stepwise Huisgen Cycloaddition Process: Copper(I)-Catalyzed Regioselective "Ligation" of Azides and Terminal Alkynes. Angew. Chem. Int. Ed. *41*, 2596–2599.

Rowe, C., Goldring, C.E.P., Kitteringham, N.R., Jenkins, R.E., Lane, B.S., Sanderson, C., Elliott, V., Platt, V., Metcalfe, P., and Park, B.K. (2010). Network Analysis of Primary Hepatocyte Dedifferentiation Using a Shotgun Proteomics Approach. J. Proteome Res. *9*, 2658–2668.

Rowe, C., Gerrard, D.T., Jenkins, R., Berry, A., Durkin, K., Sundstrom, L., Goldring, C.E., Park, B.K., Kitteringham, N.R., Hanley, K.P., et al. (2013). Proteome-wide analyses of human hepatocytes during differentiation and dedifferentiation. Hepatol. Baltim. Md *58*, 799–809.

Salic, A., and Mitchison, T.J. (2008). A chemical method for fast and sensitive detection of DNA synthesis in vivo. Proc. Natl. Acad. Sci. *105*, 2415–2420.

Samudio, I., Harmancey, R., Fiegl, M., Kantarjian, H., Konopleva, M., Korchin, B., Kaluarachchi, K., Bornmann, W., Duvvuri, S., Taegtmeyer, H., et al. (2010). Pharmacologic

inhibition of fatty acid oxidation sensitizes human leukemia cells to apoptosis induction. J. Clin. Invest. *120*, 142–156.

Sarda, P., Lepage, G., Roy, C.C., and Chessex, P. (1987). Storage of medium-chain triglycerides in adipose tissue of orally fed infants. Am. J. Clin. Nutr. *45*, 399–405.

Schaffer, J.E., and Lodish, H.F. (1994). Expression cloning and characterization of a novel adipocyte long chain fatty acid transport protein. Cell *79*, 427–436.

Schlaepfer, I.R., Rider, L., Rodrigues, L.U., Gijón, M.A., Pac, C.T., Romero, L., Cimic, A., Sirintrapun, S.J., Glodé, L.M., Eckel, R.H., et al. (2014). Lipid Catabolism via CPT1 as a Therapeutic Target for Prostate Cancer. Mol. Cancer Ther. *13*, 2361–2371.

Schwenk, R.W., Holloway, G.P., Luiken, J.J.F.P., Bonen, A., and Glatz, J.F.C. (2010). Fatty acid transport across the cell membrane: Regulation by fatty acid transporters. Prostaglandins Leukot. Essent. Fat. Acids PLEFA *82*, 149–154.

Sharma, S., Adrogue, J.V., Golfman, L., Uray, I., Lemm, J., Youker, K., Noon, G.P., Frazier, O.H., and Taegtmeyer, H. (2004). Intramyocardial lipid accumulation in the failing human heart resembles the lipotoxic rat heart. FASEB J. *18*, 1692–1700.

Shi, Y., and Cheng, D. (2009). Beyond triglyceride synthesis: the dynamic functional roles of MGAT and DGAT enzymes in energy metabolism. Am. J. Physiol. - Endocrinol. Metab. *297*, E10–E18.

Shindou, H., Hishikawa, D., Harayama, T., Yuki, K., and Shimizu, T. (2009). Recent progress on acyl CoA: lysophospholipid acyltransferase research. J. Lipid Res. *50*, S46–S51.

Smathers, R.L., and Petersen, D.R. (2011). The human fatty acid-binding protein family: Evolutionary divergences and functions. Hum. Genomics *5*, 170–191.

Smith, S.J., Cases, S., Jensen, D.R., Chen, H.C., Sande, E., Tow, B., Sanan, D.A., Raber, J., Eckel, R.H., and Farese, R.V. (2000). Obesity resistance and multiple mechanisms of triglyceride synthesis in mice lacking Dgat. Nat. Genet. *25*, 87–90.

Stone, S.J., Myers, H.M., Watkins, S.M., Brown, B.E., Feingold, K.R., Elias, P.M., and Farese, R.V. (2004). Lipopenia and Skin Barrier Abnormalities in DGAT2-deficient Mice. J. Biol. Chem. *279*, 11767–11776.

Stone, S.J., Levin, M.C., Zhou, P., Han, J., Walther, T.C., and Farese, R.V. (2009). The Endoplasmic Reticulum Enzyme DGAT2 Is Found in Mitochondria-associated Membranes and Has a Mitochondrial Targeting Signal That Promotes Its Association with Mitochondria. J. Biol. Chem. *284*, 5352–5361.

Takeuchi, K., and Reue, K. (2009). Biochemistry, physiology, and genetics of GPAT, AGPAT, and lipin enzymes in triglyceride synthesis. Am. J. Physiol. - Endocrinol. Metab. *296*, E1195–E1209.

Thiele, C., Papan, C., Hoelper, D., Kusserow, K., Gaebler, A., Schoene, M., Piotrowitz, K., Lohmann, D., Spandl, J., Stevanovic, A., et al. (2012). Tracing Fatty Acid Metabolism by Click Chemistry. ACS Chem. Biol. *7*, 2004–2011.

Thorpe, C., and Kim, J.J. (1995). Structure and mechanism of action of the acyl-CoA dehydrogenases. FASEB J. *9*, 718–725.

Tornøe, C.W., Christensen, C., and Meldal, M. (2002). Peptidotriazoles on Solid Phase: [1,2,3]-Triazoles by Regiospecific Copper(I)-Catalyzed 1,3-Dipolar Cycloadditions of Terminal Alkynes to Azides. J. Org. Chem. *67*, 3057–3064.

Veerkamp, J.H., van Moerkerk, T.B., Glatz, J.F., Zuurveld, J.G., Jacobs, A.E., and Wagenmakers, A.J. (1986). 14CO2 production is no adequate measure of [14C]fatty acid oxidation. Biochem. Med. Metab. Biol. *35*, 248–259.

Watkins, P.A., Maiguel, D., Jia, Z., and Pevsner, J. (2007). Evidence for 26 distinct acyl-coenzyme A synthetase genes in the human genome. J. Lipid Res. *48*, 2736–2750.

Wen, G.U.O., Ji-Kyung, C., Kirkland, J.L., Corkey, B.E., and Hamilton, J.A. (2000). Esterification of free fatty acids in adipocytes: a comparison between octanoate and oleate. Biochem. J. *349*, 463–471.

Wendel, A.A., Lewin, T.M., and Coleman, R.A. (2009). Glycerol-3-phosphate acyltransferases: Rate limiting enzymes of triacylglycerol biosynthesis. Biochim. Biophys. Acta *1791*, 501–506.

Wilfling, F., Wang, H., Haas, J.T., Krahmer, N., Gould, T.J., Uchida, A., Cheng, J.-X., Graham, M., Christiano, R., Fröhlich, F., et al. (2013). Triacylglycerol Synthesis Enzymes Mediate Lipid Droplet Growth by Relocalizing from the ER to Lipid Droplets. Dev. Cell *24*, 384–399.

Wu, Q., Ortegon, A.M., Tsang, B., Doege, H., Feingold, K.R., and Stahl, A. (2006). FATP1 Is an Insulin-Sensitive Fatty Acid Transporter Involved in Diet-Induced Obesity. Mol. Cell. Biol. *26*, 3455–3467.

Yamashita, A., Hayashi, Y., Matsumoto, N., Nemoto-Sasaki, Y., Oka, S., Tanikawa, T., and Sugiura, T. (2014). Glycerophosphate/Acylglycerophosphate Acyltransferases. Biology *3*, 801–830.

Yen, C.-L.E., and Farese, R.V. (2003). MGAT2, a Monoacylglycerol Acyltransferase Expressed in the Small Intestine. J. Biol. Chem. *278*, 18532–18537.

Yen, C.-L.E., Stone, S.J., Cases, S., Zhou, P., and Farese, R.V. (2002). Identification of a gene encoding MGAT1, a monoacylglycerol acyltransferase. Proc. Natl. Acad. Sci. *99*, 8512–8517.

Yen, C.-L.E., Monetti, M., Burri, B.J., and Farese, R.V. (2005). The triacylglycerol synthesis enzyme DGAT1 also catalyzes the synthesis of diacylglycerols, waxes, and retinyl esters. J. Lipid Res. *46*, 1502–1511.

Yen, C.-L.E., Stone, S.J., Koliwad, S., Harris, C., and Farese, R.V. (2008). Thematic Review Series: Glycerolipids. DGAT enzymes and triacylglycerol biosynthesis. J. Lipid Res. *49*, 2283–2301.

Yen, C.-L.E., Nelson, D.W., and Yen, M.-I. (2015). Intestinal triacylglycerol synthesis in fat absorption and systemic energy metabolism. J. Lipid Res. *56*, 489–501.

Yuhas, R., Pramuk, K., and Lien, E.L. (2006). Human milk fatty acid composition from nine countries varies most in DHA. Lipids *41*, 851–858.

van Zijl, F., and Mikulits, W. (2010). Hepatospheres: Three dimensional cell cultures resemble physiological conditions of the liver. World J. Hepatol. *2*, 1–7.

Zimmermann, R., Strauss, J.G., Haemmerle, G., Schoiswohl, G., Birner-Gruenberger, R., Riederer, M., Lass, A., Neuberger, G., Eisenhaber, F., Hermetter, A., et al. (2004). Fat Mobilization in Adipose Tissue Is Promoted by Adipose Triglyceride Lipase. Science *306*, 1383–1386.

(1988). Methods of Biochemical Analysis (Hoboken, NJ, USA: John Wiley & Sons, Inc.).

(1994). Food Components to Enhance Performance: An Evaluation of Potential Performance-Enhancing Food Components for Operational Rations (National Academies Press).

Acknowledgements

My name alone stands on the cover of this thesis, but this work could have never come to completion without the help from many people who supported me over the last few years.

Foremost, I would like to thank Prof. Christoph Thiele for possibility to work in his group and for offering me this interesting subject. Immense knowledge and precise insights of Prof. Thiele have always been a great and reliable help. I am very grateful for his support during the whole period of my PhD.

I also want to thank the members of my thesis committee. I am grateful to Prof. Klaus Willecke for reviewing my thesis. Also my sincere thanks to Prof. Sven Burgdorf and Prof. Ulrich Kubitscheck for agreeing to take part in my thesis committee.

The RNA sequencing team from AG Schultze have done a great work sequencing and analyzing RNA probes of differentiating 3T3-L1 cells and dedifferentiating hepatocytes. Special thanks to Dr. Kristian Händler, Dr. Susanne Schmidt, Dr. Thomas Ulas, Stefanie Herresthal, Kathrin Klee. I also thank Dr. Gerhard Liebisch for preliminary MS analysis.

I would like to thank Marlene Buller for differentiation experiments with 3T3-L1 cells. I also want to thank Maria Fiedler and Jennifer Saam for synthesis of oxa-FAs and experiments in cells with these FAs.

I would like to express my gratitude to Kira, Alex, Elvira, Danute and Kastytis for proof-read my thesis. I really appreciate this!

My most sincere thanks to all present and former lab members, who always created nice collegial atmosphere as well as helped me in various situations. I am especially grateful to my fellow PhD students from AG Thiele Alex, Kira, Klaus and Tina. I shared many nice moments with them in the lab and outside the lab, e.g. during sunny coffee breaks or in the “Boulder Halle”.

Last but not least I would like to thank my close ones. My warmest thanks to my parents for supporting me always in every step of my life. And finally, I wish to thank Kastytis, my friendly, encouraging and most reliable counsel, for being always there for me.

My PhD was funded in part by International Graduate School LIMES Chemical Biology and German Research Foundation “TR83”.